

2mL

RADIATION-PRESSURE AND AIR-DRAG EFFECTS ON THE ORBIT OF THE BALLOON SATELLITE

1963 30D

JACK W. SLOWEY

(NASA-CR-136794) RADIATION PRESSURE AND
AIR DRAG EFFECTS ON THE ORBIT OF THE
BALLOON SATELLITE 1963 30D (Smithsonian
Astrophysical Observatory)

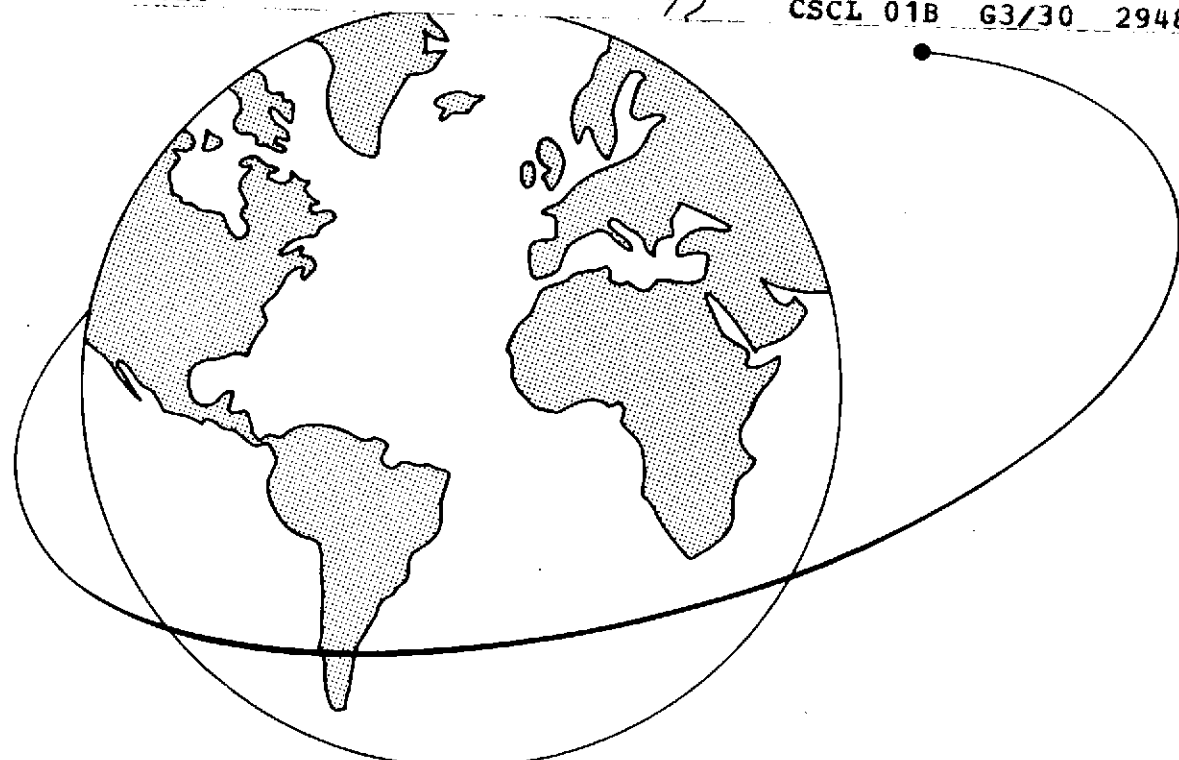
\$7.25

102 p HC
92

CSCL 01B G3/30

N74-16542

Unclassified
29483



Smithsonian Astrophysical Observatory
SPECIAL REPORT 356

Research in Space Science
SAO Special Report No. 356

RADIATION-PRESSURE AND AIR-DRAG EFFECTS ON THE ORBIT
OF THE BALLOON SATELLITE 1963 30D

Jack W. Slowey

January 18, 1974

Smithsonian Institution
Astrophysical Observatory
Cambridge, Massachusetts 02138

TABLE OF CONTENTS

	<u>Page</u>
ABSTRACT	vii
1 INTRODUCTION	1
2 ORBITS	3
3 RADIATION-PRESSURE EFFECTS	9
4 AIR-DRAG EFFECTS	27
5 AN ISOLATED EVENT	37
6 ACKNOWLEDGMENTS	39
7 REFERENCES	41

PRECEDING PAGE BLANK NOT FILMED

PRECEDING PAGE BLANK NOT FILMED

ILLUSTRATIONS

	<u>Page</u>
1 Perigee heights of 1963 30D calculated from orbits determined in the interval MJD 38396–38852	5
2 Perigee heights and the smoothed effective height of 1963 30D in the interval MJD 40230–41054	6
3 Observed and computed values of the orbital eccentricity of 1963 30D in the interval MJD 40230–41000	11
4 Observed and computed values of the orbital inclination of 1963 30D corresponding to the values of the eccentricity shown in Figure 3	12
5 Observed and computed values of the orbital acceleration of 1963 30D in the interval MJD 38470–38560	14
6 Curves showing the magnitude, relative to the total magnitude, of the right-angle component of the force of radiation pressure on a prolate spheroid as a function of the angle of incidence	16
7 Observed and computed values of the orbital acceleration of 1963 30D in the interval MJD 40230–40790	17
8 Observed and computed values of the difference from a reference integration of the derivatives of the eccentricity of 1963 30D in the interval MJD 38397–38849	20
9 Observed values and values computed by numerical integration of the orbital eccentricity of 1963 30D in the interval MJD 38396– 38850	22
10 Observed values and values computed by numerical integration of the orbital inclination of 1963 30D corresponding to the values of the eccentricity shown in Figure 9	23
11 Observed and computed values of the orbital acceleration of 1963 30D in the interval MJD 38470–38560	24
12 Densities obtained from atmospheric drag on 1963 30D in the inter- val MJD 38402–38814, during periods when the orbit was entirely in sunlight	30
13 Derived and computed densities in the intervals MJD 40237–40305 and MJD 40405–40465	32
14 Derived and computed densities in the intervals MJD 40560–40609 and MJD 40710–40770	33
15 Derived and computed densities in the interval MJD 40850–41046 . .	35
16 Residuals in mean anomaly of individual observations of 1963 30D in the vicinity of MJD 38409	38

TABLES

	<u>Page</u>
1 Orbital elements of 1963 30D in the interval MJD 38396–38852	43
2 Orbital elements of 1963 30D in the interval MJD 40230–41054	49
3 Accelerations, atmospheric densities, atmospheric temperatures, and geometric parameters from 1963 30D in the interval MJD 38397.00–38814.00	59
4 Accelerations, atmospheric densities, atmospheric temperatures, and geometric parameters from 1963 30D in the interval MJD 40237.00–41045.80	67
5 Standard heights to which densities in Tables 3 and 4 are referred ..	93

ABSTRACT

Computed orbits of the balloon satellite 1963 30D are given every 2 days over an interval of 456 days near the beginning of the satellite's lifetime and an interval of 824 days near the end of its lifetime. The effects of radiation pressure on the satellite are examined in some detail. It is found that the variations in all the elements can be represented by use of a single parameter to specify the effect of diffuse reflection from the satellite's surface, and that this parameter remains constant, or nearly so, during the entire 7-year lifetime. Success in obtaining a consistent representation of the radiation-pressure effects is ascribed to the inclusion of the effects of terrestrial radiation pressure, using a model for the earth's albedo that includes seasonal and latitudinal variations. "Anomalous" effects in the orbital acceleration, as well as in the other elements, are represented quite well by including a small force at right angles to the solar direction and by allowing this to rotate about the solar direction. This implies that the satellite is aspherical, that it is rotating, and that the axis of rotation precesses. While the period of precession decreases considerably over the lifetime, the magnitude of the right-angle force remains essentially constant at about 3% of the total force. The effects of atmospheric drag are also examined, and atmospheric densities are derived in several intervals and compared with the J71 model atmosphere. Intervals are included where hydrogen is expected to be the dominant constituent and where helium is expected to be dominant. A revised model of the hydrogen concentration is given for use with the J71 model. Densities indicative of helium are in good agreement with the model, as are densities obtained near the end of the lifetime. The densities near the end vary by about 2.5 orders of magnitude, since the satellite's perigee traverses over 400 km in height in about 200 days; the total range of the density data is over 5.5 orders of magnitude, since the effective height of the density determinations goes from over 3600 km near the beginning to about 360 km near the end of the lifetime.

RESUME

On donne les orbites calculées du satellite-ballon 1963 30D, tous les deux jours pour une période de 456 jours au début de la vie du satellite, et pour une période de 824 jours en fin de vie. On examine de façon assez détaillée les effets de la pression de radiation. On trouve que les variations de tous les éléments peuvent être représentées par un seul paramètre spécifiant l'effet de la réflexion diffuse de la surface du satellite et que ce paramètre reste constant -ou presque- durant la totalité des sept années de vie du satellite. On attribue cette réussite que constitue l'obtention d'une représentation stable des effets de la pression de radiation au fait que l'on a inclus les effets de la pression de radiation terrestre, à l'aide d'un modèle de l'albédo de la terre comportant les variations saisonnières et latitudinales. Les effets "anomaux" de l'accélération orbitale et des autres éléments sont assez bien représentés lorsque l'on inclut une force faible à angles droits par rapport à la direction solaire et que l'on fait tourner le tout autour de la direction solaire. Cela implique que le satellite est asphérique, qu'il tourne et que l'axe de rotation est soumis à une précession. Alors que la période de précession diminue considérablement au cours de la vie du satellite, l'importance de la force à angle droit reste essentiellement constante à 3% de la force totale. On examine également les effets de traînée atmosphérique, on déduit les densités atmosphériques pour diverses périodes et on les compare à l'atmosphère modèle J 71. On y inclut des périodes où l'hydrogène est supposé être l'élément constitutif dominant, et d'autre où c'est l'hélium. On donne un modèle révisé de la concentration en hydrogène à utiliser avec le modèle J 71. Les densités indiquant l'hélium correspondent bien au modèle; il en est de même pour les densités obtenues en fin de vie. Ces dernières varient d'environ 2,5 ordres de grandeur, car le périgée du satellite parcourt plus de 400 km de hauteur en 200 jours environ; l'éventail complet des données de densités couvre plus de 5,5 ordres de grandeur, car la hauteur effective des densités déterminées va de plus de 3 600 km en début de vie à environ 360 km en fin de vie.

КОНСПЕКТ

Высчитанные орбиты воздушных шаров-спутников 1963 300 даются каждых два дня за период времени в 456 дней в начале жизни спутника и за период времени в 824 дня вблизи конца его жизни. Рассматриваются довольно подробно влияния давления радиации на спутник. Было найдено что изменения во всех элементах могут быть представлены употребляя единственный параметр для характеристики влияния рассеянного отражения от площади спутника и что этот параметр остается постоянным, или почти-что в течение всей 7 летней жизни. Успех получения совместимого представления влияний давления радиации приписывается включению влияний земного давления радиации, употребляя модель земной альбедо которая включает сезонные и широтные изменения. "Аномальные" влияния на орбитное ускорение, также как и на другие элементы, довольно хорошо представляются включением малой силы под прямыми углами к солнечному направлению и позволяя этой силе вращаться вокруг солнечного направления. Это подразумевает что спутник является несферическим, что он вращается и что ось вращения прецессирует. В то время как период прецессии значительно уменьшается за время жизни, величина перпендикулярной силы остается в среднем постоянной, в 3% общей силы. Также рассматриваются влияния атмосферного драга и атмосферные плотности выводятся в нескольких промежутках и сравниваются с моделью атмосферы J71. Включаются промежутки где водород ожидается как преобладающая составная часть и где гелий ожидается преобладающим. Пересмотренная модель концентрации гелия дается для употребления с моделью J71. Плотности указывающие гелий, хорошо согласуются с моделью, также как и плотности полученные вблизи конца жизни. Плотности в конце жизни изменяются на 2,5 порядков величины, так как перигей спутника проходит на высоте больше 400 км за приблизительно 200 дней; общая область данных о плотности, простирается на 5,5 порядков величины так как эффективная высота определений плотности простирается от более чем 3600 км вблизи начала, до приблизительно 360 км вблизи конца жизни.

RADIATION-PRESSURE AND AIR-DRAG EFFECTS ON THE ORBIT
OF THE BALLOON SATELLITE 1963 30D

Jack W. Slowey

1. INTRODUCTION

The satellite 1963 30D (Dash 2) was launched on July 19, 1963, into an orbit that was nearly circular at a height of about 3700 km above the earth's surface and that had an inclination of $88^\circ 4'$ to the earth's equator. It was a balloon of about 2.4-m diameter and, because of its large area/mass ratio and the circumstances of its orbit, was strongly perturbed by solar radiation pressure. A commensurability of the motion of perigee and of the orbital plane with respect to the sun was of particular consequence. This caused the eccentricity of the orbit to increase continuously throughout most of the satellite's lifetime with an attendant continuous decrease in the height of perigee. By early April of 1971, just before rapid descent began under the influence of atmospheric drag, the height of perigee had been reduced to about 300 km, owing mainly to the effect of solar radiation pressure. The eccentricity had reached a maximum of 0.30 just 2 months earlier.

The satellite is interesting for several reasons. Until the last year or so of the lifetime, the effects of direct solar radiation pressure can be studied under conditions where atmospheric drag was a relatively minor consideration. The effect of terrestrial radiation pressure on the semimajor axis of the orbit can also be studied during a large portion of the lifetime before the last year or so. When the orbit lies entirely in sunlight so that the effect of direct radiation pressure on the semimajor axis vanishes, this effect, which is comparable in magnitude to that of atmospheric drag in this

This work was supported in part by grant NGR 09-015-002 from the National Aeronautics and Space Administration.

interval, can be clearly discerned in the observed accelerations. Finally, the atmospheric drag on the satellite can be used to determine densities in the vicinity of perigee as perigee moves through a tremendous range in height. The relative uncertainty in the contribution of direct radiation pressure to the acceleration does, however, limit such determinations to times when the contribution of direct radiation pressure vanishes or is relatively small.

2. ORBITS

Orbits of 1963 30D were determined in two intervals, one near the beginning of the lifetime and the other near the end. The orbits near the beginning cover an interval of 456 days, from January 2, 1964, to April 2, 1965, and were computed from precisely reduced Baker-Nunn observations. An accuracy of 4 arcsec was assumed for these observations, although it is actually somewhat better than that. The orbits near the end cover an interval of 824 days, from January 9, 1969, to April 13, 1971, and were computed from radar observations obtained from the U.S. Air Force. The ranges given by the observations used are considerably more accurate, relatively, than are the angular positions. The ranges were assumed to have an accuracy of 0.2 km. Biases determined by the Air Force for each observing station were applied to the observations before orbit determination. Orbits were determined at epochs 2 days apart in both intervals by using, in each case, observations within either 2 or 4 days on either side of the epoch. The shorter time span was used throughout except in the early portion of the end interval, where the number of observations was generally low. The SAO Differential Orbit Improvement (DOI) program was employed for the orbit determinations.

The orbits in the beginning and the end intervals are tabulated in Tables 1 and 2, respectively. The epoch, reckoned in Modified Julian Days ($MJD = JD - 2,400,000.5$), appears in the first column of these tables. The six columns following the epoch contain, in order, the argument of perigee ω , the right ascension of the ascending node Ω , the inclination i , the eccentricity e , the mean anomaly M , and the anomalistic mean motion n . With the exception of the mean anomaly, the angular elements are expressed in degrees. The mean anomaly is expressed in revolutions and the mean motion in revolutions per day. The single digit one space to the right of each element is the standard error in that element and refers to the last digit given. The next column contains a number, in floating-point form, that is one-half of n , the time derivative of the mean motion as determined by DOI, together with the standard error in the last two digits given. The next column contains the semimajor axis a , expressed

in megameters, as computed from the given value of the mean motion. The last three columns contain, in order, the number of observations N used in the orbit determination, the total number of days D from which observations were used, and the mean standard error σ of the observations relative to their assumed accuracy.

The tabulated orbital elements are mean elements in the sense that the short-period perturbations due to the earth's oblateness have been eliminated. In the case of the elements in Table 1, which were obtained from precisely reduced Baker-Nunn observations, perturbations due to the moon and to the tesseral harmonics in the earth's potential have also been eliminated. The lunar perturbations were computed from the expressions in an appendix of the description of the DOI program written by Gaposchkin (1964). The tesseral-harmonic perturbations were computed from the expressions derived by Kaula (1966), with the use of the L3 set of tesseral-harmonic coefficients determined by Gaposchkin (1966).

Some other facts should be mentioned concerning the element tabulations. One is that the small contribution of radiation pressure to the apparent mean motion was not allowed for in computing the tabulated values of the semimajor axis. The resulting error in the semimajor axis (Slowey, 1969) can amount to several kilometers for this satellite. The effect of radiation pressure was, however, taken into account internally in the computation of the semimajor axis during orbit determination, so that no error from this source was introduced in the directly determined elements that are tabulated. Also, the angular position and the range portions of each of the radar observations used in determining the orbits in Table 2 were treated as independent observations. The ranges, which dominate the orbit determinations because of their greater accuracy, constitute only roughly one-half the values given by N in Table 2. In this regard, we must also keep in mind that a range is only one independent quantity, while an angular-position observation consists of two independent quantities.

The heights of perigee above the geoid obtained from the orbits in Tables 1 and 2 are plotted in Figures 1 and 2, respectively. I have also plotted in Figure 2 the smoothed effective height as a function of time. The effective height is the average of the height around the orbit weighted by the local atmospheric drag. It was computed

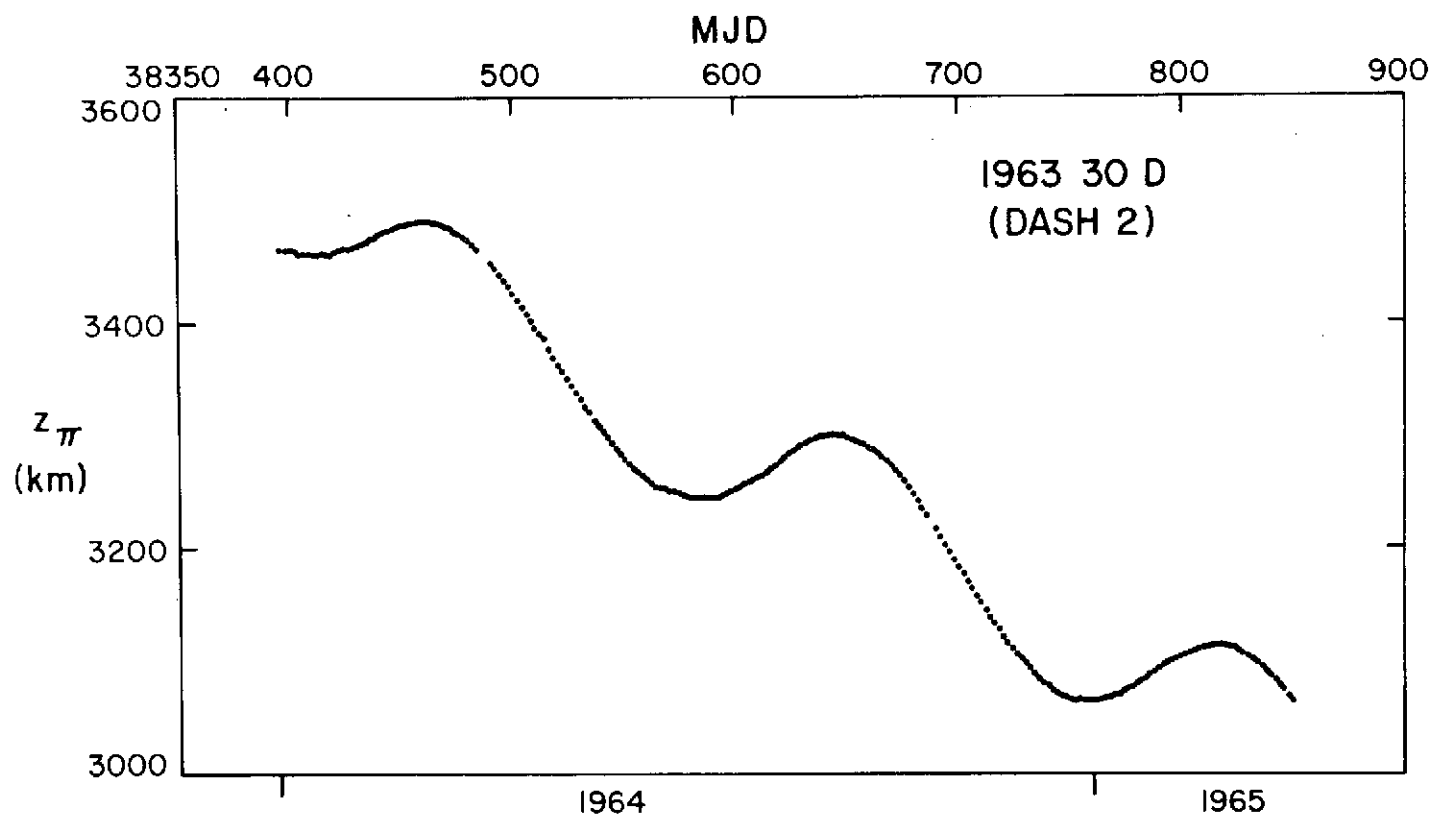


Figure 1. Perigee heights of 1963 30D calculated from orbits determined in the interval MJD 38396–38852.

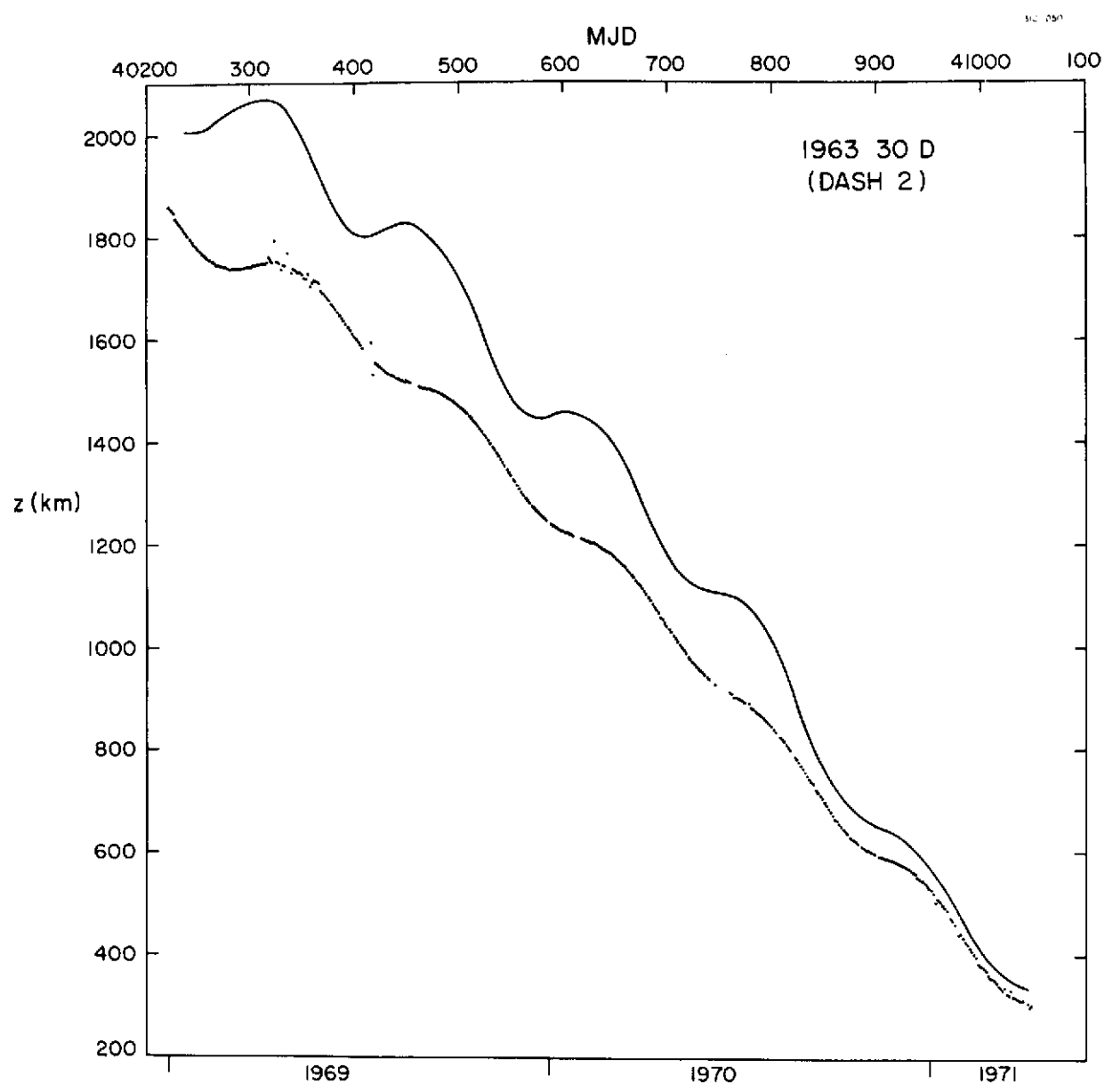


Figure 2. Perigee heights (points) and the smoothed effective height (smooth curve) of 1963 30D in the interval MJD 40230–41054.

at regular intervals by using the same atmospheric model that was used to compute densities from the observed accelerations. Since the individual points contain short-term fluctuations due to fluctuations in the density scale height of the atmosphere, the points were smoothed and a continuous curve was drawn.

3. RADIATION-PRESSURE EFFECTS

The effects of radiation pressure on the orbit of Dash 2 were studied in both the beginning interval and the earlier portion of the end interval. For this purpose, I employed a computer program that numerically integrates the Lagrangian equations of motion; this program includes both the perturbations due to direct solar radiation pressure and those due to terrestrial radiation pressure. The Gaussian form of the equations, in which the right-hand sides are functions of the components of force, are used for these perturbations. The program also includes perturbations due to the zonal harmonics in the earth's gravitational potential, air drag, and lunar and solar gravity.

Since the numerical-integration program does not deal with short-periodic perturbations, it is necessary in some cases to integrate the perturbations over one revolution to obtain the average long-term contributions to the derivatives at the time in question. In the case of direct solar radiation pressure, this integration is done analytically (Kozai, 1961), although the limits of integration, i.e., the shadow entry and exit points, must be determined numerically in each particular instance. In the case of terrestrial radiation pressure, the integration over one revolution can be done both easily and accurately only by numerical means, even with the simplest model of the terrestrial radiation. Therefore, the program does the integration by numerical quadrature, and also does a two-dimensional numerical quadrature over the visible cap of the earth at each point within the integration, in order to determine the components of force. This procedure is obviously rather expensive in terms of computing time, but it avoids the crude approximations that would otherwise be necessary and permits complete freedom in modeling the terrestrial radiation.

An area-to-mass ratio A/m of $37.9 \text{ cm}^2 \text{ g}^{-1}$ was used in all the computations. The area-to-mass ratio determined from published values of the expected in-orbit mass and diameter of the satellite is $40.2 \text{ cm}^2 \text{ g}^{-1}$. However, if this value is applied to the observed drag near the end of the lifetime, when the effective height is between

720 and 360 km, the resulting densities are systematically smaller than the corresponding densities given by the J71 model (Jacchia, 1971). Since the model is believed to be quite good in this height range, and since the satellite seems to have assumed a slightly aspherical shape, I have chosen the value $A/m = 37.9 \text{ cm}^2 \text{ g}^{-1}$ in order to give agreement with the model.

The exact value of A/m is not important as far as radiation-pressure effects are concerned. The area-to-mass ratio must be multiplied by a factor s to account for the nature of the light reflection from the satellite's surface. This factor is usually taken as unity when the total force is equal only to the force of the radiation stopped by the cross section of the satellite, as is the case for a sphere. However, s is usually slightly greater than unity, owing to a diffuse component in the reflected radiation that yields an added contribution to the force in the direction opposite the sun. If s is determined from observed variations in the orbital elements, any error in the assumed area-to-mass ratio will be absorbed in s .

I determined s for 1963 30D to be 1.120 by fitting the observed variations in the eccentricity in the interval MJD 40310–40500 by trial and error, using the integration program mentioned above. The solar constant was assumed to be $2.000 \text{ cal cm}^{-2} \text{ min}^{-1}$. Had I retained $A/m = 40.2 \text{ cm}^2 \text{ g}^{-1}$, the corresponding value of s would have been 1.056. The eccentricity was used for determining s because the error in s is least in this case. Although no attempt was made to combine the results, values of s obtained from the inclination, argument of perigee, and ascending node over the same interval agreed with the value from the eccentricity within the estimated errors of those values. This kind of agreement has not been found by others, as far as I know. The single value of the product $s \cdot A/m = 42.4 \text{ cm}^2 \text{ g}^{-1}$ given here compares, for example, with values of 41.0 and $38.0 \text{ cm}^2 \text{ g}^{-1}$ reported by Fea and Smith (1970) as the "best average" values to fit variations in the eccentricity and inclination, respectively, during the early lifetime of 1963 30D. I suspect the difference is due to the way terrestrial radiation pressure was included in the computations.

Numerical integration, starting from the observed elements as given by a least-squares fit, was carried out in the interval MJD 40230–41000 with $A/m = 37.9$ and $s = 1.120$. This includes all but 50 days or so at the very last of the end interval. The results from the integration are plotted as a smooth curve, together with the observed values, for the eccentricity and the inclination in Figures 3 and 4, respectively.

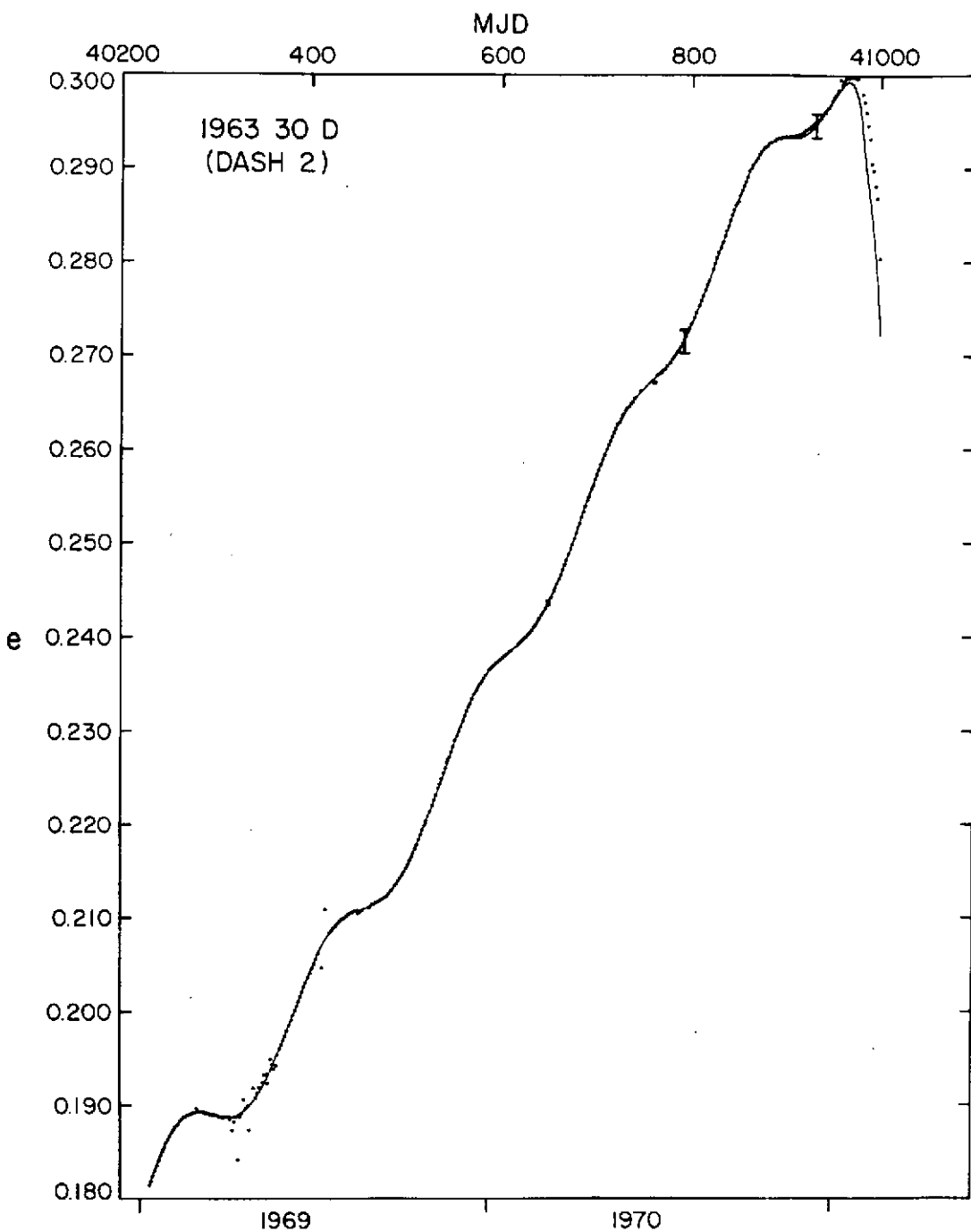


Figure 3. Observed (points) and computed (smooth curve) values of the orbital eccentricity of 1963 30D in the interval MJD 40230–41000. The computed values were obtained by numerical integration, starting from fitted values of the mean elements and taking $s = 1.120$ with $A/m = 37.9 \text{ cm}^2 \text{ g}^{-1}$. Tick marks indicate points at which the integration was restarted. Computed values of the perturbations due to the zonal harmonics in the earth's potential have been subtracted from both the observed and the computed values.

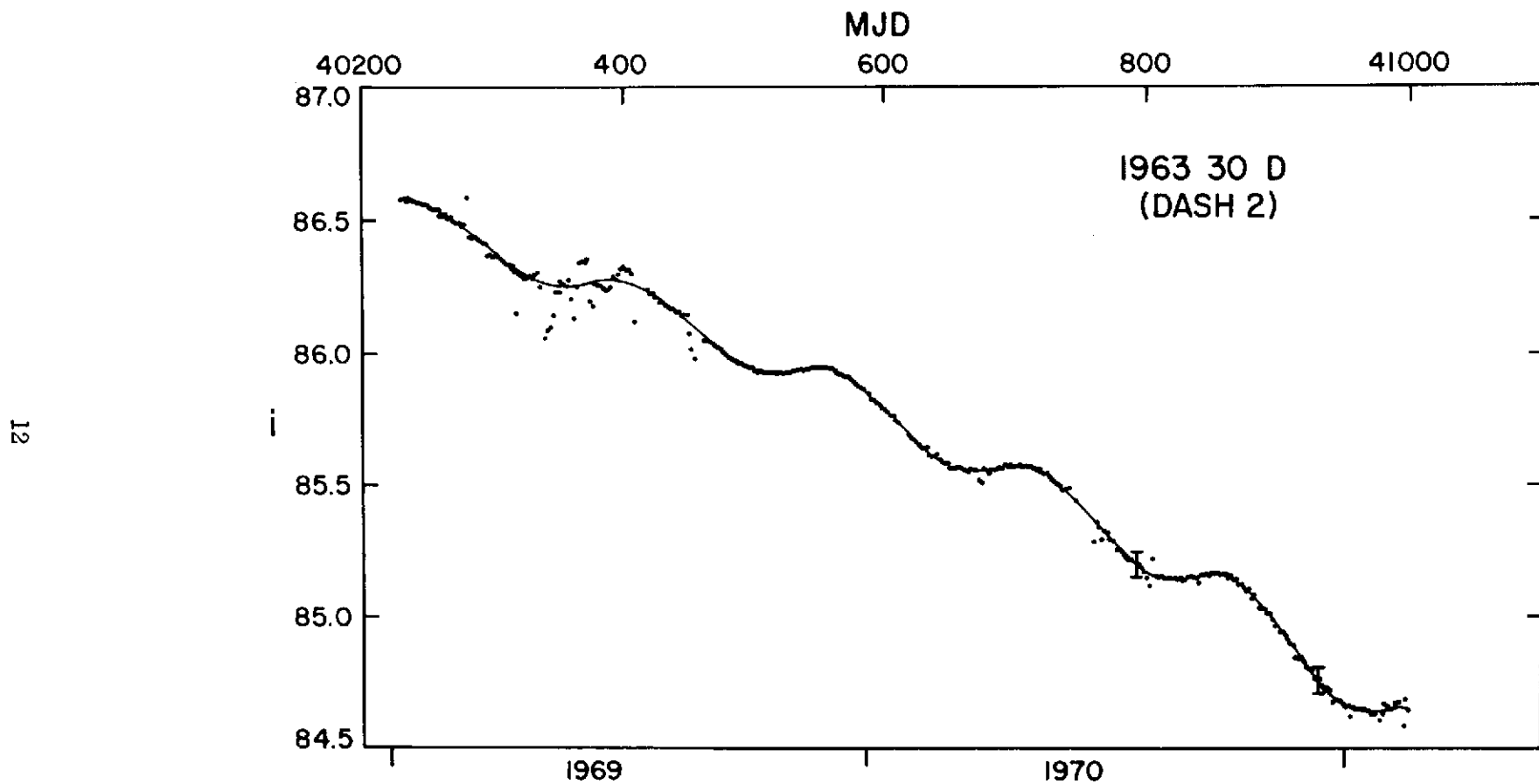


Figure 4. Observed (points) and computed (smooth curve) values of the orbital inclination of 1963 30D corresponding to the values of the eccentricity shown in Figure 3. Perturbations due to the zonal harmonics have been subtracted.

The integrated long-periodic perturbations due to the zonal harmonics have been subtracted from both the integrated elements and the elements from Table 2. I used the set of coefficients to degree 14 that Kozai (1964) determined. Tick marks on the plots indicate the points at which the integration was restarted from the observed elements. As can be seen, the changes at the first tick mark, just before atmospheric drag becomes strong, are not really perceptible at the scales on which the plots are drawn. The differences at this point are only slightly greater than the standard errors of the observed elements. This is also true for the argument of perigee and the ascending node. In particular, the value of s that was used can be seen to represent the variation in the eccentricity to about 1 part in 1000. The integration becomes much less satisfactory near the end of the lifetime, but this is clearly due to small imperfections in the atmospheric model. Had the drag effects remained small, there is little doubt that I could have represented the variations in all the elements satisfactorily over a still longer period of time using a single value of s .

Before going further, an effect that was included in the integration mentioned above should be discussed. The orbital acceleration, or time rate of change of the period, of 1963 30D exhibits features that were something of a mystery for a very long time (Fea, 1967, 1970). These features can be seen in Figure 5, where we have plotted values of the acceleration from an interval in the beginning section when the orbit is partly in shadow. The closed circles in the upper strip of the figure are the observed values determined from the orbital behavior of the satellite. The smooth curve in the lower strip represents the result computed with the integration program, on the assumption that the satellite is spherical, i.e., that the force of direct radiation pressure is in the direction exactly opposite that to the sun. I used $s = 1.068$ with $A/m = 37.9$ for this computation, but it is clear that no constant values for these parameters could reproduce the large-amplitude waves in the observed acceleration. It is possible, however, to represent the observed accelerations quite well by introducing a very small component of force at right angles to the solar direction and allowing this component to rotate with time. This is what was done to obtain the smooth curve plotted in the upper strip of Figure 5.

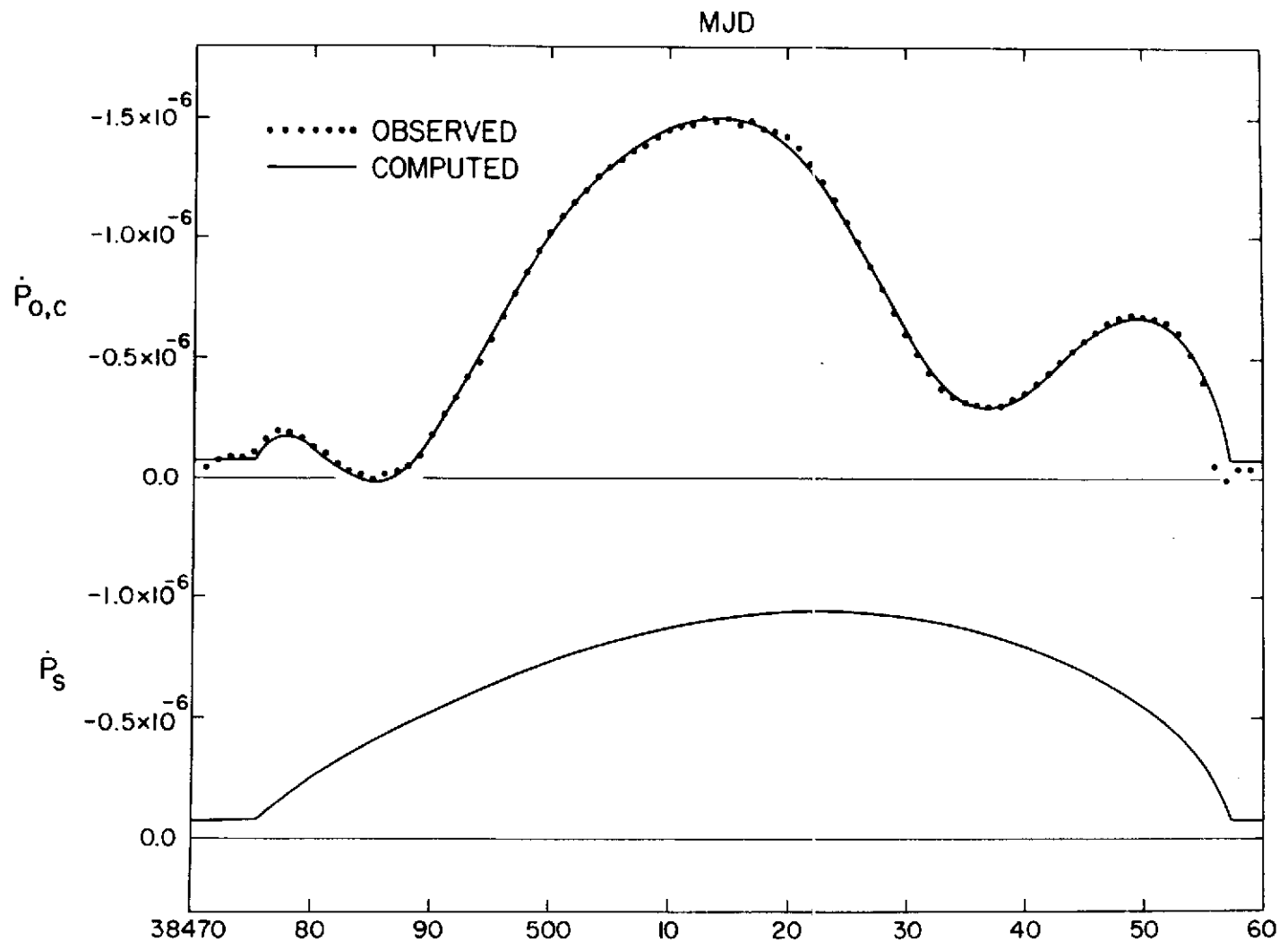


Figure 5. Observed and computed values of the orbital acceleration of 1963 30D in the interval MJD 38470–38560 are shown in the upper strip. The computed values include the effect of a small component of force due to radiation pressure at right angles to the solar direction. The orbital acceleration that would be expected in the absence of the right-angle component is shown in the lower strip.

What appears to be the explanation of the behavior of 1963 30D came from photometric studies of the Pageos satellite (Vanderburgh and Kissell, 1971), which shows "anomalous" accelerations (Fea, 1970) similar to those of 1963 30D. It was discovered that Pageos had apparently assumed a slightly prolate shape, that it was spinning rapidly about a minor axis, and that this spin axis was precessing about the solar direction. Smith and Kissell (1972) were then able to supply a suitable explanation of the accelerations of Pageos.

Reflection from a spheroid does, of course, produce a component of force at right angles to the incident direction, as long as this is not parallel to a symmetry axis of the figure. The magnitude of this force, relative to the total force, is plotted in Figure 6 for a prolate spheroid for various values of the ratio of the minor axes to the major axis. The magnitude in the figure is given as a function of the angle between the incident direction and the plane of the minor axes. A formulation based on that of Carmeli (1972) was used to compute the plotted data. For a spinning satellite, it is necessary to integrate over a complete rotation of the satellite to obtain the average right-angle force vector. The figure should, however, give some idea of how the force is related to the degree of asphericity of the satellite.

In the routine used by the integration program to compute the derivatives due to direct solar radiation pressure, I have introduced a component of force in the plane perpendicular to the solar direction. The magnitude and direction of this force are supplied externally. The direction is specified in terms of the phase angle, which is measured counterclockwise in the plane as seen from the sun, starting from the north pole of the ecliptic. Trial-and-error adjustment of the magnitude and of the phase relation proved rather successful in representing the effects observed in 1963 30D.

Orbital accelerations of 1963 30D in the end interval, up to the last 250 days or so, are plotted in Figure 7. The upper strip shows the observed values of the acceleration. The large "bumps" in the acceleration, occurring at intervals of about 150 days, are due to direct radiation pressure when the orbit is partly in shadow. We ascribe the superimposed oscillations to the right-angle component of force; the period of these oscillations is considerably shorter here than in the beginning interval. The effect of both components vanishes in the intervening intervals, when the orbit is entirely in

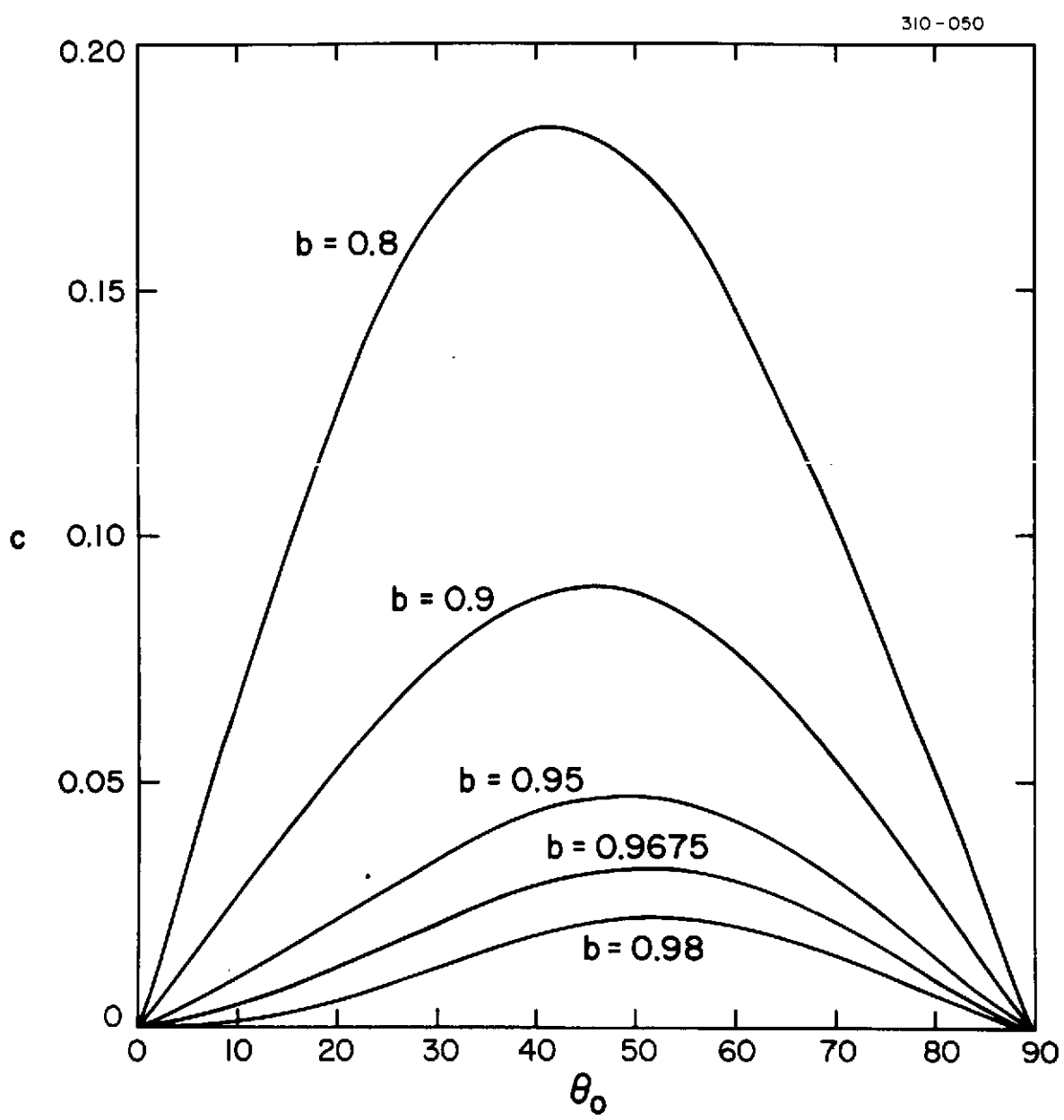


Figure 6. Curves showing the magnitude c , relative to the total magnitude, of the right-angle component of the force of radiation pressure on a prolate spheroid as a function of the angle of incidence θ_0 . The curves are drawn for various values of the ratio b of the minor axes to the major axis.

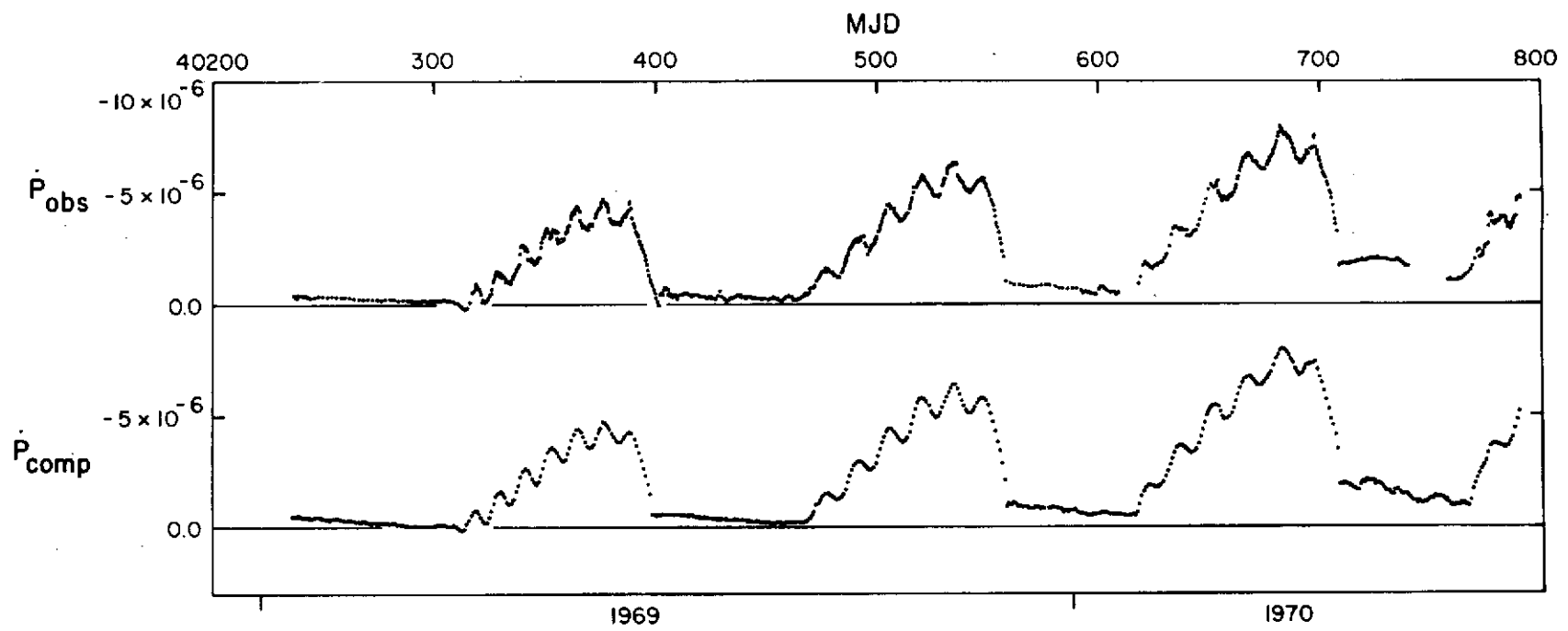


Figure 7. Observed (upper strip) and computed (lower strip) values of the orbital acceleration of 1963 30D in the interval MJD 40230–40790. The computed values include the effect of a rotating right-angle component of force due to radiation pressure that has a magnitude of 0.030 relative to the total force.

sunlight. The acceleration in those intervals is due to atmospheric drag and terrestrial radiation pressure. In the lower strip of the figure, I have plotted values of the acceleration computed by the integration program. As can be seen, agreement with the observed values is excellent in every respect. The magnitude c of the right-angle component of force was taken as 0.030 relative to the total force throughout this integration, although a slightly larger value would probably have been a better choice. The phase angle θ was specified as a function of time t by

$$\theta = 100^\circ + 33^\circ 30(t - t_0) - 0^\circ 034426(t - t_0)^2 + 0^\circ 3953E-4(t - t_0)^3 ,$$

$$t_0 = 40310.0 ,$$

in the interval MJD 40230–40650, and by

$$\theta = 300^\circ + 25^\circ 26(t - t_0) - 0^\circ 018615(t - t_0)^2 + 0^\circ 4747E-4(t - t_0)^3 ,$$

$$t_0 = 40510.0 ,$$

in the interval MJD 40650–40790.

The right-angle component has an effect on the other orbital elements even when the orbit is entirely in sunlight. It is doubtful that any of these could have been reliably detected in the end interval, however, and no attempts at detection were undertaken. Therefore, no claim is made for the above phase equations outside the intervals when the orbit is partly in shadow, even though the right-angle component as specified by the above phase equations was included throughout the integration.

It may come as something of a surprise that the observed effect on the acceleration can be explained by a right-angle component having such a relatively small amplitude. This is because it acts predominantly in one direction, either to increase or to decrease the semimajor axis, over the exposed portion of the orbit, while the portion of the orbit that would otherwise provide a balance is mostly in shadow. In the case of the in-line component, on the other hand, the intrusion of the shadow does little to upset

the symmetry that prevails when the orbit is fully in sunlight. It is only the imbalance introduced by the eccentricity of the orbit, with perigee off-center with respect to the sun, that produces any net effect at all. A similar argument can be made concerning the importance of the transverse component of radiation reflected from the earth as opposed to the radial component in the case of terrestrial radiation pressure.

I did attempt to detect the effect of the right-angle component on one of the other elements, the eccentricity, in the beginning interval. This was done in two steps: First, I took differences in the observed values of the eccentricity to obtain values of the derivative with respect to time. Then I subtracted reference values of the derivative, which were obtained by differencing the results of a numerical integration that included all the perturbations except that due to the right-angle component. The difference, representing the observed contribution to the derivative of perturbations not included in the integration, is plotted in the upper strip of Figure 8. As can be seen, there are clearly defined oscillations when the orbit is entirely in sunlight, although little information can be gained when the orbit is partly in shadow, owing to a degradation in the accuracy of the elements in these intervals. This loss of accuracy probably results mainly from a failure to include the short-periodic variations in the mean anomaly due to radiation pressure when computing orbits. In the lower strip of Figure 8, I have plotted the differences, from the same reference integration, in the derivatives of the eccentricity of an integration that included the right-angle component. This integration was made with $c = 0.032$ and the phase given by

$$\theta = 190^\circ 8 + 8^\circ 193(t - t_0) - 0^\circ 12044E^{-2}(t - t_0)^2 + 0^\circ 16227E^{-4}(t - t_0)^3 ,$$

$$t_0 = 38464^\circ 0 ,$$

and obviously yields derivatives that are in good agreement with the observed values. The fact that c turns out to be essentially identical to the value found in the end interval, as much as 6 1/2 years later, is rather striking.

The above integration, made with $s = 1.120$, did, however, show a small systematic departure from the observed elements. For the most part, this could be corrected by using a slightly smaller value of s . Another integration was, therefore, performed with $s = 1.105$. Values of the eccentricity and the inclination from this integration are plotted

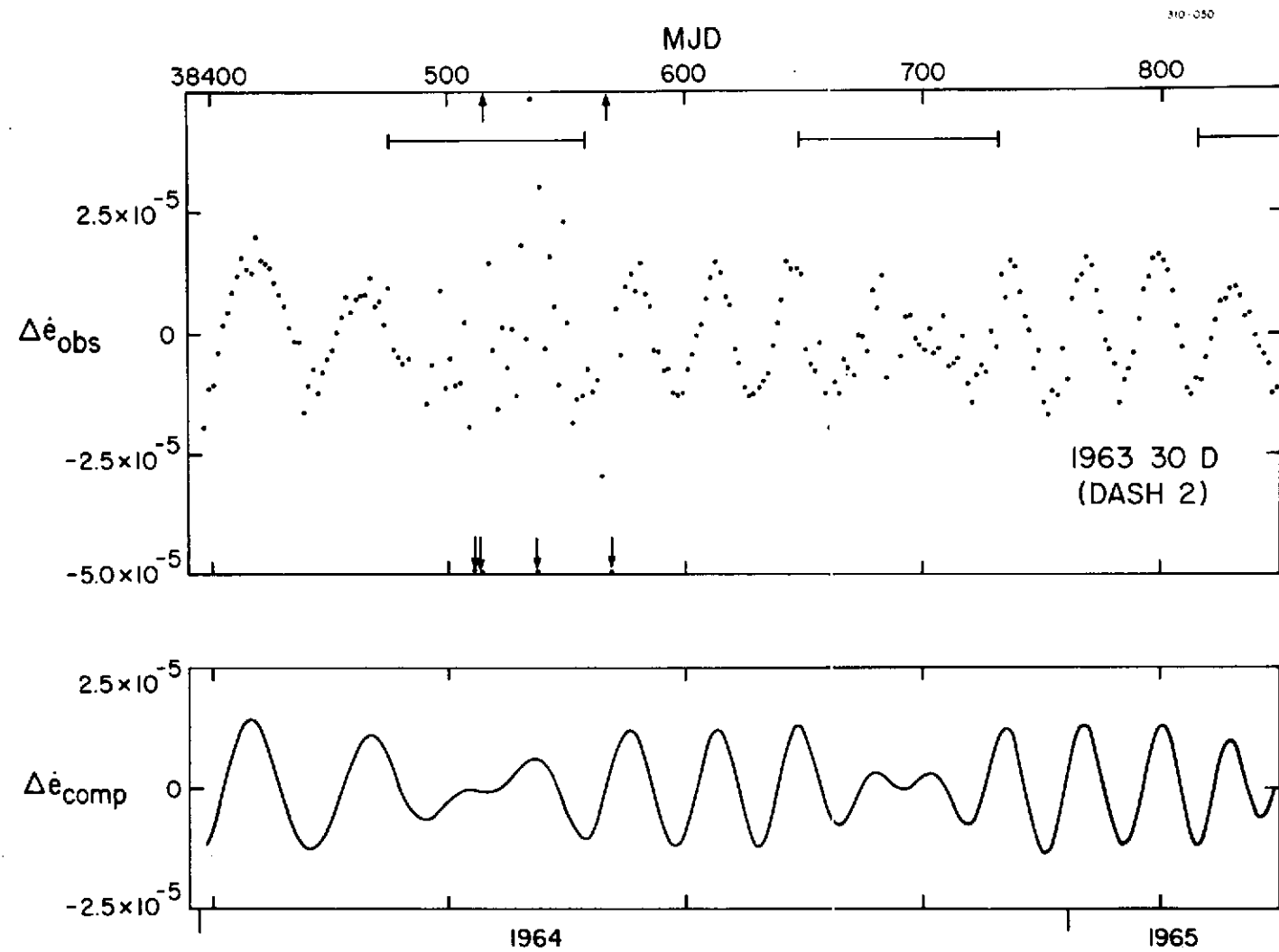


Figure 8. Observed (upper strip) and computed (lower strip) values of the difference from a reference integration of the derivatives of the eccentricity of 1963 30D in the interval MJD 38397–38849. The computed values represent entirely the effect of a right-angle component of the force of radiation pressure having a magnitude of 0.032 of the total force. Bars in the upper strip indicate periods when the orbit was partly in shadow.

as smooth curves, together with the observed values, in Figures 9 and 10, respectively. The integrated long-period perturbations due to the zonal harmonics have again been subtracted from both the computed and the observed values, as in Figures 3 and 4. Tick marks again indicate points at which the integration was restarted from fitted values of the observed elements. All things considered, agreement between the observed and the computed values is quite good. The slightly smaller value of s found here possibly indicates a slow increase with time due to deterioration of the satellite's surface.

I then looked at the accelerations during the interval MJD 38470–38560, the first interval when the orbit was partly in shadow. It quickly became obvious that the phase of the right-angle component departed somewhat from the equation derived from the eccentricity outside of shadow. To find the phase from the acceleration, I first determined s and c to fit the maxima and minima of the observed acceleration. The values were $s = 1.068$ and $c = 0.034$. The phase relation

$$\theta = 267^\circ.1 + 7^\circ.05(t - t_0) + 23^\circ.7 \sin [253^\circ.5 + 7^\circ.248(t - t_0)] ,$$

$$t_0 = 38470.0 ,$$

was then obtained from a least-squares fit of phase values determined at various points by trial and error. The acceleration, computed by using this equation and the values of s and c above, is plotted as a smooth curve in the upper strip of Figure 5. It is in almost perfect agreement with the observed acceleration. However, while the value of c that was used is probably acceptable, the value of s used is really not compatible with the variations in the other elements. In Figure 11, I again show the observed accelerations in this interval, but I compare them with the result of an integration made with the phase relation above and with $s = 1.105$ and $c = 0.032$. Agreement is not quite so good as in Figure 5, but is within the uncertainty associated with the computed contribution of atmospheric drag to the acceleration at this height. Actually, the agreement would have been about as good as that in Figure 5 had I reduced the density over the pole in the way the drag data from this satellite would appear to require.

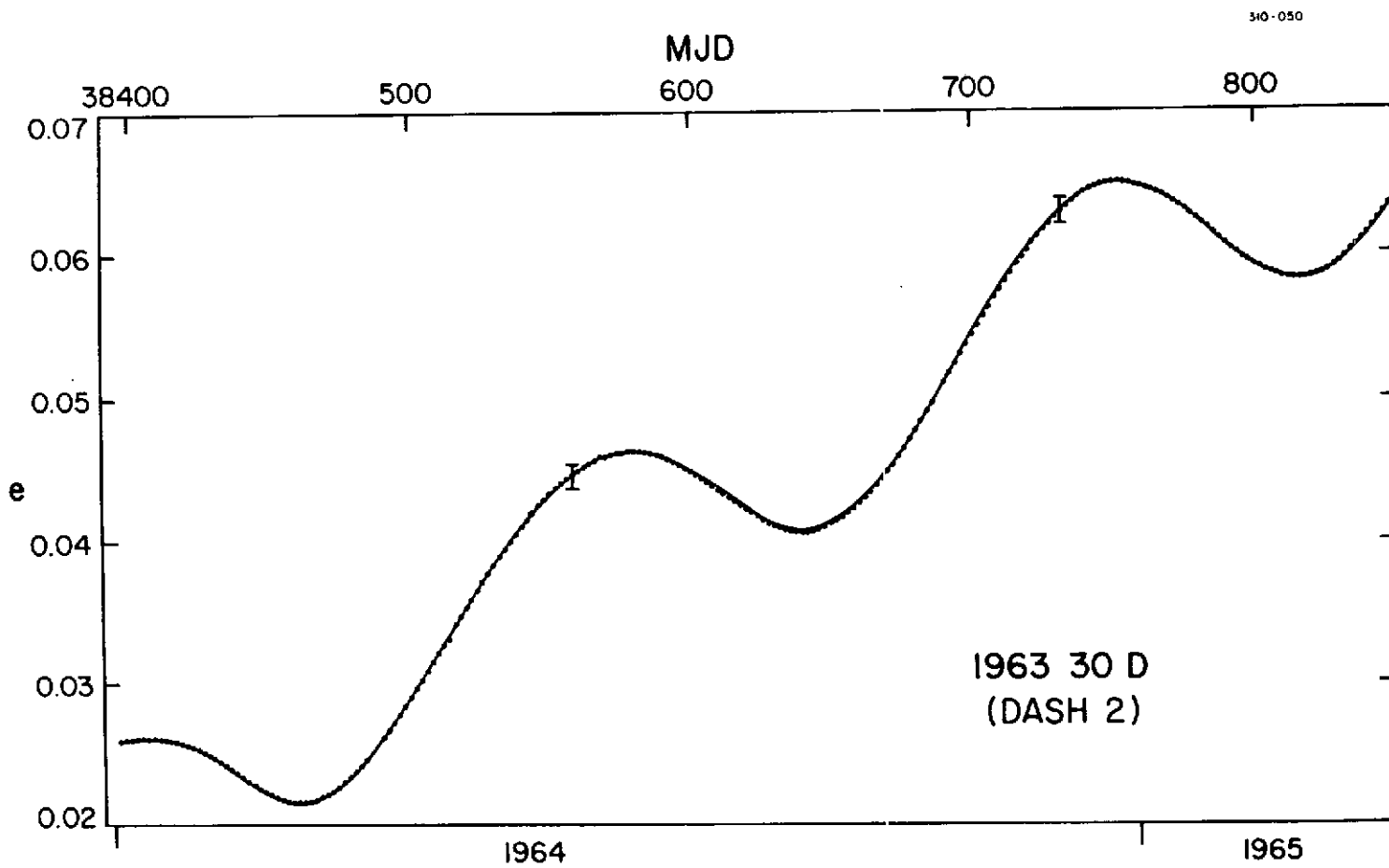


Figure 9. Observed values (points) and values computed by numerical integration (smooth curve), with $s = 1.105$ and $c = 0.032$, of the orbital eccentricity of 1963 30D in the interval MJD 38396–38850. Tick marks indicate points at which the integration was restarted. Perturbations due to the zonal harmonics have been subtracted.

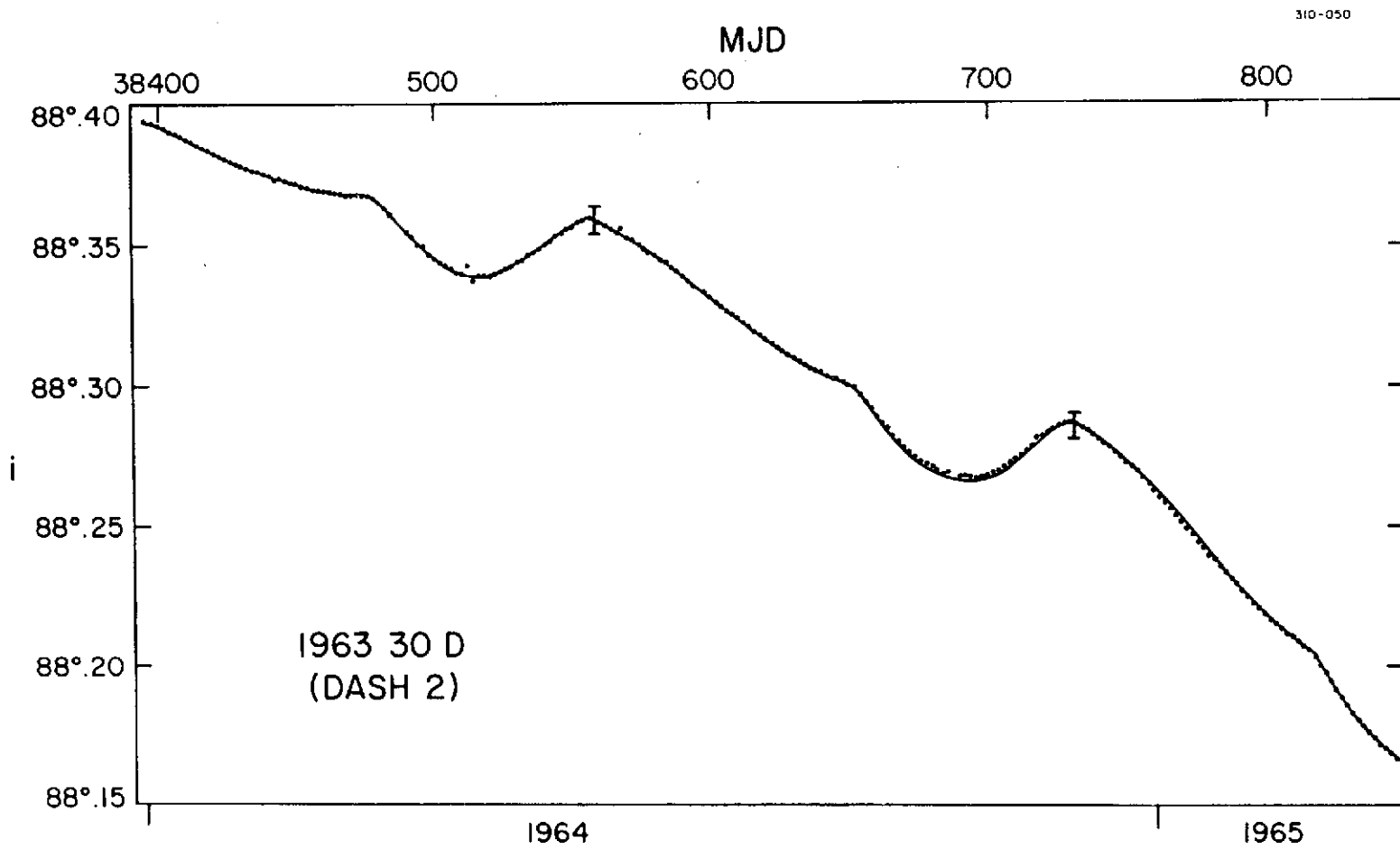


Figure 10. Observed values (points) and values computed by numerical integration (smooth curve) of the orbital inclination of 1963 30D corresponding to the values of the eccentricity shown in Figure 9. Perturbations due to the zonal harmonics have been subtracted.

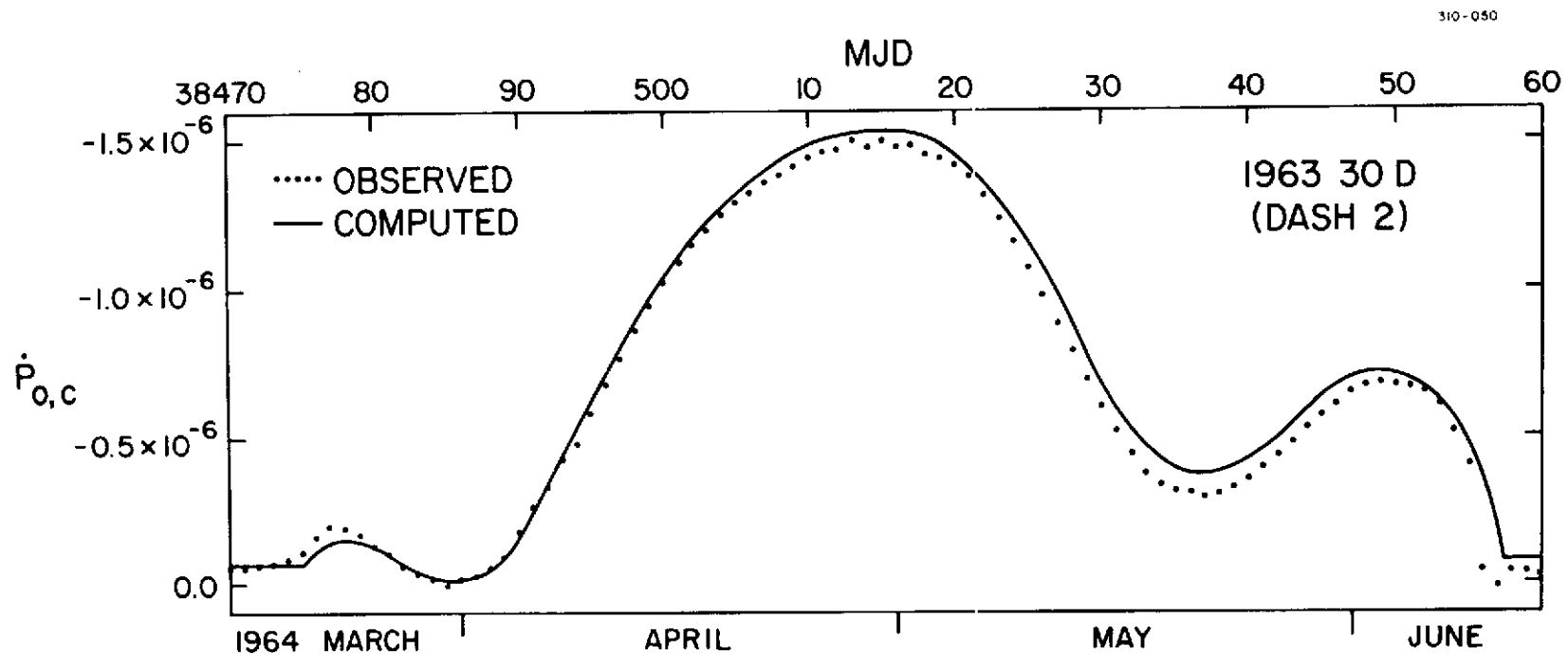


Figure 11. Observed and computed values of the orbital acceleration of 1963 30D in the interval MJD 38470–38560. The computed values were obtained with $s = 1.105$ and $c = 0.032$. The assumed phase of the right-angle component is given in the text and is the same as in Figure 5.

Not much has been said about terrestrial radiation pressure, although it has been included in all the computations. The effects of terrestrial radiation pressure are discussed in some detail in another paper (Slowey, 1973). It should be mentioned, however, that I found it inadequate to use a constant value for the earth's albedo. The relative distribution of albedo over the earth's surface is quite important in determining the sizes of the integrated effects at any time – a fact that would seem to preclude the use of the effects to model the albedo directly, as suggested by Prior (1970). A model including both latitudinal and seasonal variations in albedo did, on the other hand, seem to give good results. This model consisted of four mean seasonal models of the albedo as a function of latitude determined from Tiros observations (NASA Scientific and Technical Information Division, 1966), which were used with linear interpolation to obtain interseasonal values. It was used throughout that part of the lifetime where the effect of terrestrial radiation pressure was significant, compared to that of atmospheric drag.

PRECEDING PAGE BLANK NOT FILMED

4. AIR-DRAG EFFECTS

Values of the acceleration, the time rate of change of the anomalistic period, for Dash 2 were determined by analysis of the mean anomaly throughout both the beginning and the end interval. Wherever the contribution of radiation pressure to the accelerations could be specified with reasonable accuracy, it was applied to the total accelerations to determine which portions should be ascribed to atmospheric drag. When the relative accuracy of the resulting accelerations was deemed sufficient, these were then used to compute atmospheric densities. All these results are tabulated in Tables 3 and 4 for the beginning interval and the end interval, respectively. Densities in these tables are given both at the height of perigee and at a standard height, which was kept constant for some period of time. The standard heights that apply are given in Table 5.

The time is given in the first column of Tables 3 and 4. The observed total acceleration is given in the second; the combined contribution of direct solar radiation pressure and of terrestrial radiation pressure is in the third. The fourth column lists the difference — the portion ascribed to atmospheric drag. The common logarithms of the density, in grams per cubic centimeter, at the height of perigee and at the standard height appear in columns five and six, respectively. The local exospheric temperature in the J71 model corresponding to the computed densities is given in column seven; the last three columns contain, in order, the perigee height, the difference in right ascension between perigee and the sun, and the difference in declination between perigee and the sun.

The densities in Tables 3 and 4 were computed using the J71 model to represent the variation in density around the orbit. However, it was necessary to modify the model for use in the beginning interval. The derivation of densities in this interval is unusually sensitive to the model because of the relatively small orbital eccentricities and large density scale heights that prevail. The diurnal density variation that would be given by the J71 model at heights where hydrogen is the dominant constituent appears,

on the other hand, to be far too large. Hydrogen concentrations in the model vary with temperature according to the theory of Kockarts and Nicolet (1962, 1963). This variation is intended to represent the variation with the solar cycle and does not necessarily apply to the diurnal variation of hydrogen. If the diurnal temperature variation of the models is applied to the hydrogen model, the resulting densities vary by a factor of up to 8 or more.

I first substituted

$$\log_{10} n(H)_{500} = 102.69 - 59.618 \log_{10}(T_{500}) + 9.00 \log_{10}^2(T_{500})$$

for Jacchia's (1971) equation (7) for the hydrogen concentration at 500 km as a function of temperature. This change was not really necessary for my purposes, but it puts the mean model concentrations into better agreement with recent observational data. The equation increases the hydrogen concentrations by very nearly the factors, relative to the Kockarts-Nicolet values, recommended by Vidal-Madjar, Blamont, and Phissamay (1973) on the basis of Lyman α observations from the OSO 5 spacecraft. These factors are 2.3 for low solar activity, 2.5 for moderate solar activity, and 4.0 for high solar activity. I took the mean temperatures corresponding to the three levels of solar activity to be 700, 1000, and 1300 K.

Jacchia's equation (17) for the diurnal temperature variation can be written as

$$T_\ell = T_c(1 + Rd) ,$$

where d is given by

$$d = \sin^m \theta + (\cos^m \eta - \sin^m \theta) \cos^n \frac{\tau}{2} .$$

The constant R is the ratio of the increase in the maximum temperature above the minimum to the minimum temperature. To reduce the amplitude of the diurnal density variation for hydrogen, I introduced a separate temperature equation for it into the model. This has the form

$$T_H = T_{1/2} \left[1 + r_H \left(d - \frac{1}{2} \right) \right] ,$$

where $T_{1/2}$ is the mean diurnal temperature given by

$$T_{1/2} = T_c \left(1 + \frac{R}{2} \right) .$$

A value of $r_H = 0.090$, with $R = 0.30$, gives diurnal density ratios of very nearly 2.0, 1.7, and 1.4 for mean temperatures of 700, 1000, and 1300 K, respectively. These values agree with the theoretical relation given by Quessette (1972), which was confirmed over a considerable range by the data of Vidal-Madjar et al. (1973).

An area-to-mass ratio of $37.9 \text{ cm}^2 \text{ g}^{-1}$ was assumed in all the density computations. I used a variable drag coefficient (Jacchia and Slowey, 1972) that is based on the work of Cook (1965, 1966). In the beginning interval, the average effective drag coefficient was 3.6. The average value decreased from 3.0 at the beginning of the end interval to 2.2 toward the end of the lifetime.

Densities from the beginning section are plotted as a function of time in Figure 12. Apart from dust or other contamination, they should represent essentially pure hydrogen. The data are limited, however, to a time of minimum solar activity and to locations in moderate and low latitudes, near the maximum of the diurnal density variation for hydrogen. A detailed discussion of these data will not be given here. The densities are, for the most part, substantially greater than the average of $1.8 \times 10^{-20} \text{ g cm}^{-3}$ at 3500 km given by Fea and Smith (1970) as determined from 1963 30D in the same period. Analysis indicates, however, that the data are in quite good agreement at low latitudes with the revised hydrogen model. Variations exist that seem to be related to latitude, although it is possible that these variations reflect short-term variations in the latitudinal distribution of the earth's albedo rather than any real variations in the atmosphere. There is also an indication of a marked decrease in density toward the summer pole. This may be evidence of a seasonal-latitudinal variation for hydrogen similar to that for helium. Such a variation, with an even larger amplitude than that for helium, appears to be a distinct possibility (Jacchia, 1973).

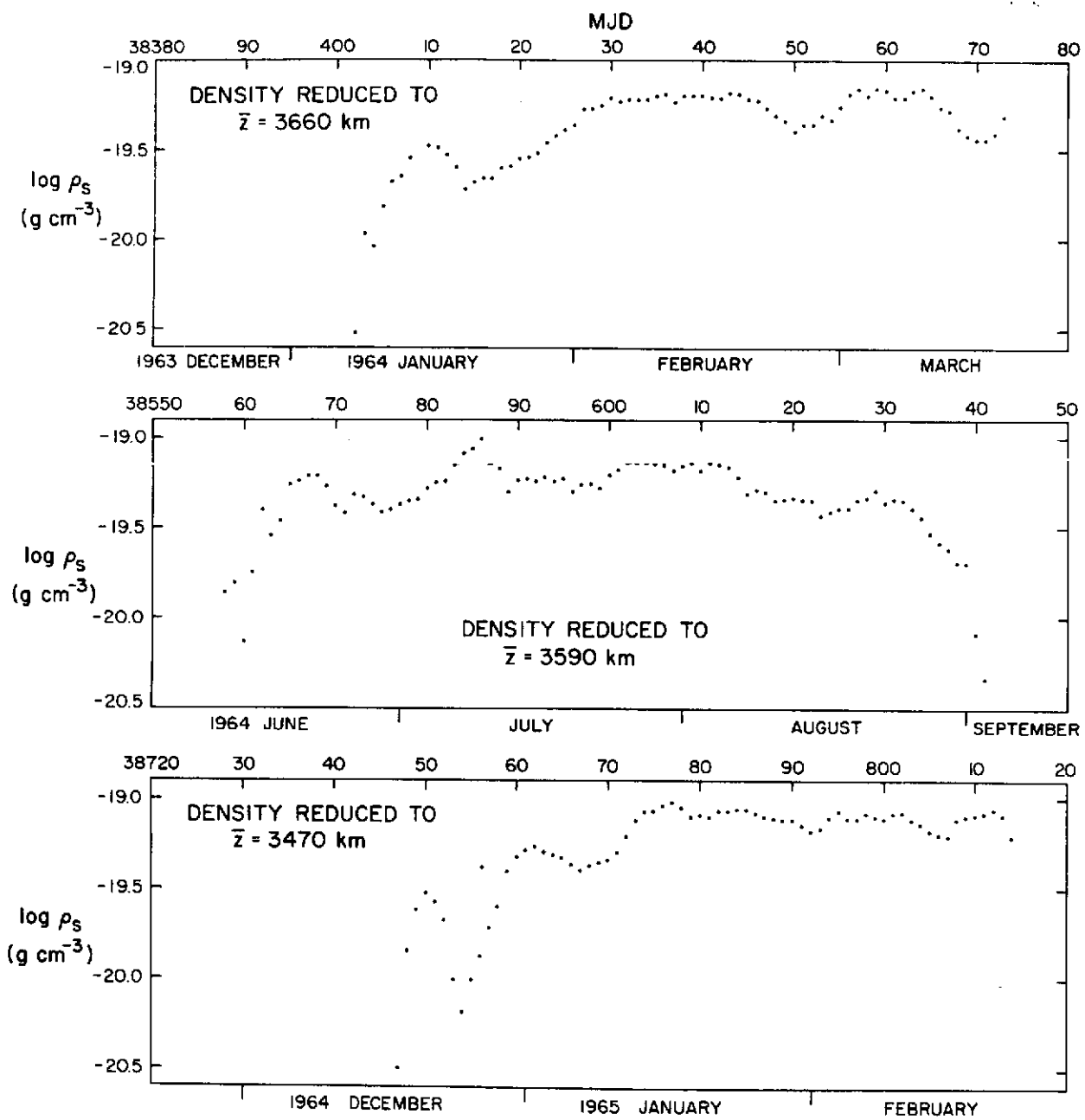


Figure 12. Densities obtained from atmospheric drag on 1963 30D in the interval MJD 38402–38814, during periods when the orbit was entirely in sunlight. In each strip, the perigee is at about 60° latitude in the summer hemisphere at the beginning and moves toward lower latitudes. Low values of density near the beginning in each case may be an indication of a seasonal-latitudinal variation for hydrogen. Other features in the plots may also be related to latitude.

Densities were derived in the end interval during five time periods, each separated from the next by a period when the orbit was partly in shadow and when the effect of radiation pressure was either too large or too uncertain to permit reliable derivation of densities. The first four of these periods are each about 60 days long and the fifth is about 200 days long. The intervening periods are each roughly 100 days long.

The densities from the first two periods are plotted in Figure 13, together with the corresponding densities computed from the J71 model. The derived densities in large parts of these two periods are not terribly accurate, and I have stretched the rules considerably in giving them. The effective heights to which the densities correspond are above 1800 km, and the atmospheric portions of the observed accelerations were, in places, only on the order of 10% of those due to terrestrial radiation pressure. The good agreement of the derived densities with the model is primarily an indication of how well terrestrial radiation pressure has been taken into account.

The densities plotted in Figure 13 are for different heights than any that apply in Table 4. In the figure, I have plotted the densities at the effective heights of the individual density determinations. This is also the case for Figures 14 and 15, discussed below. As a result, short-term variations are slightly exaggerated in the plots. This is because the increase in temperature associated with an increase in density gives a small decrease in the computed effective height due to the corresponding decrease in the assumed density scale height. It would have been better had the smoothed effective heights been used; the purpose of the figures, however, is only to provide a visual representation of the data and a comparison with the model.

The densities from the second two periods are plotted in Figure 14, again with the corresponding densities computed from the J71 model. The average effective heights for the two intervals are, in order, 1450 and 1120 km, and the data, though rather limited in scope, are of some interest since they refer to an atmosphere expected to consist of 90% or more helium. The agreement between the derived and the computed densities is, in general, quite good, considering the very large seasonal-latitudinal variation of helium that the model must accommodate. The short-term variations in the computed densities, which are associated with similar variations in the solar decimetric flux and in the geomagnetic index, do not fit the derived densities at all well,

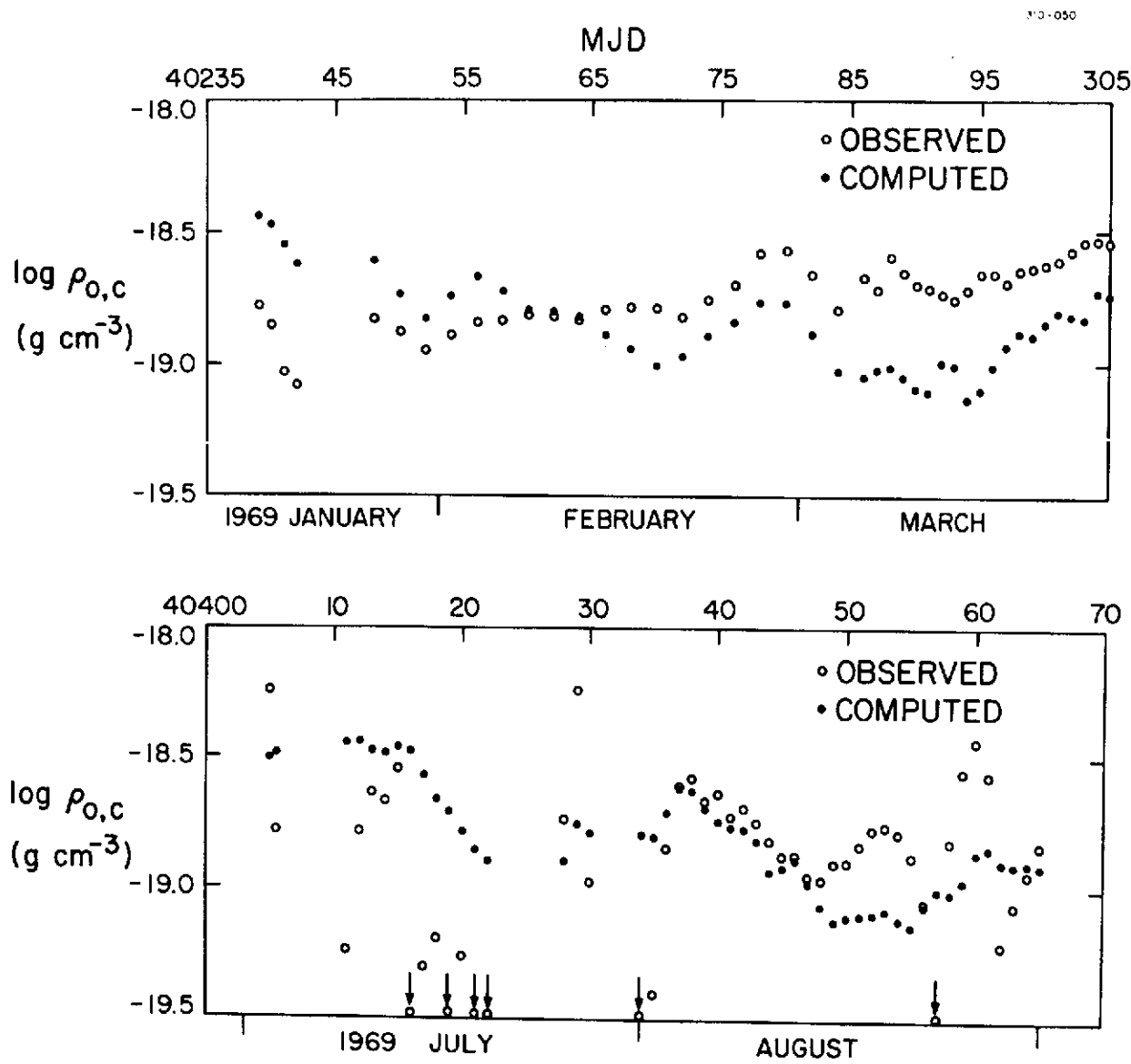


Figure 13. Derived and computed densities in the intervals MJD 40237–40305 and MJD 40405–40465. The effect of atmospheric drag was rather small compared to that of terrestrial radiation pressure, especially in the earlier portions of the intervals, and the derived and computed values do not agree too well. The densities are those at the effective heights of the individual density derivations (see text).

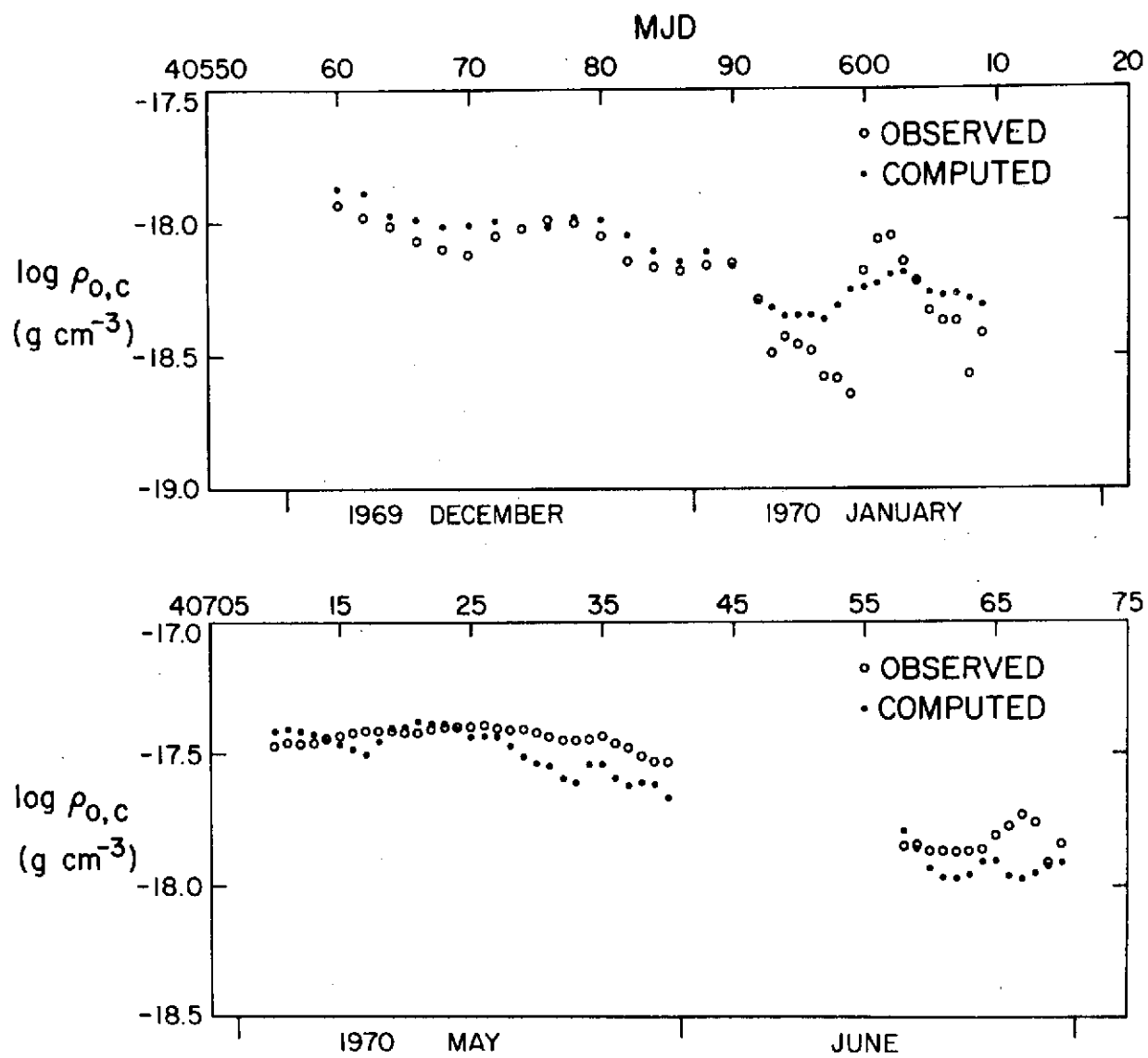


Figure 14. Derived and computed densities in the intervals MJD 40560–40609 and MJD 40710–40770. Helium is expected to be the dominant constituent in both intervals. Densities are at individual effective heights.

however. As in the case of the hydrogen densities, it may be that the derived densities should be smoother than they appear and that the short-term variations that seem to exist are, in fact, due to albedo effects. This argument is strengthened somewhat by the smoothness of the derived data in the fourth period, where the effects of terrestrial radiation pressure are relatively much smaller. An exception is the small increase in the derived density in the vicinity of MJD 40735, which seems clearly associated with a geomagnetic disturbance where the 3-hourly K_p index reached a maximum value of 7. However, at this height, the increase can probably be ascribed to an increase in the atomic oxygen concentration rather than to an increase in the helium concentration.

In the final period, the effective height goes from about 760 km to about 340 km and the densities range over about 2.5 orders of magnitude, owing mainly to the variation in height. The derived densities are plotted in the upper strip of Figure 15. The corresponding densities computed from the J71 model are plotted in the lower strip of the same figure. As can be seen, the agreement between the derived and computed densities is quite good throughout. Of course, no overall systematic difference exists between the two plots, because of the way the area-to-mass ratio was selected. The two plots do, however, agree quite well in detail also. A plot of the differences between the two indicates the short-term systematic difference to be, with one exception, within about 10% everywhere and generally much less than that. The exception occurs in the vicinity of MJD 40975, where the difference reaches about 25% for a short time. This may be due to a departure from the average relation between the atmosphere and the decimetric flux. Aside from this, no systematic differences that could be related to height or to any of the other parameters usually employed were detected. This is not too surprising when one considers that the model is based on a large body of drag data that pertains mainly to the height range involved here. These data do, however, constitute a unique test, in capsule form, of the model over a wide range of most of the variations involved, at least for conditions of average solar activity.

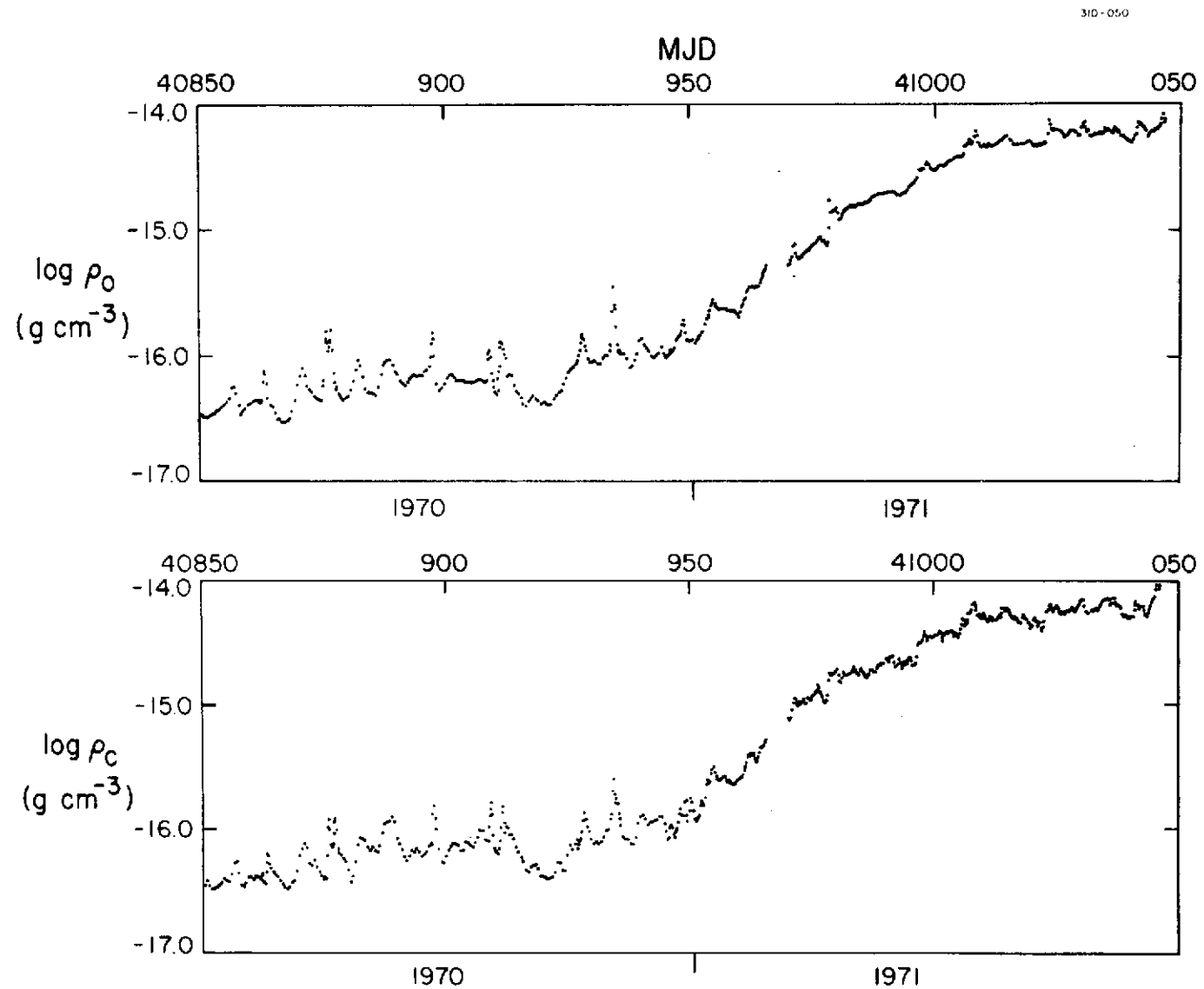


Figure 15. Derived (upper strip) and computed (lower strip) densities in the interval MJD 40850–41046. Densities are at individual effective heights that vary from about 760 km at the beginning to about 340 km at the end of the interval.

5. AN ISOLATED EVENT

No observed acceleration is given in Table 3 for MJD 38409. The reason for this omission is the presence, near that time, of a relatively large and unusual acceleration. In Figure 16, I have plotted residuals with respect to a reference polynomial of values of the mean anomaly obtained by fitting the individual observations of 1963 30D in the vicinity of MJD 38409 to the derived trajectory. The abrupt change in slope, centered at about MJD 38408.9, represents the acceleration referred to. Its appearance in the figure is similar to that observed for satellites at lower heights in association with short-lived increases in atmospheric density correlated with geomagnetic disturbances. The acceleration here, however, is a relatively enormous spike of very short duration that is not related to anything expected from the atmosphere.

The orbital elements given in Table 1 indicate that there was a decrease in the semimajor axis of about 20 m associated with this event. The corresponding decrease in velocity would be about 0.6 cm sec^{-1} , which, assuming 1.25 kg for the satellite's mass, implies a decrease in energy of about 50 joules. If this energy loss were due to neutral atmospheric drag and if it occurred over one orbital period — about the longest interval the data would seem to permit — an effective density of more than $2 \times 10^{-18} \text{ g cm}^{-3}$ would be required. This is roughly 70 times the density derived just before and after the event. A transient increase of this magnitude does not seem especially plausible and some other explanation is required. It is entirely possible that this acceleration is due to a collision with a meteor or to an outgassing of the satellite, possibly as a result of meteor impact. To my knowledge, this is the only event of this kind ever detected by orbital analysis.

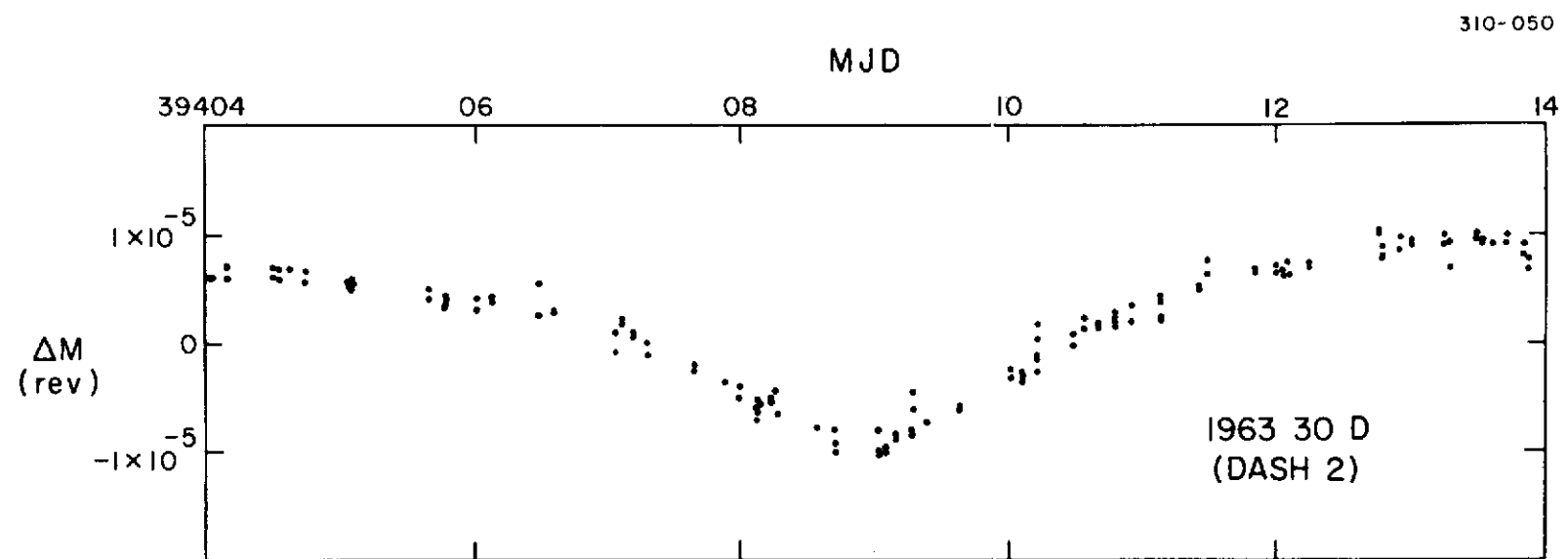


Figure 16. Residuals in mean anomaly of individual observations of 1963 30D in the vicinity of MJD 38409.

6. ACKNOWLEDGMENTS

The author appreciates the assistance of the 14th Aerospace Force, U.S. Air Force, in providing the radar observations of 1963 30D that were used for the end interval in this paper. The encouragement of L. G. Jacchia throughout the course of this analysis is also greatly appreciated.

PRECEDING PAGE BLANK NOT FILMED

7. REFERENCES

CARMELI, M.

1972. Solar radiation pressure on high altitude satellites. Aerospace Res. Lab. Tech. Doc. Rep. ARL 72-0034, February, 9 pp.

COOK, G. E.

1965. Satellite drag coefficients. *Planet. Space Sci.*, vol. 13, pp. 929-946.

1966. Drag coefficients of spherical satellites. *Ann. de Géophys.*, vol. 22, pp. 53-64.

FEA, K.

1967. Satellite accelerations and air densities at extreme altitudes. *Phil. Trans. Roy. Soc. London, Ser. A.*, vol. 262, pp. 200-202.

1970. The orbital accelerations of high balloon satellites. In Dynamics of Satellites (1969), ed. by B. Morando, Springer-Verlag, New York, pp. 295-302.

FEA, K. H., and SMITH, D. E.

1970. Some further studies of perturbations of satellites at great altitude. *Planet. Space Sci.*, vol. 18, pp. 1499-1525.

GAPOSCHKIN, E. M.

1964. Differential orbit improvement (DOI-3). *Smithsonian Astrophys. Obs. Spec. Rep.* No. 161, 70 pp.

1966. Tesserai harmonic coefficients and station coordinates from the dynamic method. In Geodetic Parameters for a 1966 Smithsonian Institution Standard Earth, ed. by C. A. Lundquist and G. Veis, *Smithsonian Astrophys. Obs. Spec. Rep.* No. 200, vol. 2, pp. 105-258.

JACCHIA, L. G.

1971. Revised static models of the thermosphere and exosphere with empirical temperature profiles. *Smithsonian Astrophys. Obs. Spec. Rep.* No. 332, 113 pp.

1973. Variations in thermospheric composition: A model based on mass-spectrometer and satellite-drag data. *Smithsonian Astrophys. Obs. Spec. Rep.* No. 354, 19 pp.

JACCHIA, L. G., and SLOWEY, J. W.

1972. A supplemental catalog of atmospheric densities from satellite-drag analysis. *Smithsonian Astrophys. Obs. Spec. Rep.* No. 348, 323 pp.

KAULA, W. M.

1966. Theory of Satellite Geodesy. Blaisdell Publ. Co., Waltham, Mass., 124 pp.

KOCKARTS, G., and NICOLET, M.

1962. Le problème aéronomique de l'hélium et de l'hydrogène neutres. *Ann. de Géophys.*, vol. 18, pp. 269-290.

KOCKARTS, G., and NICOLET, M.

1963. L'hélium et l'hydrogène atomique au cours d'un minimum d'activité solaire.
Ann. de Géophys., vol. 19, pp. 370-385.

KOZAI, Y.

1961. Effects of solar radiation pressure on the motion of an artificial satellite.
Smithsonian Astrophys. Obs. Spec. Rep. No. 56, pp. 25-33.
1964. New determination of zonal harmonics coefficients of the earth's gravitational potential. Smithsonian Astrophys. Obs. Spec. Rep. No. 165, 38 pp.

NASA SCIENTIFIC AND TECHNICAL INFORMATION DIVISION

1966. Significant achievements in satellite meteorology 1958-1964. NASA SP-96, 141 pp.

PRIOR, E. J.

1970. Earth albedo effects on the orbital variations of Echo I and Pageos I. In Dynamics of Satellites, ed. by B. Morando, Springer-Verlag, New York, pp. 303-312.

QUESETTE, J. A.

1972. Atomic hydrogen densities of the exobase. Journ. Geophys. Res., vol. 77, pp. 2997-3000.

SLOWEY, J. W.

1969. The effect of solar-radiation pressure on determination of the semimajor axis in satellite-orbit computation. In Space Research IX, ed. by K. S. W. Champion, P. A. Smith, and R. L. Smith-Rose, North-Holland Publ. Co., Amsterdam, pp. 76-82.
1973. Earth radiation pressure and the determination of density from satellite drag. In Space Research XIV, in press.

SMITH, D. E., and KISSELL, K. E.

1972. Anomalous orbital accelerations of the Pageos spacecraft. In Space Research XII, ed. by S. A. Bowhill, L. D. Jaffe, and M. J. Rycroft, Akademie-Verlag, Berlin, pp. 1523-1527.

VANDERBURGH, R. C., and KISSELL, K. E.

1971. Measurements of deformation and spin dynamics of the Pageos balloon-satellite by photoelectric photometry. Planet. Space Sci., vol. 19, pp. 223-231.

VIDAL-MADJAR, A., BLAMONT, J. E., and PHISSAMAY, B.

1973. Solar Lyman Alpha changes and related hydrogen density distribution at the earth's exobase (1969-1970). Journ. Geophys. Res., vol. 78, pp. 1115-1144.

Table 1. Orbital elements of 1963 30 D in the interval MJD 38398–38852.

T	ω	Ω	i	e	M	n	$\delta/2$	a	N	D	o
38398.0	229.227 9	45.60896 9	88.3938 2	.025281 3	.67055 3	8.57301 3	.275E-3 19	10.08543	42	4	.39
38398.0	228.362 7	45.49501 7	88.3933 1	.025356 3	.81339 2	8.57299 3	.10E-4 16	10.08544	34	4	.31
38400.0	227.493 7	45.38124 5	88.3924 1	.025422 3	.95623 2	8.57299 2	.164E-4 97	10.08544	34	4	.35
38402.0	226.587 5	45.26720 9	88.3910 1	.025464 2	.09917 2	8.57298 1	.39E-5 74	10.08544	34	4	.29
38404.0	225.653 4	45.15315 9	88.3898 2	.025493 2	.24218 1	8.57298 3	.29E-4 16	10.08544	46	4	.35
38406.0	224.688 3	45.03940 9	88.3891 1	.025508 1	.385335 9	8.572987 7	.386E-4 73	10.085442	96	4	.42
38408.0	223.626 2	44.92523 7	88.3883 1	.025505 1	.528655 7	8.572990 5	.426E-4 64	10.085440	144	4	.44
38410.0	222.509 3	44.81107 7	88.3874 2	.025485 1	.672202 9	8.573007 6	.277E-4 44	10.085426	168	4	.75
38412.0	221.352 2	44.69665 6	88.38623 8	.025448 1	.815887 5	8.573012 4	.282E-4 25	10.085423	108	4	.40
38414.0	220.108 3	44.58210 6	88.38491 8	.025396 1	.959817 8	8.573013 6	.198E-4 38	10.085422	58	4	.40
38416.0	218.808 2	44.48786 8	88.3845 1	.025317 1	.103899 7	8.573012 8	.212E-4 52	10.085422	50	4	.38
38418.0	217.434 3	44.35344 7	88.3836 1	.025216 2	.248188 8	8.573014 4	.405E-4 38	10.085421	67	4	.39
38420.0	215.955 2	44.23909 5	88.38234 7	.025111 1	.392773 6	8.573014 4	.197E-4 48	10.085421	105	4	.46
38422.0	214.414 2	44.12439 5	88.38134 8	.024977 1	.537529 6	8.573014 4	.256E-4 39	10.085421	129	4	.50
38424.0	212.788 2	44.00980 4	88.38049 6	.024825 1	.682524 4	8.573016 3	.312E-4 30	10.085419	125	4	.47
38426.0	212.596 2	43.89514 4	88.37950 5	.024657 1	.827764 4	8.573019 2	.288E-4 17	10.085417	139	4	.42
38428.0	209.280 2	43.78066 5	88.37881 5	.024469 1	.973239 4	8.573023 3	.371E-4 26	10.085414	112	4	.42
38430.0	207.387 2	43.66622 7	88.37803 8	.024266 1	.118996 5	8.573029 3	.356E-4 27	10.085410	91	4	.51
38432.0	205.398 1	43.55162 5	88.37693 6	.024050 1	.265030 4	8.573035 2	.237E-4 28	10.085405	129	4	.43
38434.0	203.330 2	43.43712 7	88.37646 8	.023819 2	.411297 5	8.573040 6	.208E-4 38	10.085401	95	4	.46
38436.0	201.179 4	43.3225 2	88.3760 2	.023580 3	.55780 1	8.573047 7	.393E-4 69	10.085395	25	4	.56
38438.0	198.98 1	43.2075 2	88.3754 4	.023342 3	.70446 3	8.57306 4	.131E-3 34	10.08538	27	4	.67
38440.0	196.593 8	43.0926 5	88.3744 2	.023078 2	.85165 2	8.57306 3	.435E-4 16	10.08539	34	4	.51
38442.0	194.200 6	42.9783 1	88.3733 2	.022832 2	.99887 2	8.573067 8	.58E-4 19	10.085379	39	4	.54
38444.0	191.71 1	42.86338 5	88.3738 2	.022594 1	.14099 3	8.57373 1	.28E-4 13	10.08537	39	4	.58
38446.0	189.128 7	42.37265 8	88.3726 1	.022370 1	.29414 2	8.57308 2	.140E-3 24	10.08537	34	4	.45
38448.0	186.53 1	42.63417 9	88.3723 1	.022172 1	.44198 3	8.57309 2	.49E-4 11	10.08536	35	4	.47
38450.0	183.81 1	42.51955 7	88.3715 1	.022001 1	.59015 3	8.57309 3	.168E-3 23	10.08536	43	4	.46
38452.0	180.95 2	42.40501 7	88.3709 1	.021860 1	.73873 4	8.57310 2	.6E-5 15	10.08536	33	4	.45
38454.0	178.09 3	42.2904 1	88.3704 2	.021754 2	.88732 9	8.5731 1	.185E-3 35	10.0854	30	4	.60
38456.0	175.06 1	42.1761 1	88.3698 2	.021688 1	.03639 4	8.57311 3	.37E-4 14	10.08535	34	4	.46
38458.0	172.07 3	42.0616 2	88.3695 4	.021661 3	.18539 7	8.57312 5	.93E-4 27	10.08534	30	4	.52
38460.0	168.915 6	41.94752 8	88.3690 1	.021675 1	.33484 2	8.57313 2	.21E-8 18	10.08533	44	4	.54
38462.0	165.749 7	41.83311 6	88.3693 1	.021733 1	.48435 2	8.57314 2	.129E-4 89	10.08532	63	4	.47
38464.0	162.506 5	41.71884 5	88.36854 8	.021837 1	.63409 1	8.57315 1	.360E-4 71	10.08532	71	4	.41
38466.0	159.269 6	41.60445 5	88.36800 8	.021986 1	.78384 2	8.57316 1	.191E-4 71	10.08531	71	4	.46
38468.0	155.962 6	41.48990 5	88.36787 9	.022190 1	.93381 2	8.57317 1	.411E-4 75	10.08530	59	4	.45
38470.0	152.732 5	41.37560 7	88.36775 1	.022430 1	.08357 1	8.573178 8	.5E-6 55	10.085292	64	4	.45
38472.0	149.451 5	41.26142 5	88.36810 8	.022721 1	.23350 1	8.573187 8	.326E-4 56	10.085285	65	4	.42
38474.0	146.235 6	41.14716 6	88.3678 1	.023050 1	.32326 2	8.57320 1	.270E-4 87	10.08528	51	4	.52
38476.0	142.987 5	41.03282 5	88.36758 8	.023439 2	.53313 2	8.57321 1	.748E-4 71	10.08527	68	4	.48
38478.0	139.880 4	40.91843 5	88.36638 6	.023835 1	.68266 1	8.573241 9	.90E-5 70	10.085243	77	4	.40
38480.0	136.851 6	40.80406 8	88.36476 9	.024256 2	.83203 2	8.57326 1	.9E-5 10	10.08522	57	4	.53
38482.0	133.89 1	40.6898 1	88.3631 1	.024707 5	.98124 3	8.57328 1	.7E-5 15	10.08521	37	4	.57
38484.0	130.99 1	40.5754 1	88.3610 1	.025187 6	.13032 3	8.57328 5	.5E-5 46	10.08521	19	4	.52
38490.0	122.849 3	40.23046 9	88.3547 1	.026753 1	.575981 7	8.573302 9	.5E-5 10	10.085195	112	4	.41
38492.0	120.45 1	40.1142 3	88.3532 3	.027307 3	.72375 3	8.57335 3	.249E-3 17	10.08516	99	4	.61

Table 1 (Cont.)

T	w	Ω	i	e	M	n	b/2	a	N	D	σ
38494.0	117.94 3	39.9994 4	88.3499 4	.027896 5	.87188 8	8.57337 6	.353E-3 41	10.08514	60	4	.53
38496.0	115.71 4	39.882 1	88.350 1	.02846 1	.0194 1	8.57349 8	.388E-3 37	10.08505	40	4	.84
38498.0	113.195 5	39.7677 2	88.3464 2	.029108 3	.16791 1	8.57361 3	.212E-3 16	10.08495	82	4	.64
38500.0	111.007 4	39.6515 2	88.3453 2	.029725 2	.31577 1	8.573737 9	.583E-4 84	10.084854	90	4	.49
38502.0	108.845 4	39.5352 2	88.3438 2	.030360 2	.46385 1	8.573898 5	.61E-5 75	10.084728	87	4	.57
38504.0	106.787 4	39.4188 2	88.3424 2	.030992 2	.611977 9	8.574073 4	.545E-4 64	10.084591	165	4	.53
38506.0	104.772 4	39.3020 1	88.3416 2	.031629 2	.76035 1	8.574264 6	.64E-4 11	10.084441	138	4	.49
38508.0	102.80 1	39.1854 2	88.3406 3	.032293 4	.90899 3	8.57446 5	.138E-3 17	10.08429	75	4	.56
38510.0	100.93 4	39.0682 6	88.3401 6	.03290 1	.0578 1	8.5747 1	.124E-3 42	10.0841	57	4	.51
38512.0	99.39 2	38.9490 5	88.3428 6	.03341 1	.20610 5	8.57485 5	.779E-3 31	10.08398	68	4	.75
38514.0	98.17 3	38.8274 9	88.347 1	.03382 2	.35406 7	8.57502 5	.2804E-2 36	10.08385	114	4	1.44
38516.0	95.528 8	38.7189 2	88.3391 2	.034790 5	.50609 2	8.57533 1	.1819E-2 80	10.08360	207	4	.56
38518.0	93.686 5	38.60225 9	88.3388 1	.035465 3	.65650 1	8.575542 9	.389E-4 60	10.083440	202	4	.45
38520.0	91.972 6	38.4854 1	88.3385 2	.036095 3	.80700 2	8.57575 1	.118E-4 70	10.08328	161	4	.45
38522.0	90.332 8	38.3677 2	88.3395 2	.036692 6	.95772 2	8.57596 1	.78E-4 10	10.08311	158	4	.54
38524.0	88.66 1	38.2510 2	88.3405 3	.037312 8	.10890 3	8.57613 2	.122E-3 13	10.08298	99	4	.64
38526.0	87.04 1	38.1343 4	88.3414 4	.03790 1	.26028 3	8.57630 2	.78E-4 16	10.08285	111	4	.81
38528.0	85.430 9	38.0179 3	88.3419 3	.038800 9	.41193 2	8.57644 2	.5E-5 17	10.08274	100	4	.71
38530.0	83.86 2	37.9003 4	88.3437 5	.03906 2	.56370 4	8.57653 2	.52E-4 14	10.08266	100	4	.90
38532.0	82.264 4	37.7840 1	88.3444 2	.039660 6	.71572 1	8.576611 8	.19E-5 68	10.082603	105	4	.47
38534.0	80.725 3	37.6672 1	88.3461 2	.040208 3	.867712 7	8.57667 1	.8E-6 64	10.08256	92	4	.48
38536.0	79.13 2	37.5508 2	88.3473 4	.04084 2	.01994 4	8.57666 3	.158E-3 15	10.08258	48	4	.48
38538.0	77.73 1	37.4348 3	88.3484 4	.04123 2	.17176 3	8.57675 3	.45E-4 14	10.08250	55	4	.45
38540.0	76.21 1	37.3183 3	88.3501 4	.04179 1	.32397 2	8.57681 1	.15E-4 11	10.08245	65	4	.49
38542.0	74.748 8	37.2026 3	88.3510 4	.04227 1	.47614 2	8.57686 2	.19E-4 17	10.08241	52	4	.60
38544.0	73.291 6	37.0860 2	88.3531 4	.04276 1	.62841 1	8.576934 7	.10E-4 11	10.082351	50	4	.51
38546.0	71.875 9	36.9702 2	88.3541 4	.04321 2	.78074 2	8.57701 3	.57E-4 16	10.08229	56	4	.51
38548.0	70.477 9	36.8537 3	88.3559 5	.04361 3	.93320 2	8.57711 2	.62E-4 10	10.08221	49	4	.46
38550.0	69.06 1	36.7380 3	88.3562 5	.04405 3	.08589 2	8.57722 2	.00E-6 11	10.08212	34	4	.40
38552.0	67.66 1	36.6212 3	88.3578 6	.04444 3	.23874 2	8.57729 1	.132E-3 21	10.08207	35	4	.58
38554.0	66.332 2	36.50600 8	88.3586 1	.044757 2	.391582 5	8.577405 3	.138E-4 45	10.081982	74	4	.48
38556.0	64.999 2	36.3896 1	88.3590 2	.045077 6	.544584 8	8.577447 6	.581E-4 58	10.081949	91	4	.73
38558.0	63.650 1	36.27275 4	88.35837 8	.045363 3	.697668 4	8.577454 3	.96E-5 28	10.081944	110	4	.50
38560.0	62.336 2	36.15528 4	88.35749 8	.045643 3	.850656 5	8.577459 5	.83E-5 32	10.081940	84	4	.38
38562.0	61.003 3	36.03790 6	88.3568 1	.045881 5	.00371 1	8.577464 9	.48E-5 83	10.081936	41	4	.45
38564.0	59.666 5	35.9204 1	88.3556 2	.046092 8	.15679 2	8.577476 8	.291E-4 98	10.081926	27	4	.47
38566.0	58.279 7	35.8028 2	88.3543 4	.04623 2	.31004 2	8.57749 7	.55E-4 68	10.08191	18	4	.50
38568.0	57.00 2	35.6871 8	88.3558 9	.04654 4	.46296 7	8.57752 4	.209E-3 45	10.08189	17	4	.53
38570.0	55.519 9	35.5678 1	88.3523 4	.04652 1	.61654 3	8.57751 3	.43E-4 19	10.08190	24	4	.45
38572.0	54.111 8	35.44993 9	88.3513 2	.046635 8	.76990 2	8.57752 2	.23E-4 16	10.08190	28	4	.41
38574.0	52.663 5	35.33205 7	88.3498 2	.046700 5	.92340 2	8.577526 9	.60E-5 70	10.081888	36	4	.44
38576.0	51.220 5	35.21389 6	88.3482 1	.046764 4	.07688 2	8.577526 8	.120E-4 64	10.081888	40	4	.41
38578.0	49.766 4	35.09564 6	88.3471 1	.046803 4	.23040 1	8.57754 2	.27E-4 12	10.08188	37	4	.43
38580.0	48.291 3	34.97748 8	88.3458 2	.046813 3	.38399 1	8.577534 9	.126E-4 77	10.081881	41	4	.40
38582.0	46.824 1	34.85926 6	88.3446 1	.046802 1	.537564 4	8.577541 2	.76E-5 39	10.081876	46	4	.40
38584.0	45.332 2	34.74088 9	88.3430 2	.046752 1	.691221 5	8.577548 2	.48E-5 26	10.081870	37	4	.49
38586.0	43.822 2	34.6220 1	88.3414 2	.046670 2	.844950 8	8.57751 1	.198E-4 88	10.08186	29	4	.48
38588.0	42.288 3	34.5032 1	88.3401 2	.046544 2	.00123 1	8.57757 1	.20E-4 13	10.08186	23	4	.48

Table 1 (Cont.)

T	ω	Ω	I	e	M	n	b/2	a	N	D	o
38590.0	40.717 2	34.38462 9	88.3384 2	.046393 2	.152693 7	8.57757 1	.90E-5 90	10.08185	25	4	.40
38592.0	39.116 5	34.2658 2	88.3372 2	.046211 5	.30671 2	8.57757 1	.256E-4 85	10.08185	30	4	.48
38594.0	37.464 3	34.1469 1	88.3353 2	.046007 4	.46087 1	8.577575 5	.102E-4 70	10.081849	34	4	.52
38596.0	35.783 2	34.0286 1	88.3341 2	.045770 2	.615120 6	8.577577 4	.155E-4 62	10.081847	35	4	.55
38598.0	35.053 2	33.9095 1	88.3330 2	.045512 4	.769506 7	8.577578 8	.290E-4 93	10.081846	26	4	.46
38600.0	32.280 5	33.7910 2	88.3316 2	.045239 5	.92401 1	8.577578 7	.277E-4 77	10.081846	26	4	.54
38602.0	30.446 2	33.6714 1	88.3290 2	.044958 2	.078693 6	8.577582 9	.164E-4 55	10.081843	30	4	.63
38604.0	28.565 2	33.5522 1	88.3276 2	.044669 2	.233512 4	8.577584 6	.129E-4 52	10.081842	31	4	.60
38606.0	26.628 2	33.4330 2	88.3263 2	.044376 3	.388491 6	8.577587 2	.82E-5 32	10.081839	31	4	.56
38608.0	24.656 1	33.31394 9	88.3254 2	.044079 1	.543573 3	8.577589 2	.208E-4 29	10.081838	41	4	.51
38610.0	22.631 2	33.19500 9	88.3238 2	.043786 2	.698802 4	8.577591 2	.111E-4 23	10.081836	44	4	.59
38612.0	20.573 1	33.07589 6	88.32233 9	.043498 1	.854132 3	8.577592 6	-.83E-5 38	10.081835	60	4	.46
38614.0	18.495 4	32.95645 6	88.3209 1	.043215 1	.00953 1	8.577597 7	.354E-4 50	10.081831	58	4	.40
38616.0	16.349 7	32.8370 1	88.3193 2	.042929 2	.16511 2	8.577597 1	.20E-4 10	10.081831	47	4	.52
38618.0	14.171 6	32.71803 7	88.3178 1	.042638 2	.32078 2	8.57760 1	-.19E-4 12	10.08183	50	4	.51
38620.0	11.980 6	32.5987 1	88.3167 2	.042352 2	.47649 2	8.577594 9	.40E-4 11	10.081833	39	4	.47
38622.0	9.703 5	32.47951 6	88.3146 1	.042058 1	.63243 1	8.577595 9	.10E-4 12	10.081833	48	4	.46
38624.0	7.372 5	32.36036 5	88.3135 1	.041772 1	.78852 1	8.577595 6	-.64E-5 55	10.081832	56	4	.40
38626.0	5.018 5	32.24115 7	88.3125 1	.041494 1	.94468 1	8.577592 9	.469E-4 81	10.081834	58	4	.52
38628.0	2.548 7	32.12193 8	88.3108 2	.041233 1	.10115 2	8.57760 1	.17E-5 99	10.08183	53	4	.61
38630.0	.049 6	32.00248 8	88.3095 2	.040996 1	.25771 2	8.57760 1	.6E-5 11	10.08183	40	4	.55
38632.0	357.504 6	31.88297 8	88.3086 2	.040789 1	.41442 2	8.57760 1	.43E-4 13	10.08183	43	4	.57
38634.0	354.884 6	31.76361 7	88.3080 1	.040613 1	.57133 2	8.57760 1	.11E-4 12	10.08182	56	4	.64
38636.0	352.214 6	31.64465 8	88.3070 1	.040472 1	.72838 2	8.57760 1	.22E-4 11	10.08182	57	4	.62
38638.0	349.506 4	31.52552 5	88.30593 9	.040375 1	.86555 1	8.577610 8	.27E-5 67	10.081820	64	4	.50
38640.0	346.765 4	31.40614 4	88.30500 9	.040324 1	.04281 1	8.577639 5	.44E-5 43	10.081820	68	4	.39
38642.0	343.999 4	31.28654 5	88.30390 9	.040320 1	.20015 1	8.577612 8	.198E-4 57	10.081819	66	4	.47
38644.0	341.202 3	31.16719 4	88.30323 8	.040373 1	.357565 8	8.577613 7	-.18E-5 62	10.081818	70	4	.40
38646.0	338.415 4	31.04796 4	88.30250 9	.040464 1	.514963 9	8.577613 5	.1E-6 48	10.081818	68	4	.39
38648.0	335.620 5	30.92888 6	88.3019 1	.040602 2	.67239 1	8.577620 7	-.171E-4 67	10.081813	59	4	.52
38650.0	332.817 6	30.80976 9	88.3009 1	.040782 2	.82984 1	8.57763 1	-.734E-4 77	10.08180	66	4	.77
38652.0	330.095 2	30.69085 4	88.29931 6	.040970 1	.987142 6	8.577671 6	.8E-6 41	10.081772	85	4	.44
38654.0	327.370 2	30.57174 6	88.29705 7	.041189 1	.144517 6	8.577706 3	.107E-4 27	10.081745	92	4	.43
38656.0	324.649 2	30.45213 6	88.29425 7	.041444 1	.301949 6	8.577734 6	.70E-5 39	10.081723	80	4	.49
38658.0	321.940 6	30.3327 4	88.2919 4	.04175 1	.45939 1	8.577748 7	.19E-5 51	10.081712	53	4	.48
38660.0	319.250 4	30.2121 5	88.2890 5	.04206 1	.61681 1	8.577771 9	-.24E-5 64	10.081694	41	4	.44
38662.0	316.596 3	30.09247 8	88.28728 9	.042406 2	.774155 8	8.577777 4	-.13E-5 37	10.081690	56	4	.51
38664.0	313.958 3	29.97258 9	88.28516 9	.042797 2	.931474 7	8.577792 5	-.157E-4 45	10.081678	62	4	.54
38666.0	311.361 3	29.8522 1	88.2826 1	.043214 2	.088722 8	8.5777817 7	-.25E-5 60	10.081658	65	4	.60
38668.0	308.788 2	29.73109 9	88.28015 8	.043677 2	.245960 6	8.577855 4	-.107E-4 28	10.081629	81	4	.59
38670.0	306.262 2	29.61023 9	88.27826 8	.044164 2	.403164 5	8.577910 3	-.108E-4 30	10.081586	98	4	.62
38672.0	303.785 2	29.48914 9	88.27649 8	.044674 2	.560354 4	8.577983 3	.61E-5 29	10.081529	98	4	.58
38674.0	301.344 2	29.3679 1	88.2749 1	.045218 3	.717615 6	8.578079 4	.34E-5 36	10.081453	90	4	.72
38676.0	298.950 3	29.2466 2	88.2735 2	.045793 4	.874960 9	8.578203 6	.137E-4 57	10.081356	75	4	.85
38678.0	296.617 3	29.1256 1	88.2726 1	.046376 3	.032417 6	8.578357 4	.490E-4 46	10.081236	57	4	.62
38680.0	294.312 3	29.0036 2	88.2715 2	.047003 5	.190132 8	8.578544 5	.346E-4 63	10.081089	42	4	.65
38682.0	292.061 4	28.8816 3	88.2704 2	.047637 9	.34811 1	8.57877 1	.484E-4 99	10.08091	27	4	.62
38684.0	289.855 6	28.7607 3	88.2685 2	.04830 2	.50644 2	8.57900 4	.120E-3 31	10.08073	13	4	.36

Table 1 (Cont.)

T	w	Ω	i	e	M	n	$\hbar/2$	a	N	D	o
38686.0	287.72 4	28.639 2	88.270 2	.04092 5	.6651 1	8.5793 1	.8E-4 12	10.0805	18	4	.47
38690.0	289.520 1	28.3933 2	88.2678 1	.050232 4	.983890 3	8.579847 9	.379E-4 49	10.080070	27	4	.51
38692.0	281.473 2	28.2711 2	88.2680 2	.050886 2	.143948 4	8.580100 2	.549E-4 15	10.079872	62	4	.79
38694.0	279.4512 7	28.1484 1	88.26758 7	.051559 2	.304415 2	8.580330 2	.598E-4 15	10.079692	112	4	.65
38696.0	277.4542 8	28.0257 1	88.26741 9	.052232 2	.465237 2	8.580522 1	.345E-4 12	10.079541	171	4	.79
38698.0	275.4886 7	27.9030 1	88.26764 8	.052893 3	.626329 2	8.580688 1	.307E-4 13	10.079412	169	4	.77
38700.0	273.5519 7	27.7802 1	88.26823 8	.053547 3	.787646 2	8.580829 1	.263E-4 11	10.079301	99	4	.54
38702.0	271.6390 8	27.6578 1	88.26921 9	.054193 3	.949159 2	8.580953 2	.192E-4 19	10.079205	43	4	.46
38704.0	269.756 1	27.5355 1	88.2704 1	.054840 4	.110820 3	8.581067 3	.186E-4 27	10.079115	37	4	.53
38706.0	267.8975 6	27.41282 9	88.27168 8	.055469 3	.272637 2	8.581175 1	.178E-4 11	10.079031	51	4	.40
38708.0	266.0641 8	27.2904 1	88.27260 8	.056087 3	.434596 3	8.581283 2	.149E-4 17	10.078946	63	4	.52
38710.0	264.2631 9	27.1677 1	88.27381 9	.056706 3	.596680 3	8.581394 2	.208E-4 18	10.078859	66	4	.50
38712.0	262.4834 9	27.04511 8	88.27492 7	.057290 3	.758938 3	8.581514 2	.220E-4 18	10.078766	65	4	.44
38714.0	260.730 1	26.92264 9	88.27674 8	.057859 3	.921365 4	8.581641 3	.237E-4 26	10.078667	49	4	.42
38716.0	259.001 2	26.8004 2	88.2790 1	.058414 6	.083991 7	8.581781 5	.230E-4 35	10.078557	32	4	.53
38718.0	257.31 5	26.679 2	88.281 1	.05896 1	.2468 2	8.5819 3	.03E-5 12	10.0784	21	4	.65
38720.0	255.617 3	26.5561 2	88.2825 1	.059470 6	.409957 9	8.58211 2	.573E-4 79	10.07829	40	4	.45
38722.0	253.958 1	26.43359 6	88.28360 7	.059950 2	.573376 4	8.582296 3	.358E-4 33	10.078154	78	4	.48
38724.0	252.327 2	26.31120 7	88.28486 9	.060420 2	.737083 5	8.582475 3	.370E-4 28	10.078014	111	4	.62
38726.0	250.717 1	26.18873 6	88.28608 8	.060872 2	.901072 5	8.582636 3	.422E-4 25	10.077888	154	4	.58
38728.0	249.119 2	26.06633 6	88.28682 8	.061300 2	.065320 6	8.582768 7	.458E-4 40	10.077785	163	4	.53
38730.0	247.544 1	25.94402 5	88.28721 8	.061724 2	.229710 4	8.582215 6	.370E-4 56	10.078204	393	4	.67
38732.0	245.989 2	25.82087 8	88.2861 1	.062127 2	.394132 7	8.582199 7	.65E-5 35	10.078216	378	4	.65
38734.0	244.4361 9	25.69761 4	88.28525 7	.062519 1	.558520 3	8.582219 4	.302E-4 36	10.078201	374	4	.46
38736.0	242.866 1	25.57407 4	88.28401 6	.062867 1	.722932 3	8.582179 2	.21E-5 17	10.078232	371	4	.48
38738.0	241.297 1	25.45020 6	88.28240 9	.063196 2	.887353 4	8.582207 3	.45E-5 21	10.078210	164	4	.45
38740.0	239.720 2	25.32616 6	88.2809 1	.063487 2	.051809 6	8.582212 3	.57E-5 32	10.078206	148	4	.46
38742.0	238.131 2	25.20190 8	88.2795 1	.063735 2	.216303 6	8.582240 6	.67E-5 36	10.078184	151	4	.46
38744.0	236.526 2	25.07783 8	88.2781 1	.063933 1	.380839 6	8.582259 5	.122E-4 43	10.078170	129	4	.53
38746.0	234.909 3	24.9534 2	88.2763 2	.064090 4	.54541 1	8.582267 6	.21E-5 55	10.078163	114	4	.55
38748.0	233.291 3	24.82891 9	88.2746 1	.064196 3	.709971 9	8.58225 1	.67E-5 96	10.07817	81	4	.58
38750.0	231.672 1	24.70361 4	88.2725 1	.064275 1	.874535 3	8.582284 6	.75E-5 35	10.078150	128	4	.41
38752.0	230.037 1	24.57861 7	88.27092 9	.064296 1	.039157 3	8.582294 3	.32E-5 26	10.078142	142	4	.44
38754.0	228.403 2	24.4535 1	88.2690 2	.064278 1	.203772 5	8.582294 2	.78E-5 24	10.078142	77	4	.45
38756.0	226.755 2	24.3286 1	88.2672 1	.064237 1	.368422 5	8.582318 8	.08E-4 10	10.078123	51	4	.46
38758.0	225.102 2	24.2035 1	88.2648 1	.064162 1	.533076 5	8.582322 3	.64E-5 28	10.078120	84	4	.47
38760.0	223.427 1	24.07806 7	88.2627 1	.064074 1	.697786 3	8.582353 3	.93E-5 28	10.078096	84	4	.49
38762.0	221.732 1	23.95264 8	88.2606 1	.063967 1	.862545 4	8.582375 5	.69E-5 38	10.078079	45	4	.52
38764.0	220.012 1	23.82715 8	88.2584 1	.063842 1	.027373 4	8.582414 3	.84E-5 20	10.078048	52	4	.43
38766.0	218.259 1	23.70132 6	88.25609 8	.063698 1	.192288 3	8.582460 3	.121E-4 20	10.078013	55	4	.41
38768.0	216.472 2	23.57556 9	88.2536 1	.063530 2	.357288 5	8.582509 2	.168E-4 20	10.077974	42	4	.48
38770.0	214.639 1	23.4496 1	88.2514 1	.063346 2	.522403 4	8.582557 3	.121E-4 31	10.077937	50	4	.53
38772.0	212.770 1	23.32386 8	88.2492 1	.063138 2	.687608 3	8.582604 2	.85E-5 24	10.077899	56	4	.50
38774.0	210.8661 8	23.19803 7	88.24696 8	.062901 2	.852901 2	8.582653 2	.132E-4 15	10.077861	53	4	.52
38776.0	208.9213 8	23.07174 8	88.2444 1	.062639 1	.018307 2	8.582706 2	.104E-4 21	10.077819	45	4	.50
38778.0	206.941 1	22.9454 1	88.2422 2	.062350 2	.183813 3	8.582758 2	.141E-4 25	10.077779	30	4	.55
38780.0	204.927 1	22.8191 1	88.2397 2	.062045 3	.349411 4	8.582792 3	.66E-5 21	10.077752	25	4	.54

Table 1 (Cont.)

T	w	Ω	i	e	M	n	$\hbar/2$	a	N	D	σ	
38782.0	202.886	1	22.6928	1	88.2383	2	.061726	2	.515081	3	8.582844	6
38784.0	201.815	2	22.5668	2	88.2356	2	.061388	2	.680827	4	8.582869	2
38786.0	198.721	1	22.4407	1	88.2331	2	.061055	2	.846638	3	8.582909	2
38788.0	196.5953	8	22.31431	9	88.2310	1	.060727	2	.012532	2	8.582949	1
38790.0	194.438	1	22.18779	7	88.2291	1	.060411	1	.178510	3	8.582997	3
38792.0	192.246	1	22.06144	7	88.2268	1	.060116	1	.344579	3	8.583053	4
38794.0	190.003	1	21.93499	3	88.22423	7	.059845	1	.510782	4	8.583118	2
38796.0	187.72	1	21.80851	4	88.22227	8	.059593	1	.677097	4	8.583183	2
38798.0	185.301	2	21.68214	8	88.22036	8	.059369	1	.543561	4	8.583248	2
38800.0	183.013	2	21.55584	7	88.21868	8	.059167	1	.010112	5	8.583300	2
38802.0	180.600	2	21.42943	6	88.21653	8	.058988	1	.176790	5	8.583374	3
38804.0	178.139	2	21.30274	7	88.21484	8	.058832	1	.343606	4	8.583437	4
38806.0	175.642	3	21.17592	8	88.2132	1	.058697	1	.510525	7	8.583471	8
38808.0	173.118	3	21.04928	8	88.2119	1	.058583	1	.677521	8	8.583541	5
38810.0	170.569	2	20.92278	8	88.2104	1	.058496	1	.844594	4	8.583552	3
38812.0	167.994	2	20.79629	5	88.2088	1	.058429	1	.011746	5	8.583597	2
38814.0	165.424	2	20.66966	3	88.20725	7	.058400	1	.178907	4	8.583604	3
38816.0	162.842	2	20.54311	4	88.20559	7	.058412	1	.346107	5	8.583615	2
38818.0	160.269	2	20.41679	7	88.20322	8	.058472	1	.513274	4	8.583609	3
38820.0	157.714	2	20.29025	7	88.20035	8	.058580	1	.680389	5	8.583570	3
38822.0	155.159	2	20.1638	1	88.1971	1	.058736	1	.847552	6	8.583650	5
38824.0	152.633	4	20.0371	1	88.1942	2	.058939	2	.014755	9	8.583699	5
38826.0	150.089	2	19.9102	1	88.1913	1	.059188	1	.182185	5	8.583776	4
38828.0	147.562	2	19.7831	1	88.1884	1	.059476	1	.349820	5	8.583904	4
38830.0	145.054	2	19.6557	1	88.1854	1	.059805	1	.517698	5	8.584057	2
38832.0	142.551	2	19.5277	1	88.1827	1	.060170	1	.683900	5	8.584198	3
38834.0	140.067	3	19.3994	2	88.1802	1	.060567	2	.854401	8	8.584360	5
38836.0	137.606	4	19.2714	2	88.1781	2	.060989	3	.02320	1	8.58450	2
38838.0	135.150	5	19.1429	3	88.1759	3	.061442	5	.19231	1	8.58463	1
38840.0	132.725	4	19.0138	3	88.1741	3	.061915	3	.361628	9	8.584756	4
38842.0	130.292	4	18.8856	2	88.1717	2	.062413	1	.53121	1	8.58487	8
38844.0	127.932	2	18.7563	1	88.17019	7	.062933	1	.700811	4	8.584891	5
38846.0	125.561	4	18.6273	2	88.1684	2	.063471	2	.870636	9	8.58517	2
38848.0	123.420	8	18.4980	7	88.1666	6	.064018	5	.04012	2	8.58645	5
38850.0	120.70	1	18.3805	7	88.1578	5	.064590	3	.21137	3	8.58483	2
38852.0	118.71	3	18.241	1	88.1620	7	.065218	5	.38105	8	8.58602	6
											.448E-3	37
											10.07522	82
												.92

PRECEDING PAGE BLANK NOT FILMED

Table 2. Orbital elements of 1963 30D in the interval MJD 40230-41054.

T	ω	Ω	i	e	M	n	$h/2$	a	N	D	σ
40230.0	81.05 1	249.949 3	86.578 2	.18211 2	.73210 4	8.66585 1	.79E-4 10	10.01331	16	8	.16
40232.0	78.906 8	249.680 2	86.583 2	.18268 1	.06415 2	8.666299 8	.9478E-4 41	10.012965	33	8	.22
40234.0	76.720 3	249.406 1	86.576 1	.183223 6	.397092 6	8.666648 3	.6906E-4 54	10.012696	31	8	.16
40236.0	74.537 9	249.140 3	86.581 3	.18374 2	.73058 2	8.66683 1	.270E-4 11	10.01255	24	8	.18
40238.0	72.37 1	248.874 2	86.574 3	.18431 2	.06424 2	8.66688 1	.1623E-4 75	10.01252	24	8	.16
40240.0	70.18 2	248.602 4	86.569 2	.18481 4	.39807 4	8.66696 1	.143E-4 13	10.01246	24	8	.21
40242.0	67.99 1	248.333 3	86.567 2	.18530 2	.73202 2	8.66697 2	.120E-4 14	10.01245	26	8	.20
40244.0	65.823 6	248.062 2	86.565 1	.185747 8	.06601 1	8.667048 6	.1420E-4 33	10.012390	36	8	.20
40246.0	63.660 8	247.793 2	86.563 1	.18619 1	.40011 2	8.667092 6	.1370E-4 28	10.012357	35	8	.21
40248.0	61.49 1	247.520 2	86.561 2	.18664 2	.73434 2	8.66713 1	.1267E-4 48	10.01233	31	8	.16
40250.0	59.312 8	247.250 1	86.555 1	.187020 6	.06868 1	8.667178 6	.1271E-4 29	10.012290	30	8	.30
40252.0	57.14 1	246.977 1	86.548 2	.18736 2	.40311 2	8.667213 8	.1368E-4 33	10.012263	26	8	.18
40254.0	55.00 2	246.704 2	86.547 3	.18774 3	.73758 3	8.66727 2	.1437E-4 44	10.01222	23	8	.22
40256.0	52.86 6	246.431 3	86.546 5	.1881 1	.0722 1	8.66733 4	.1233E-4 87	10.01217	19	8	.25
40258.0	50.71 8	246.160 1	86.541 4	.1883 1	.4069 1	8.66736 4	.1176E-4 36	10.01215	19	8	.23
40260.0	48.5 1	245.883 3	86.532 1	.1885 2	.7418 2	8.66745 5	.1211E-4 58	10.01208	17	8	.20
40262.0	46.35 7	245.610 3	86.532 1	.1888 1	.0767 1	8.66751 1	.1222E-4 59	10.0120	17	8	.23
40264.0	44.18 1	245.338 3	86.531 1	.18899 3	.41174 2	8.66756 1	.1018E-4 88	10.01200	18	8	.21
40266.0	42.01 1	245.063 3	86.507 8	.18915 3	.74686 2	8.66757 1	.985E-5 45	10.01199	22	8	.29
40268.0	39.84 1	244.792 2	86.509 7	.18932 2	.08206 3	8.66766 1	.1110E-4 36	10.01192	25	8	.24
40270.0	37.669 6	244.518 2	86.499 4	.18939 1	.41735 1	8.667681 4	.1021E-4 27	10.011904	27	8	.22
40272.0	35.506 8	244.241 2	86.491 4	.18944 2	.75271 1	8.667722 6	.797E-5 26	10.011873	29	8	.22
40274.0	33.34 1	243.964 2	86.491 3	.18944 2	.08814 2	8.66772 2	.834E-5 29	10.01187	24	8	.22
40276.0	31.25 6	243.685 3	86.475 6	.18956 6	.4235 1	8.66772 4	.967E-5 62	10.01188	19	8	.28
40278.0	29.0 2	243.412 2	86.484 6	.1895 2	.7593 4	8.6679 1	.1078E-4 42	10.0118	16	8	.16
40280.0	27.4 3	243.158 8	86.539 5	.1900 2	.0938 5	8.6677 2	.971E-5 53	10.0118	14	8	.16
40282.0	24.56 7	242.856 2	86.437 4	.18958 4	.4308 1	8.66795 4	.696E-5 34	10.01170	19	8	.24
40284.0	22.32 2	242.578 2	86.438 3	.18958 3	.76675 3	8.66798 1	.661E-5 36	10.01168	25	8	.28
40286.0	20.090 8	242.301 2	86.437 2	.18954 3	.10272 1	8.668008 7	.697E-5 38	10.011653	26	8	.27
40288.0	17.857 5	242.023 2	86.430 2	.18945 2	.438757 8	8.668044 3	.641E-5 33	10.011625	32	8	.31
40290.0	15.612 4	241.746 2	86.426 2	.18940 2	.774863 8	8.668062 4	.554E-5 50	10.011611	24	8	.28
40292.0	13.375 4	241.466 3	86.418 3	.18932 3	.111007 8	8.668099 5	.33E-5 18	10.011582	18	8	.22
40294.0	11.115 8	241.190 2	86.418 4	.18912 3	.44724 1	8.668129 5	.609E-5 55	10.011559	20	8	.27
40296.0	8.91 1	240.907 3	86.372 7	.18910 4	.78341 2	8.66818 2	.641E-5 53	10.01152	19	8	.26
40298.0	6.60 1	240.630 3	86.376 7	.18898 4	.11983 2	8.66822 1	.66E-5 16	10.01149	21	8	.23
40300.0	4.25 3	240.349 2	86.365 8	.18894 3	.45636 5	8.66829 5	.516E-5 38	10.01143	23	8	.22
40302.0	1.964 8	240.071 1	86.376 4	.18889 2	.79282 1	8.668268 8	.588E-5 18	10.011452	20	8	.15
40304.0	359.9 2	239.791 3	86.37 1	.18871 6	.1288 3	8.6685 2	.1030E-4 84	10.0112	16	8	.19
40306.0	357.45 8	239.512 3	86.36 1	.18868 5	.4658 1	8.6682 2	.737E-5 58	10.0115	16	8	.14
40308.0	355.16 4	239.231 3	86.348 9	.18855 4	.80245 7	8.66836 1	.571E-5 39	10.01138	17	8	.19
40310.0	352.94 8	238.946 4	86.34 1	.18847 6	.1390 1	8.66850 6	.357E-5 61	10.01127	17	8	.23
40312.0	350.50 3	238.669 4	86.34 1	.18854 5	.47600 6	8.66849 3	.330E-5 66	10.01128	20	8	.32
40314.0	348.10 4	238.382 4	86.32 1	.18854 7	.81288 7	8.66847 4	.56E-5 12	10.01130	20	8	.42
40316.0	346.1 2	238.111 7	86.31 3	.1882 2	.1490 4	8.6680 2	.105E-4 12	10.0116	15	8	.25
40318.0	345.1 1	237.80 1	86.15 7	.187 1	.484 2	8.6679 5	.213E-4 22	10.0118	12	8	.29
40320.0	341.7 2	237.55 1	86.30 4	.1880 3	.8222 4	8.6688 2	.2135E-4 99	10.0111	10	8	.09
40322.0	338.9 6	237.26 1	86.29 5	.1884 9	.160 1	8.667 3	.98E-5 74	10.012	10	8	.35

Table 2 (Cont.)

T	ω	Ω	i	e	M	n	$\hbar/2$	a	N	D	σ
40326.0	334.39 7	236.690 6	86.28 1	.1883 1	.8346 1	8.66881 4	.289E-4 11	10.01104	17	8	.37
40328.0	331.86 2	236.411 5	86.292 9	.18872 6	.17250 3	8.66868 2	.396E-4 12	10.01114	20	8	.22
40330.0	329.29 6	236.112 9	86.28 1	.1901 2	.51055 7	8.66924 3	.755E-4 41	10.01070	20	8	.22
40332.0	327.19 3	235.850 9	86.30 1	.1891 1	.84876 4	8.66932 2	.435E-4 34	10.01064	21	8	.22
40334.0	324.84 4	235.556 1	86.31 3	.1894 1	.18751 7	8.66947 4	.374E-4 10	10.01052	16	8	.24
40336.0	324. 1	235.27 1	86.25 7	.187 2	.524 2	8.6686 8	.466E-4 35	10.0112	12	8	.25
40340.0	317.2 5	234.681 5	86.06 3	.191 1	.2070 8	8.6699 2	.874E-4 12	10.0102	18	8	.27
40342.0	315.5 1	234.406 5	86.09 3	.1902 4	.5467 2	8.6706 2	.881E-4 12	10.0097	16	8	.28
40344.0	313.08 3	234.106 6	86.10 3	.1906 1	.88825 3	8.67085 6	.726E-4 29	10.00946	16	8	.33
40346.0	310.64 8	233.822 6	86.14 3	.1912 2	.2304 1	8.67119 5	.724E-4 12	10.00920	15	8	.24
40348.0	308.4 2	233.554 4	86.23 3	.1912 7	.5728 4	8.6713 2	.875E-4 16	10.0091	12	8	.12
40350.0	306.0 1	233.269 7	86.23 7	.1917 4	.9161 2	8.67178 4	.1137E-3 44	10.00875	12	8	.11
40352.0	303.5 1	232.986 4	86.27 2	.1925 3	.2605 2	8.6721 1	.1242E-3 15	10.0085	12	8	.13
40354.0	301.4 1	232.69 1	86.26 6	.1926 5	.6054 1	8.6730 2	.1222E-3 49	10.0078	10	8	.07
40356.0	299.4 9	232.40 1	86.25 8	.192 3	.951 1	8.6731 4	.1067E-3 69	10.0077	10	8	.25
40358.0	296.5 6	232.11 3	86.3 3	.194 3	.194 3	8.6736 2	.1038E-3 94	10.0074	10	8	.14
40360.0	294.5 2	231.81 2	86.2 4	.1934 8	.6463 2	8.67419 8	.1248E-3 63	10.00690	8	8	.04
40362.0	292.29 7	231.51 2	86.1 1	.1931 4	.99496 7	8.67463 2	.1421E-3 18	10.00656	8	8	.03
40364.0	290.03 4	231.234 9	86.25 6	.1933 2	.34481 4	8.67532 1	.1582E-3 29	10.00603	10	8	.10
40366.0	287.578 8	230.946 3	86.35 1	.19458 2	.69612 2	8.67584 1	.1529E-3 14	10.00563	14	8	.17
40368.0	285.247 5	230.662 3	86.35 1	.19516 1	.04853 2	8.67643 1	.1319E-3 14	10.00518	20	8	.25
40370.0	282.939 7	230.361 4	86.35 2	.19561 1	.40196 2	8.67695 1	.12729E-3 93	10.00478	23	8	.35
40372.0	280.640 8	230.071 4	86.35 2	.19606 1	.75634 3	8.67744 1	.1452E-3 11	10.00440	23	8	.36
40374.0	278.359 8	229.771 3	86.20 7	.19662 1	.11185 3	8.67805 1	.1576E-3 13	10.00393	22	8	.24
40376.0	276.06 1	229.479 3	86.18 9	.19710 2	.46868 3	8.67867 2	.1679E-3 20	10.00346	17	8	.29
40378.0	273.792 7	229.182 3	86.26 9	.197660 9	.82674 2	8.67939 1	.16179E-3 80	10.00291	17	8	.23
40380.0	271.518 7	228.887 2	86.26 5	.19820 1	.18614 2	8.68000 1	.14702E-3 89	10.00244	19	8	.21
40382.0	269.248 7	228.593 3	86.26 4	.19872 1	.54670 3	8.68053 1	.1362E-3 19	10.00202	18	8	.25
40384.0	266.987 7	228.294 3	86.25 2	.19922 2	.90831 3	8.68106 1	.1394E-3 11	10.00162	24	8	.24
40386.0	264.733 5	227.995 3	86.24 1	.19975 1	.27098 2	8.68161 1	.1531E-3 25	10.00120	20	8	.17
40388.0	262.483 4	227.698 3	86.24 1	.20027 2	.63487 2	8.68223 1	.15317E-3 84	10.00072	18	8	.17
40390.0	260.220 6	227.404 4	86.25 2	.20079 2	.00005 2	8.68285 1	.1389E-3 15	10.00025	20	8	.20
40392.0	257.969 4	227.110 3	86.29 2	.20132 2	.36630 2	8.68339 1	.1161E-3 13	9.99984	16	8	.16
40394.0	255.705 4	226.813 2	86.28 2	.20186 1	.73353 1	8.683803 6	.936E-4 14	9.999520	16	8	.16
40396.0	253.45 1	226.514 7	86.30 5	.20235 4	.10148 4	8.68411 2	.637E-4 12	9.99928	14	8	.16
40398.0	251.214 5	226.215 3	86.32 4	.20287 1	.46988 2	8.684276 8	.343E-4 11	9.999158	12	8	.19
40400.0	248.97 5	225.912 5	86.33 7	.2034 2	.83856 9	8.68432 6	.17E-4 35	9.99912	10	8	.17
40402.0	246.75 1	225.613 5	86.32 6	.20391 5	.20729 7	8.6844 1	.175E-4 36	9.9991	10	8	.18
40404.0	244.509 5	225.313 3	86.31 4	.20435 2	.57619 2	8.68446 2	.182E-4 14	9.99902	12	8	.20
40406.0	242.282 6	225.014 4	86.30 5	.20487 3	.94524 2	8.68455 1	.120E-4 26	9.99895	12	8	.13
40408.0	240.1 4	224.68 2	86.1 3	.205 1	.3144 6	8.6846 5	.185E-4 75	9.9989	14	8	1.43
40416.0	230.1 3	223.60 3	86.6 2	.2040 9	.7937 4	8.68494 4	.1845E-4 51	9.99864	12	8	.09
40418.0	230. 4	223.20 2	86.24 5	.21 1	.161 5	8.685 2	.16E-4 40	9.998	11	8	.33
40420.0	226.76 3	222.912 3	86.223 8	.2078 1	.53183 5	8.68499 2	.115E-4 16	9.99861	17	8	.20
40422.0	224.50 1	222.608 3	86.224 7	.20803 5	.90188 1	8.68503 2	.1060E-4 65	9.99858	17	8	.20
40424.0	222.262 8	222.305 4	86.213 3	.20830 5	.27196 1	8.685050 5	.1265E-4 88	9.998567	19	8	.19
40426.0	220.037 8	222.000 3	86.208 4	.20857 5	.642118 9	8.685108 4	.161E-4 12	9.998523	21	8	.19

Table 2 (Cont.)

T	ω	Ω	I	e	M	n	b/2	a	N	D	o
40428.0	217.81 1	221.695 4	86.193 4	.20886 6	.01241 1	8.685154 7	.1477E-4 74	9.998487	22	8	.25
40430.0	215.573 9	221.390 4	86.191 4	.20910 6	.382812 8	8.685221 5	.1273E-4 70	9.998436	23	8	.28
40432.0	213.34 1	221.094 5	86.179 4	.20934 8	.753310 8	8.685264 5	.130E-4 66	9.998403	27	8	.26
40434.0	211.097 9	220.784 3	86.174 3	.20948 5	.123890 7	8.685300 4	.1086E-4 46	9.998375	30	8	.23
40436.0	208.846 8	220.477 2	86.169 2	.20961 4	.694566 8	8.685362 5	.1156E-4 68	9.998328	28	8	.26
40438.0	206.593 6	220.172 2	86.165 2	.20975 3	.865343 7	8.685343 3	.1331E-4 29	9.998292	32	8	.23
40440.0	204.35 1	219.865 2	86.155 4	.20997 5	.23622 1	8.685481 9	.1347E-4 46	9.998236	25	8	.18
40442.0	202.12 2	219.558 3	86.156 6	.21016 5	.60719 3	8.68552 2	.1381E-4 95	9.99821	23	8	.23
40444.0	199.86 2	219.250 2	86.146 6	.21026 5	.97830 4	8.68555 1	.1083E-4 34	9.99818	22	8	.11
40446.0	197.65 3	218.939 2	86.148 6	.21041 4	.34941 5	8.6855 1	.984E-5 42	9.9982	18	8	.12
40448.0	195.31 8	218.631 2	86.146 9	.21048 9	.7208 1	8.68569 6	.887E-5 46	9.99807	18	8	.16
40450.0	192.7 5	218.34 3	86.142	.2103 5	.0928 9	8.6859 2	.80E-5 15	9.9979	14	8	.13
40452.0	190.4 2	218.04 1	86.02 8	.2104 2	.4643 3	8.6856 1	.111E-4 13	9.9981	12	8	.11
40454.0	188.0 3	217.73 2	86.0 2	.2105 2	.8361 6	8.6857 2	.6E-5 32	9.9981	8	8	.04
40452.0	178.8 1	216.471 5	86.052 6	.21105 6	.3231 2	8.68576 6	.203E-4 53	9.99802	12	8	.15
40464.0	176.71 3	216.158 4	86.052 5	.21133 3	.69467 6	8.68582 5	.62E-5 22	9.99798	12	8	.15
40466.0	174.49 3	215.844 6	86.047 7	.21148 4	.06655 5	8.68601 2	.1349E-4 92	9.99783	17	8	.17
40468.0	172.18 2	215.538 4	86.037 4	.21156 4	.43868 3	8.686073 8	.1442E-4 73	9.997782	18	8	.30
40470.0	169.92 1	215.231 4	86.029 3	.21169 3	.81085 2	8.68616 1	.182E-4 28	9.99771	21	8	.32
40472.0	167.590 5	214.922 3	86.025 2	.21184 3	.183294 7	8.686291 4	.3341E-4 46	9.997615	24	8	.29
40474.0	165.255 6	214.604 4	86.017 3	.21200 4	.556020 9	8.686450 5	.4803E-4 90	9.997493	22	8	.27
40476.0	162.915 9	214.292 3	86.006 3	.21219 3	.92914 2	8.686671 6	.5460E-4 37	9.997324	29	8	.41
40478.0	160.51 1	213.981 2	85.996 3	.21228 2	.30280 2	8.686936 8	.5487E-4 62	9.997120	23	8	.29
40480.0	158.13 2	213.669 2	85.985 2	.21250 3	.67688 3	8.68708 2	.5062E-4 44	9.99701	26	8	.34
40482.0	155.84 1	213.350 3	85.982 2	.21281 2	.05120 2	8.68726 1	.492BE-4 32	9.99688	32	8	.37
40484.0	153.572 9	213.039 2	85.975 2	.21312 3	.42588 2	8.687495 9	.5699E-4 34	9.996692	32	8	.35
40486.0	151.246 7	212.721 2	85.970 2	.21343 2	.80110 1	8.687763 6	.7446E-4 33	9.996487	33	8	.29
40488.0	148.930 9	212.405 2	85.965 2	.21374 2	.17690 2	8.687101 6	.9334E-4 22	9.996228	35	8	.28
40490.0	146.550 8	212.087 2	85.963 2	.21400 2	.55356 1	8.688513 5	.10567E-3 31	9.995912	34	8	.30
40492.0	144.222 7	211.774 3	85.951 2	.21437 2	.93099 1	8.688968 7	.10811E-3 49	9.995863	30	8	.27
40494.0	142.868 5	211.459 2	85.948 2	.21468 2	.309339 9	8.689393 5	.10296E-3 33	9.995237	32	8	.23
40496.0	139.522 6	211.143 2	85.947 2	.21501 2	.68850 1	8.689781 5	.9602E-4 34	9.994941	27	8	.25
40498.0	137.18 2	210.818 2	85.945 2	.21591 4	.06840 3	8.69014 1	.9983E-4 93	9.99467	21	8	.21
40500.0	134.845 5	210.501 1	85.934 1	.21580 3	.449080 9	8.690584 3	.11668E-3 23	9.994326	24	8	.20
40502.0	132.488 6	210.177 2	85.931 1	.21622 1	.83072 1	8.691083 7	.13963E-3 51	9.993943	24	8	.18
40504.0	130.144 5	209.860 1	85.932 1	.21662 1	.21346 1	8.691681 7	.15611E-3 42	9.993485	28	8	.25
40506.0	127.799 5	209.542 1	85.9316 8	.21704 1	.59747 1	8.692328 4	.15834E-3 68	9.992990	32	8	.25
40508.0	125.472 5	209.218 2	85.928 1	.21753 1	.98273 1	8.692954 6	.15380E-3 61	9.992511	29	8	.22
40510.0	123.130 7	208.890 2	85.930 2	.21797 1	.36926 2	8.693571 6	.14449E-3 75	9.992083	29	8	.32
40512.0	120.819 4	208.575 1	85.9267 8	.218516 6	.756887 7	8.694134 3	.14417E-3 43	9.991607	29	8	.19
40514.0	118.487 8	208.254 2	85.925 2	.21900 1	.14570 1	8.694717 6	.15654E-3 42	9.991161	28	8	.25
40516.0	116.15 1	207.931 2	85.922 1	.21952 2	.53576 2	8.69537 1	.17786E-3 49	9.99066	25	8	.28
40518.0	113.82 1	207.606 2	85.924 2	.22010 2	.92723 2	8.696137 6	.19905E-3 46	9.990075	23	8	.24
40520.0	111.52 1	207.277 2	85.930 1	.22060 2	.32026 2	8.696952 9	.20990E-3 43	9.988451	28	8	.23
40522.0	109.206 7	206.953 1	85.9265 8	.22116 1	.71500 1	8.697803 4	.20621E-3 31	9.988800	33	8	.22
40524.0	106.899 4	206.627 1	85.9280 9	.221719 7	.111391 7	8.698618 5	.19581E-3 30	9.988176	37	8	.21
40526.0	104.580 4	206.301 2	85.928 1	.222275 7	.509367 8	8.699375 5	.18645E-3 24	9.987597	37	8	.23

Table 2 (Cont.)

T	ω	Ω	I	e	M	n	$\hbar/2$	a	N	D	σ
40528.0	102.280 6	205.974 2	85.931 1	.22286 1	.90878 1	8.700086 4	.18790E-3 49	9.987052	36	8	.31
40530.0	99.964 6	205.646 2	85.933 1	.223450 7	.30970 1	8.700861 4	.20306E-3 24	9.986462	49	8	.25
40532.0	97.665 5	205.316 1	85.9342 8	.224025 6	.712215 9	8.701703 4	.22108E-3 40	9.985818	49	8	.24
40534.0	95.374 4	204.988 1	85.9353 6	.224612 5	.116487 7	8.702605 3	.23016E-3 23	9.985129	52	8	.25
40536.0	93.081 4	204.656 1	85.9378 7	.225186 5	.522626 7	8.703533 3	.22515E-3 24	9.984420	55	8	.26
40538.0	90.801 4	204.328 1	85.9385 7	.225760 6	.930552 8	8.704421 4	.21184E-3 37	9.983741	40	8	.25
40540.0	88.513 5	203.996 1	85.9393 7	.226335 6	.340190 9	8.705221 6	.19592E-3 50	9.983130	41	8	.26
40542.0	86.213 4	203.665 1	85.9419 6	.226908 5	.731411 8	8.705991 4	.18991E-3 30	9.982542	50	8	.24
40544.0	83.938 4	203.3330 9	85.9440 7	.227485 5	.164090 8	8.706748 3	.19679E-3 39	9.981964	54	8	.23
40546.0	81.652 3	203.0009 8	85.9446 7	.228060 4	.578364 6	8.707554 3	.20563E-3 21	9.981349	68	8	.23
40548.0	79.374 2	202.6655 8	85.944 1	.228613 5	.994284 4	8.708387 3	.20559E-3 28	9.980713	62	8	.25
40550.0	77.095 3	202.3317 8	85.944 2	.229158 8	.411860 6	8.709200 2	.19334E-3 43	9.980098	51	8	.25
40552.0	74.823 3	201.998 1	85.944 3	.229713 8	.830990 5	8.709933 3	.16827E-3 37	9.979533	56	8	.22
40554.0	72.554 3	201.6620 9	85.945 2	.230207 7	.251468 5	8.710552 3	.13783E-3 46	9.979061	41	8	.18
40556.0	70.282 2	201.327 2	85.942 3	.23074 1	.673063 5	8.711041 3	.10158E-3 78	9.978688	45	8	.20
40558.0	68.012 3	200.994 2	85.941 3	.23128 1	.095473 6	8.711366 4	.58380E-4 71	9.978440	46	8	.23
40560.0	65.740 3	200.657 1	85.942 3	.231806 9	.518286 7	8.711493 3	.37711E-4 39	9.978344	33	8	.29
40562.0	63.444 5	200.323 1	85.924 3	.23240 2	.041404 2	8.711608 4	.31475E-4 52	9.978257	37	8	.33
40564.0	61.214 3	199.984 1	85.924 2	.232825 7	.364731 5	8.711752 2	.3161E-4 60	9.978147	51	8	.31
40566.0	58.948 2	199.6469 7	85.922 1	.233271 5	.788344 4	8.711882 2	.3067E-4 23	9.978048	55	8	.26
40568.0	56.669 2	199.3099 6	85.914 1	.233718 5	.212219 3	8.712001 2	.3075E-4 24	9.977957	60	8	.21
40570.0	54.400 2	198.9704 6	85.913 1	.234141 5	.636322 4	8.712121 2	.3030E-4 17	9.977866	64	8	.22
40572.0	52.123 4	198.6327 9	85.910 2	.234531 7	.060678 6	8.712247 3	.3074E-4 26	9.977770	49	8	.32
40574.0	49.856 3	198.2902 8	85.902 2	.234923 6	.485263 5	8.712361 2	.3098E-4 26	9.977683	52	8	.34
40576.0	47.591 3	197.952 1	85.894 2	.235240 7	.910089 6	8.712493 3	.3301E-4 27	9.977583	44	8	.37
40578.0	45.316 3	197.6125 9	85.882 2	.235580 5	.335201 5	8.712640 3	.3376E-4 35	9.977471	42	8	.30
40580.0	43.032 2	197.2705 8	85.877 2	.235870 6	.760595 4	8.712767 2	.3065E-4 26	9.977375	54	8	.28
40582.0	40.749 3	196.9286 9	85.871 2	.236150 5	.186234 5	8.712885 3	.2862E-4 20	9.977285	49	8	.26
40584.0	38.468 3	195.586 1	85.864 2	.612101 7	.812101 6	8.712996 3	.2571E-4 53	9.977200	46	8	.27
40586.0	33.899 3	195.905 1	85.849 2	.236927 8	.464459 7	8.71323 1	.52E-4 14	9.97702	16	4	.23
40590.0	31.609 4	195.551 1	85.826 2	.237096 5	.891003 6	8.713358 6	.242E-4 11	9.976924	24	4	.18
40592.0	29.299 4	195.210 1	85.823 2	.237272 6	.317770 7	8.713432 7	.215E-4 22	9.976868	22	4	.22
40594.0	26.985 9	194.866 2	85.812 4	.237455 9	.74472 2	8.71352 2	.170E-4 29	9.97680	21	4	.33
40596.0	24.672 4	194.522 1	85.805 2	.237698 6	.171826 7	8.713607 7	.172E-4 13	9.976735	25	4	.27
40598.0	22.358 6	194.179 2	85.796 4	.23780 1	.59909 1	8.71368 1	.194E-4 60	9.97668	20	4	.40
40600.0	20.05 2	193.831 6	85.79 1	.23793 2	.02651 3	8.71376 4	.196E-4 55	9.97661	14	4	.27
40602.0	17.722 5	193.481 2	85.778 4	.23809 1	.454144 8	8.713872 9	.284E-4 15	9.976532	20	4	.25
40604.0	15.399 6	193.134 2	85.766 5	.23819 2	.88200 1	8.71403 2	.246E-4 15	9.97641	19	4	.29
40606.0	13.04 2	192.791 3	85.768 8	.23831 2	.31012 3	8.71407 3	.192E-4 19	9.97638	18	4	.43
40608.0	10.696 8	192.440 2	85.748 3	.23852 1	.73836 1	8.71418 2	.241E-4 17	9.97630	24	4	.28
40610.0	8.4 1	192.101 7	85.743 5	.2387 1	.1673 5	8.716 1	.15E-2 15	9.975	15	4	.27
40618.0	358.88 2	190.690 3	85.692 7	.23910 4	.88214 4	8.71468 2	.178E-3 32	9.97592	16	4	.29
40620.0	356.508 6	190.337 2	85.684 4	.23932 1	.311606 9	8.714831 8	.617E-3 18	9.975801	28	4	.23
40622.0	354.135 4	189.989 1	85.676 3	.239500 9	.741522 8	8.715087 8	.644E-3 15	9.975606	27	4	.22
40624.0	351.756 7	189.635 2	85.662 4	.23968 1	.17198 1	8.71536 1	.688E-4 21	9.97540	23	4	.26
40626.0	349.383 8	189.280 2	85.651 7	.23984 2	.60296 1	8.71557 1	.648E-4 21	9.97524	22	4	.41
40628.0	347.01 1	188.927 2	85.643 5	.23999 2	.03444 2	8.71587 1	.667E-4 22	9.97501	20	4	.31

Table 2 (Cont.)

T	w	Ω	i	e	M	n	$\delta/2$	a	N	D	σ
40630.0	344.613 6	188.574 2	85.641 5	.24021 1	.46651 1	8.71619 1	.790E-4 32	9.97476	23	4	.33
40632.0	342.196 5	188.225 2	85.645 4	.24045 1	.899262 9	8.71656 1	.1007E-3 20	9.97449	23	4	.30
40634.0	339.816 6	187.863 2	85.616 4	.24071 1	.332772 9	8.717009 7	.1231E-3 18	9.974141	25	4	.44
40636.0	337.412 6	187.508 2	85.612 3	.24101 2	.767300 9	8.71754 1	.1367E-3 28	9.97373	26	4	.32
40638.0	335.003 6	187.154 2	85.611 4	.24134 2	.20288 2	8.71800 2	.1422E-3 94	9.97338	18	4	.33
40640.0	332.621 7	186.798 3	85.622 5	.24159 2	.63944 3	8.71840 5	.84E-4 21	9.97308	12	4	.25
40642.0	330.211 1	186.435 2	85.598 5	.24192 3	.07708 2	8.71896 2	.98E-4 26	9.97266	19	4	.26
40644.0	327.832 4	186.079 1	85.585 3	.24218 1	.51554 1	8.71947 1	.1437E-3 60	9.97226	21	4	.16
40646.0	325.438 5	185.721 2	85.581 4	.24250 1	.95511 1	8.72001 1	.126E-3 13	9.97185	15	4	.17
40648.0	323.035 7	185.359 2	85.583 5	.24290 2	.39580 1	8.72064 1	.1680E-3 27	9.97137	18	4	.25
40650.0	320.626 6	184.995 2	85.565 4	.24335 2	.837830 8	8.721366 8	.1924E-3 22	9.970822	23	4	.20
40652.0	318.236 4	184.633 2	85.562 3	.24373 2	.281369 7	8.722161 8	.1969E-3 49	9.970216	26	4	.24
40654.0	315.829 4	184.274 2	85.564 3	.24420 2	.726523 8	8.72296 2	.1961E-3 28	9.96961	22	4	.20
40656.0	313.433 5	183.914 3	85.568 5	.24464 2	.173216 8	8.723724 9	.1875E-3 42	9.969026	21	4	.22
40658.0	311.017 8	183.537 3	85.570 7	.24506 3	.62141 2	8.72442 3	.175E-3 16	9.96850	15	4	.23
40660.0	308.62 3	183.177 3	85.56 1	.2455 1	.07100 3	8.72514 3	.179E-3 27	9.96795	15	4	.17
40662.0	306.258 4	182.820 1	85.558 3	.24599 2	.521967 6	8.725891 7	.2045E-3 31	9.967377	30	4	.19
40664.0	303.855 3	182.452 1	85.552 3	.24655 1	.974599 8	8.72673 1	.2217E-3 51	9.96674	30	4	.21
40666.0	301.462 3	182.085 1	85.559 3	.24708 1	.428998 8	8.727660 9	.2452E-3 39	9.966032	27	4	.16
40668.0	299.076 3	181.719 2	85.559 4	.24763 2	.885322 8	8.72864 1	.2569E-3 26	9.96528	33	4	.21
40670.0	296.701 3	181.352 2	85.555 4	.24814 1	.343675 8	8.72967 1	.2344E-3 48	9.96450	33	4	.29
40672.0	294.324 4	180.989 2	85.518 7	.24867 3	.80394 1	8.73061 1	.2629E-3 76	9.96379	25	4	.36
40674.0	291.548 7	180.637 6	85.51 1	.24915 4	.26620 3	8.73148 3	.207E-3 14	9.96313	17	4	.43
40676.0	289.557 4	180.243 2	85.563 4	.24973 2	.73025 1	8.73245 2	.227E-3 14	9.96239	15	4	.15
40678.0	287.179 6	179.873 4	85.56 1	.25035 5	.19616 1	8.73343 2	.2459E-3 75	9.96164	20	4	.24
40680.0	284.803 5	179.497 3	85.546 8	.25092 4	.664060 9	8.73446 1	.2717E-3 70	9.96086	21	4	.18
40682.0	282.432 2	179.127 2	85.555 5	.25148 1	.134066 9	8.73552 1	.2989E-3 42	9.96006	31	4	.24
40684.0	280.065 2	178.756 2	85.557 4	.25204 2	.60637 1	8.73674 2	.293E-3 12	9.95913	29	4	.24
40686.0	277.701 2	178.383 2	85.559 5	.25265 2	.08098 2	8.73785 2	.203E-3 13	9.95829	19	4	.17
40688.0	275.336 1	178.0113 9	85.561 2	.253208 5	.557943 5	8.739003 6	.2615E-3 64	9.957414	28	4	.11
40690.0	272.968 2	177.636 1	85.561 3	.253773 9	.037032 7	8.74005 1	.2393E-3 44	9.95662	40	4	.22
40692.0	270.602 5	177.259 7	85.58 1	.2543 1	.51807 4	8.74099 5	.241E-3 67	9.95591	22	4	.34
40694.0	268.250 4	176.891 4	85.570 7	.25515 7	.00116 3	8.74201 5	.267E-3 30	9.95514	20	4	.32
40696.0	265.885 2	176.509 2	85.578 5	.25546 1	.48621 1	8.74308 1	.2653E-3 65	9.95432	35	4	.34
40698.0	263.523 2	176.132 2	85.571 5	.25604 1	.97336 1	8.74412 2	.2819E-3 68	9.95353	29	4	.29
40700.0	261.180 2	175.746 2	85.570 4	.25661 2	.46264 1	8.74510 2	.2539E-3 63	9.95279	26	4	.14
40702.0	258.827 1	175.3684 8	85.575 2	.257133 6	.953919 5	8.746097 7	.2337E-3 29	9.952035	36	4	.14
40704.0	256.468 2	174.990 1	85.573 3	.25768 2	.447033 7	8.746955 9	.1924E-3 31	9.951384	31	4	.16
40706.0	254.109 3	174.612 2	85.566 5	.25820 3	.94170 1	8.74768 2	.1728E-3 45	9.95084	24	4	.27
40708.0	251.757 2	174.228 1	85.570 4	.25873 1	.437737 8	8.74831 1	.1216E-3 49	9.95036	25	4	.24
40710.0	249.404 2	173.848 1	85.568 3	.25926 1	.934750 7	8.74867 1	.771E-4 30	9.95010	33	4	.19
40712.0	247.057 2	173.465 1	85.569 3	.25977 2	.432356 6	8.748916 8	.699E-4 30	9.949900	33	4	.18
40714.0	244.714 2	173.083 1	85.564 3	.26028 1	.930506 6	8.749198 8	.626E-4 27	9.949687	31	4	.15
40716.0	242.359 4	172.701 2	85.559 5	.26072 2	.42919 1	8.74948 1	.740E-4 35	9.94948	30	4	.19
40718.0	240.016 3	172.316 1	85.560 4	.26124 1	.928464 6	8.749769 8	.739E-4 24	9.949254	25	4	.17
40720.0	237.662 2	171.936 1	85.547 2	.26167 1	.428338 7	8.75008 1	.74E-4 15	9.94902	23	4	.16
40722.0	235.314 8	171.550 2	85.541 5	.26212 4	.92882 2	8.75040 2	.800E-4 85	9.94878	22	4	.18
40724.0	232.936 6	171.161 2	85.544 5	.26238 3	.429925 8	8.750705 9	.795E-4 32	9.948546	23	4	.27

Table 2 (Cont.)

T	w	R	I	e	M	n	n/2	a	N	D	o
40726.0	230.596 4	170.777 2	85.530 4	.26280 2	.931610 8	8.75097 1	.751E-4 30	9.94635	23	4	.25
40728.0	228.251 3	170.391 1	85.517 4	.26321 2	.433924 5	8.751315 6	.770E-4 16	9.948085	21	4	.17
40730.0	225.897 4	170.005 2	85.507 4	.26358 2	.936882 4	8.751638 6	.808E-4 22	9.936882	20	4	.15
40732.0	223.535 4	169.616 2	85.503 4	.26392 2	.440465 7	8.75193 1	.685E-4 25	9.94762	20	4	.16
40734.0	221.163 5	169.225 2	85.496 4	.26418 2	.944617 6	8.752241 9	.807E-4 13	9.947384	18	4	.16
40736.0	218.81 1	168.838 4	85.482 9	.26449 2	.44937 1	8.75251 2	.24E-4 50	9.94718	12	4	.12
40738.0	216.45 2	168.444 4	85.485 8	.26477 3	.95469 7	8.7529 1	.79E-4 23	9.9469	12	4	.36
40740.0	214.09 1	168.044 4	85.490 7	.26510 4	.46059 4	8.75305 3	.11E-3 12	9.94677	14	4	.35
40746.0	206.98 7	168.881 5	85.44 1	.2659 1	.98136 2	8.75380 4	-.22E-3 35	9.94621	8	4	.13
40760.0	190.1 1	164.16 2	85.28 4	.267 2	.5456 2	8.7556 2	.06E-3 15	9.9449	8	4	.18
40762.0	187.8 1	163.73 1	85.36 2	.2671 4	.053 2	8.758 2	.73E-2 56	9.943	8	4	.23
40764.0	185.33 2	163.335 4	85.335 8	.26791 3	.5668 1	8.75612 7	.229E-3 47	9.94444	10	4	.23
40766.0	182.90 1	162.956 6	85.29 1	.26807 2	.07880 2	8.75576 4	.695E-4 43	9.94472	12	4	.40
40768.0	180.38 3	162.535 2	85.318 4	.26823 4	.59085 4	8.75599 4	.05E-4 17	9.94455	10	4	.19
40770.0	177.99 6	162.130 4	85.322 6	.26855 6	.10318 9	8.75648 9	.827E-4 39	9.94417	8	4	.16
40772.0	175.4 1	161.737 8	85.29 1	.2686 1	.6165 2	8.7565 2	.919E-4 46	9.9442	10	4	.47
40774.0	173.157 4	161.328 3	85.287 5	.26905 1	.13007 1	8.75709 1	.847E-4 53	9.94371	9	4	.15
40778.0	168.287 2	160.520 2	85.2531 8	.269490 9	.160131 5	8.758173 3	.917E-4 50	9.942896	8	4	.06
40780.0	165.850 5	160.129 3	85.247 5	.269977 7	.676876 8	8.75865 1	.1386E-3 23	9.94253	13	4	.15
40782.0	163.407 9	159.729 2	85.236 4	.270339 1	.19470 2	8.75930 2	.356E-3 68	9.94204	10	4	.10
40784.0	160.95 1	159.331 2	85.221 6	.27065 2	.71320 8	8.76021 6	.345E-3 27	9.94136	8	4	.11
40786.0	158.508 9	158.914 3	85.216 4	.27105 3	.23395 1	8.76037 2	.68E-5 23	9.94124	12	4	.28
40788.0	156.059 5	158.513 2	85.214 3	.27139 2	.75515 1	8.76099 2	.1687E-3 36	9.94077	11	4	.16
40790.0	153.5 4	158.093 6	85.240 9	.2781 6	.2781 6	8.7622 6	.35E-4 43	9.9398	8	4	.21
40792.0	151.22 4	157.692 7	85.22 1	.27224 2	.80104 9	8.76237 2	.48E-3 11	9.93972	10	4	.39
40794.0	148.738 9	157.287 4	85.20 1	.27264 3	.32742 2	8.76334 2	.218E-3 15	9.93899	14	4	.55
40796.0	146.30 1	156.883 2	85.186 5	.27311 2	.85493 2	8.76423 1	.216E-3 33	9.93832	13	4	.23
40798.0	143.832 9	156.476 5	85.166 7	.27362 2	.38427 1	8.76506 3	.2040E-3 48	9.93767	14	4	.63
40800.0	141.3 1	156.067 4	85.143 9	.27409 7	.9154 1	8.7661 1	.2198E-3 42	9.9369	12	4	.27
40802.0	138.6 1	155.671 8	85.11 2	.27470 5	.4484 2	8.7671 2	.2173E-3 25	9.9361	10	4	.29
40804.0	136.2 2	155.21 1	85.22 2	.2753 3	.9829 3	8.7677 4	.10E-3 14	9.9357	8	4	.13
40806.0	131.643 3	154.41 1	85.148 2	.27611 1	.057505 5	8.769920 7	.2864E-3 18	9.934022	19	4	.31
40810.0	129.210 2	153.9898 9	85.145 2	.276688 5	.598443 4	8.771019 5	.2722E-3 18	9.933193	28	4	.22
40812.0	126.771 4	153.579 2	85.151 4	.27729 2	.141552 6	8.772098 8	.2711E-3 23	9.932380	24	4	.18
40814.0	124.325 3	153.161 2	85.145 2	.27786 1	.686831 6	8.77317 1	.2817E-3 25	9.93156	17	4	.31
40816.0	121.888 2	152.7403 8	85.144 1	.278403 8	.234373 4	8.774436 4	.3320E-3 14	9.930616	21	4	.26
40818.0	119.46 1	152.317 5	85.143 6	.27897 4	.78451 2	8.7756 1	.09E-4 12	9.9298	10	4	.13
40822.0	114.61 2	151.486 2	85.143 3	.28016 3	.89290 2	8.77853 1	.3495E-3 30	9.92753	14	4	.25
40824.0	112.187 4	151.061 1	85.140 2	.28078 1	.451371 6	8.779987 7	.3717E-3 24	9.926434	17	4	.22
40826.0	109.761 2	150.6392 9	85.144 2	.281378 5	.012817 4	8.781460 5	.3541E-3 14	9.925325	17	4	.16
40828.0	107.321 5	150.218 2	85.134 3	.28200 1	.577142 7	8.782877 7	.3626E-3 17	9.924258	20	4	.20
40830.0	104.911 6	149.789 3	85.140 4	.28257 1	.14436 1	8.78442 1	.4102E-3 36	9.92310	17	4	.40
40832.0	102.50 1	149.364 3	85.149 6	.28316 3	.71492 2	8.78619 2	.459E-3 15	9.92177	11	4	.22
40834.0	100.076 2	148.9396 5	85.149 1	.289146 5	.289146 3	8.788055 4	.4610E-3 11	9.920363	21	4	.16
40836.0	97.665 2	148.5124 6	85.147 1	.284323 6	.867048 3	8.789873 4	.4528E-3 11	9.918996	25	4	.20

Table 2 (Cont.)

T	ω	Ω	i	c	M	n	$\delta/2$	a	N	D	σ
40838.0	95.252 6	148.087 2	85.146 4	.28485 2	.448605 9	8.79174 1	.4656E-3 61	9.91760	16	4	.37
40840.0	93.0 2	147.666 9	85.12 2	.2849 7	.0338 2	8.7934 3	.4300E-3 92	9.9163	10	4	.26
40842.0	90.390 8	147.224 2	85.154 5	.28612 3	.62282 1	8.79530 2	.4823E-3 56	9.91492	15	4	.58
40844.0	88.00 1	146.798 2	85.158 3	.28654 4	.21552 1	8.79745 1	.5216E-3 60	9.91331	15	4	.21
40846.0	85.58 3	146.368 2	85.159 4	.2871 1	.81236 2	8.79935 3	.4552E-3 73	9.91188	14	4	.22
40848.0	83.23 2	145.933 1	85.156 4	.2874 1	.41287 2	8.80123 2	.4841E-3 37	9.91047	15	4	.23
40850.0	80.77 2	145.496 2	85.161 5	.28816 7	.01743 1	8.80332 1	.5316E-3 30	9.90890	20	4	.20
40852.0	78.363 4	145.0619 8	85.161 2	.28861 1	.626174 6	8.805421 5	.5326E-3 16	9.907324	23	4	.21
40854.0	75.901 5	144.629 2	85.164 2	.28830 2	.239110 6	8.807546 7	.5300E-3 34	9.905731	15	4	.21
40856.0	73.55 1	144.195 2	85.158 4	.28947 8	.856269 9	8.90416 2	.5788E-3 87	9.90416	10	4	.19
40858.0	71.13 3	143.757 3	85.158 8	.2900 2	.47785 1	8.81179 2	.3857E-3 50	9.90256	15	4	.21
40860.0	68.7 1	143.317 7	85.158 7	.2907 8	.10279 6	8.81330 6	.520E-3 82	9.90142	11	4	.22
40862.0	66.308 5	142.878 2	85.145 4	.29086 3	.730711 7	8.81468 1	.4120E-3 14	9.90039	16	4	.25
40864.0	63.897 6	142.440 2	85.157 4	.29126 1	.361950 8	8.816624 9	.4341E-3 22	9.898935	24	4	.49
40866.0	61.493 3	141.9978 7	85.139 1	.29164 7	.996622 4	8.818001 5	.31085E-3 84	9.897905	29	4	.17
40868.0	59.086 2	141.5582 9	85.1374 9	.29197 5	.633801 3	8.819196 3	.3076E-3 10	9.897011	27	4	.16
40870.0	56.662 5	141.118 2	85.117 3	.29229 2	.273491 8	8.820647 8	.5082E-3 27	9.895927	19	4	.18
40872.0	54.252 4	140.666 1	85.120 2	.292571 9	.917130 7	8.823010 5	.5307E-3 14	9.894160	20	4	.16
40874.0	51.822 6	140.222 2	85.114 5	.29285 1	.56504 1	8.82485 1	.4281E-3 28	9.89278	20	4	.20
40876.0	49.39 1	139.792 3	85.089 8	.29305 3	.21671 2	8.82724 2	.9005E-3 53	9.89100	20	4	.70
40878.0	46.95 1	139.333 4	85.104 4	.29303 2	.87521 1	8.83081 1	.401E-3 11	9.88834	14	4	.31
40880.0	44.526 4	138.878 2	85.063 4	.29326 1	.538345 9	8.832483 7	.4677E-3 31	9.887087	12	4	.09
40882.0	42.07 2	138.43 1	85.08 2	.29347 7	.20529 5	8.8324 5	.63E-3 17	9.8877	21	4	.10
40884.0	41.1 5	138.00 3	85.14 3	.2948 5	.8751 8	8.8361 4	.526E-3 31	9.8844	16	4	.11
40886.0	37.1 1	137.526 4	85.031 6	.2935 1	.5535 2	8.83884 7	.4467E-3 43	9.88235	12	4	.10
40888.0	34.744 4	137.073 1	85.026 3	.293679 6	.233348 6	8.841274 7	.70011E-3 94	9.880533	23	4	.14
40890.0	32.287 3	136.623 1	85.029 4	.29370 1	.918793 5	8.844111 8	.6343E-3 13	9.878421	35	4	.24
40892.0	29.821 4	136.172 1	85.013 4	.29369 1	.609354 7	8.846402 7	.5676E-3 24	9.876716	31	4	.27
40894.0	27.341 5	135.719 2	85.013 3	.293743 9	.304470 9	8.848773 8	.635E-3 12	9.874952	16	4	.25
40896.0	24.866 8	135.253 3	84.986 8	.29376 2	.00442 3	8.85117 2	.679E-3 15	9.87317	13	4	.30
40898.0	22.404 8	134.795 3	84.960 7	.29376 2	.70992 1	8.85450 2	.750E-3 23	9.87069	14	4	.24
40902.0	17.39 1	133.888 3	84.942 7	.29370 3	.13671 3	8.85896 2	.563E-3 10	9.86738	15	4	.25
40904.0	14.879 6	133.423 2	84.939 6	.29370 2	.85680 1	8.86110 1	.5382E-3 60	9.86579	17	4	.27
40906.0	12.36 1	132.959 1	84.927 4	.29362 9	.58121 7	8.8633 1	.510E-3 14	9.8641	13	4	.15
40908.0	9.848 8	132.504 2	84.907 7	.29369 4	.30968 2	8.86521 2	.506E-3 13	9.86274	17	4	.26
40910.0	7.36 1	132.041 4	84.897 7	.29367 1	.04263 1	8.86788 1	.5879E-3 20	9.86076	20	4	.44
40912.0	4.79 1	131.572 2	84.89 1	.29370 3	.78070 3	8.87048 4	.7328E-3 61	9.85884	15	4	.21
40914.0	2.257 8	131.120 5	84.841 8	.29368 4	.52422 3	8.87291 4	.585E-3 20	9.85704	16	4	.22
40916.0	359.731 5	130.640 2	84.844 3	.29378 9	.272042 7	8.874811 7	.3978E-3 16	9.855631	21	4	.20
40918.0	357.156 6	130.179 2	84.843 4	.29390 1	.023145 8	8.876305 9	.466E-3 21	9.854526	15	4	.13
40920.0	354.596 4	129.710 2	84.826 4	.29402 9	.77749 1	8.87805 1	.4401E-3 21	9.85323	16	4	.13
40922.0	352.049 4	129.238 2	84.802 5	.29416 1	.535282 8	8.87975 1	.4430E-3 33	9.85198	18	4	.17
40924.0	349.497 6	128.770 2	84.803 5	.29425 1	.296671 8	8.881694 8	.539E-3 12	9.850540	18	4	.22
40926.0	346.936 7	128.305 2	84.798 5	.29438 2	.06244 1	8.88427 2	.6929E-3 85	9.84864	14	4	.20
40928.0	344.36 1	127.825 4	84.762 7	.29450 3	.83385 2	8.88750 1	.1059E-2 25	9.84625	14	4	.20
40930.0	341.769 5	127.356 2	84.769 5	.29466 1	.612736 6	8.891137 7	.81936E-3 91	9.843566	22	4	.19
40932.0	339.204 9	126.875 2	84.760 8	.29483 2	.39423 1	8.894316 9	.8046E-3 92	9.841221	17	4	.20

Table 2 (Cont.)

T	w	Ω	i	e	M	n	$\dot{n}/2$	a	N	D	o
40934.0	336.64 1	126.410 3	84.730 9	.29498 3	.19013 2	8.89814 4	.12817E-2 59	9.83840	17	4	.30
40936.0	334.021 8	125.926 3	84.723 6	.29513 3	.99198 2	8.90346 1	.952E-3 75	9.83449	14	4	.11
40938.0	331.35 6	125.455 9	84.73 2	.2956 2	.80253 8	8.9068 1	.8166E-3 44	9.8320	12	4	.14
40940.0	328.81 6	124.98 1	84.72 2	.2956 2	.6195 1	8.91035 6	.118E-2 22	9.82941	12	4	.15
40942.0	326.2 4	124.47 4	84.67 9	.296 1	.4449 5	8.914 1	.957E-3 26	9.827	12	4	.140
40944.0	323.687 7	123.996 5	84.68 1	.29610 3	.27736 1	8.91816 1	.9720E-3 22	9.82368	20	4	.21
40946.0	321.088 3	123.516 2	84.682 5	.29646 1	.117632 4	8.921979 5	.9546E-3 13	9.820875	24	4	.17
40948.0	318.489 5	123.028 3	84.68 7	.29684 2	.965631 8	8.926157 6	.12090E-2 22	9.817811	21	4	.19
40950.0	315.890 4	122.541 3	84.665 8	.29712 3	.82310 1	8.93118 1	.12013E-2 65	9.81413	17	4	.24
40952.0	313.310 4	122.040 3	84.649 6	.29737 2	.690124 8	8.93570 1	.1120E-2 13	9.81082	18	4	.17
40954.0	310.708 2	121.556 2	84.653 4	.29776 1	.566596 3	8.941074 4	.16333E-2 15	9.806892	24	4	.15
40958.0	305.513 4	120.569 2	84.652 7	.29835 2	.359594 5	8.955289 5	.17229E-2 16	9.796515	22	4	.14
40960.0	302.914 3	120.076 2	84.645 6	.29864 2	.27690 1	8.96191 1	.16764E-2 55	9.79169	28	4	.25
40962.0	300.313 2	119.573 2	84.640 5	.29895 2	.207898 9	8.96955 1	.22874E-2 51	9.78613	30	4	.31
40964.0	297.717 2	119.075 2	84.643 5	.29914 1	.156740 7	8.979230 9	.24672E-2 43	9.779099	30	4	.25
40966.0	295.119 6	118.569 7	84.644 6	.29913 9	.12575 9	8.9900 3	.262E-2 34	9.7713	15	4	.10
40970.0	289.89 1	117.569 5	84.637 7	.29927 6	.14256 7	9.0198 4	.187E-2 53	9.7498	14	4	.13
40972.0	287.282 2	117.049 3	84.629 8	.29911 1	.195320 8	9.03461 1	.40810E-2 52	9.73910	25	4	.25
40974.0	284.662 2	116.541 2	84.629 6	.29896 1	.280463 8	9.05067 1	.42841E-2 27	9.72759	25	4	.20
40978.0	279.40 2	115.51 1	84.61 4	.2992 1	.5602 1	9.0909 1	.560E-2 13	9.6988	24	4	1.58
40980.0	276.767 3	114.981 3	84.630 6	.29722 2	.77167 2	9.12317 2	.8391E-2 17	9.67599	27	4	.24
40982.0	274.115 3	114.450 2	84.665 5	.29636 1	.05150 1	9.15699 1	.88364E-2 45	9.65216	34	4	.36
40984.0	271.431 3	113.923 4	84.654 4	.29531 7	.40225 1	9.1943 1	.947E-2 25	9.6260	17	4	.17
40986.0	268.740 3	113.393 2	84.647 4	.29387 4	.82930 1	9.23208 3	.97211E-2 41	9.59976	27	4	.22
40988.0	266.045 2	112.856 1	84.651 4	.292420 7	.334332 8	9.27363 1	.108538E-1 3	9.57107	34	4	.20
40990.0	263.306 6	112.299 3	84.67 1	.29082 1	.92609 2	9.31829 2	.114183E-1 5	9.54047	18	4	.33
40992.0	260.562 6	111.758 5	84.67 5	.28904 1	.60932 2	9.36499 2	.113103E-1 7	9.50873	14	4	.28
40994.0	257.81 1	111.24 1	84.69 7	.28742 5	.38292 6	9.40871 7	.11536E-1 46	9.47926	14	4	1.02
40996.0	255.040 8	110.624 9	84.58 5	.28607 4	.24926 4	9.45924 5	.13957E-1 26	9.44547	18	4	.72
40998.0	252.24 1	110.09 1	84.68 4	.2831 1	.2309 1	9.52587 9	.18384E-1 44	9.40139	24	4	1.26
41000.0	249.343 3	109.498 2	84.646 6	.27957 4	.35720 2	9.59890 2	.18294E-1 37	9.35360	20	4	.21
41002.0	246.460 6	108.917 4	84.618 9	.27619 6	.62979 5	9.67340 8	.19248E-1 39	9.30558	26	4	.56
41004.0	243.513 9	108.294 6	84.68 2	.27239 6	.05899 3	9.75825 4	.21933E-1 13	9.25157	39	4	1.61
41006.0	240.601 3	107.716 2	84.644 5	.26856 2	.66369 1	9.85079 2	.27857E-1 20	9.19355	35	4	.36
41008.0	237.64 1	107.11 1	84.63 3	.26303 6	.48474 5	9.97377 5	.32685E-1 20	9.11763	38	4	1.50
41010.0	234.389 8	106.446 7	84.59 2	.25684 3	.56388 3	10.10038 4	.288199E-1 9	9.04149	55	4	1.07
41012.0	231.209 5	105.807 5	84.61 1	.25140 3	.87855 3	10.21594 7	.29294E-1 23	8.97320	46	4	.71
41014.0	228.024 4	105.146 3	84.607 8	.24573 2	.43050 1	10.34061 1	.34104E-1 16	8.90094	35	4	.29
41016.0	224.687 5	104.842 2	84.608 6	.23966 2	.25082 2	10.47712 2	.317586E-1 6	8.82347	47	4	.67
41018.0	221.329 4	103.772 2	84.574 4	.23388 1	.32648 1	10.59920 1	.317638E-1 4	8.75560	60	4	.50
41020.0	217.89 1	103.030 4	84.478 7	.22827 4	.65567 3	10.72971 2	.320754E-1 8	8.68448	61	4	1.20
41022.0	214.02 1	102.356 5	84.588 8	.22120 5	.24222 3	10.85751 3	.33871E-1 10	8.61621	50	4	1.41
41024.0	210.736 3	101.565 2	84.562 2	.21471 2	.106311 7	11.921759 6	.462226E-1 2	8.530416	37	4	.32
41026.0	206.603 5	100.767 2	84.557 2	.20614 2	.33182 2	11.20071 2	.426790E-1 8	8.43933	35	4	.31
41028.0	202.95 3	100.064 4	84.463 6	.19830 9	.89965 2	11.37060 2	.43750E-1 76	8.35508	36	4	.81
41030.0	198.92 7	99.19 2	84.63 3	.1883 3	.8193 2	11.5521 3	.48058E-1 72	8.2674	41	4	4.83

Table 2 (Cont.)

T	ω	Ω	j	e	M	n	$\hbar/2$	a	N	D	σ
41032.0	194.787 4	98.352 2	84.483 1	.18121 2	.12166 1	11.74147 2	.440064E-1 3	8.17825	49	4	.30
41034.0	190.446 6	97.473 2	84.467 2	.17278 2	.78266 1	11.92112 1	.480807E-1 2	8.09590	74	4	.73
41036.0	186.071 4	96.5741 9	84.453 1	.16358 2	.829439 9	12.128196 8	.528070E-1 2	8.003506	94	4	.55
41038.0	181.490 3	95.6460 7	84.4448 7	.15432 1	.298463 6	12.338130 7	.486427E-1 1	7.912485	89	4	.34
41040.0	176.98 1	95.550 2	84.340 2	.14610 4	.15703 2	12.51893 2	.474983E-1 4	7.83614	86	4	1.14
41042.0	171.36 5	93.85 1	84.48 1	.1357 2	.40973 9	12.7516 1	.63496E-1 21	7.7406	98	4	4.65
41044.0	166.63 1	92.618 1	84.371 1	.12548 3	.15968 2	12.99618 2	.630043E-1 3	7.64316	69	4	.54
41046.0	162.446 8	91.82 1	84.47 2	.1128 2	.4371 2	13.3076 2	.84233E-1 20	7.5235	61	4	6.28
41048.0	157.01 5	90.308 6	84.273 7	.0968 1	.3898 1	13.6541 2	.88989E-1 19	7.3957	65	4	2.98
41050.0	150.4 2	89.07 1	84.69 2	.0781 2	.0627 4	14.0392 3	.133072 26	7.2599	70	4	7.42
41052.0	144.8 3	88.04 2	84.52 1	.0576 4	.8300 6	14.7923 7	.22292 19	7.0114	58	4	7.61
41054.0	125.53 8	86.439 5	84.2696 9	.00717 9	.8362 7	16.522 1	.68479 80	6.513	32	4	.30

Table 3. Accelerations, atmospheric densities, atmospheric temperatures, and geometric parameters from 1963 30D in the interval MJD 38397.00– 38814.00

PRECEDING PAGE BLANK NOT FILMED

MJD	$-10^7 \dot{P}$	$10^7 \dot{P}_r$	$-10^7 \dot{P}_a$	$\log \rho_\pi$	$\log \rho_s$	T_π (°K)	z (km)	$a_\pi - a_\odot$ (deg)	$\delta_\pi - \delta_\odot$ (deg)
38397.00	-0.17	0.01	-.14			3464.0	304.9	-25.8	
98.00	-0.34	0.03	-.30			3463.4	303.7	-25.5	
99.00	-0.30	0.05	-.24			3462.9	302.5	-25.2	
38400.00	-0.20	0.06	-.12			3462.5	301.4	-24.8	
01.00	-0.18	0.08	-.09			3462.1	300.2	-24.5	
02.00	-0.06	0.10	0.04	-20.46	-20.52	1014	3461.7	299.0	-24.2
03.00	0.03	0.11	0.14	-19.92	-19.97	1207	3461.3	297.8	-23.8
04.00	-0.01	0.13	0.12	.99	-20.04	1159	3461.0	296.6	-23.5
05.00	0.06	0.14	0.20	.76	-19.82	1280	3460.7	295.5	-23.2
06.00	0.12	0.15	0.27	.63	.68	1346	3460.4	294.3	-22.8
07.00	0.13	0.17	0.29	.59	.65	1362	3460.2	293.1	-22.5
08.00	0.18	0.18	0.36	.50	.55	1409	3460.0	292.0	-22.1
09.00							3459.8	290.8	-21.7
10.00	0.21	0.21	0.42	-19.43	-19.48	1442	3459.7	289.6	-21.3
11.00	0.20	0.22	0.42	.43	.49	1438	3459.6	288.5	-21.0
12.00	0.15	0.23	0.38	.47	.53	1416	3459.6	287.3	-20.6
13.00	0.08	0.24	0.32	.54	.60	1380	3459.6	286.2	-20.1
14.00	-0.01	0.25	0.24	.66	.72	1319	3459.6	285.0	-19.7
15.00	0.00	0.26	0.26	.63	.68	1335	3459.7	283.9	-19.3
16.00	0.00	0.27	0.27	.61	.66	1344	3460.1	282.7	-18.8
17.00	0.00	0.28	0.27	.61	.66	1343	3460.2	281.6	-18.4
18.00	0.03	0.29	0.31	.54	.60	1370	3460.5	280.4	-17.9
19.00	0.03	0.29	0.32	.53	.59	1375	3460.7	279.3	-17.4
20.00	0.05	0.30	0.35	.49	.55	1393	3461.0	278.2	-16.9
21.00	0.05	0.31	0.35	.49	.54	1393	3461.3	277.0	-16.4
22.00	0.06	0.31	0.37	.46	.52	1405	3461.7	275.9	-15.9
23.00	0.11	0.31	0.42	.41	.46	1430	3462.1	274.8	-15.4
24.00	0.14	0.31	0.46	.37	.42	1448	3462.6	273.7	-14.8
25.00	0.18	0.32	0.50	.33	.39	1468	3463.1	272.6	-14.2
26.00	0.22	0.32	0.53	.30	.36	1480	3463.6	271.4	-13.6
27.00	0.32	0.31	0.64	.22	.27	1526	3464.2	270.3	-13.0
28.00	0.33	0.31	0.64	.21	.27	1527	3464.8	269.2	-12.4
29.00	0.35	0.31	0.66	.20	.25	1533	3465.5	268.1	-11.8
30.00	0.42	0.31	0.73	.15	.21	1557	3466.2	267.0	-11.1
31.00	0.38	0.31	0.69	.18	.23	1538	3466.9	265.9	-10.4
32.00	0.41	0.31	0.72	.16	.22	1546	3468.3	264.8	-9.7
33.00	0.40	0.30	0.71	.16	.22	1543	3469.1	263.7	-9.0
34.00	0.40	0.30	0.70	.17	.22	1537	3470.0	262.6	-8.3
35.00	0.44	0.30	0.74	.14	.20	1550	3470.8	261.5	-7.5
36.00	0.46	0.29	0.75	.13	.19	1554	3471.7	260.5	-6.8
37.00	0.39	0.29	0.68	.17	.23	1527	3472.6	259.4	-6.0
38.00	0.45	0.28	0.73	.14	.20	1540	3473.6	258.3	-5.2
39.00	0.46	0.28	0.73	.14	.20	1538	3474.5	257.2	-4.4
40.00	0.45	0.27	0.72	.14	.20	1535	3475.5	256.1	-3.5
41.00	0.43	0.26	0.69	.16	.21	1523	3476.5	255.1	-2.7
42.00	0.45	0.25	0.70	.15	.21	1526	3477.5	254.0	-1.8
43.00	0.49	0.25	0.74	.13	.18	1538	3478.4	252.9	-0.9
44.00	0.48	0.24	0.72	.14	.19	1530	3479.4	251.9	0.0
45.00	0.44	0.23	0.67	.17	.22	1510	3480.3	250.8	0.9
46.00	0.44	0.22	0.66	.18	.23	1502	3481.9	249.8	1.8
47.00	0.40	0.21	0.61	.21	.27	1481	3482.7	248.7	2.8
48.00	0.35	0.20	0.55	.26	.31	1456	3483.5	247.7	3.7
49.00	0.33	0.18	0.51	.29	.34	1437	3484.2	246.6	4.7
50.00	0.27	0.17	0.45	.35	.40	1407	3484.9	245.6	5.7
51.00	0.33	0.16	0.49	.31	.36	1422	3485.6	244.5	6.8
52.00	0.34	0.15	0.49	.31	.36	1420	3486.2	243.5	7.8
53.00	0.41	0.14	0.55	.26	.31	1445	3486.7	242.4	8.9
54.00	0.39	0.13	0.52	.28	.33	1432	3487.2	241.4	10.0
55.00	0.50	0.11	0.61	.21	.26	1469	3487.5	240.4	11.1
56.00	0.61	0.10	0.71	.14	.19	1507	3487.9	239.3	12.2

Table 3 (Cont.)

MJD	$-10^7 \dot{P}$	$10^7 \dot{P}_r$	$-10^7 \dot{P}_a$	$\log \rho_\pi$	$\log \rho_s$	T_π (°K)	z (km)	$a_\pi - a_\odot$ (deg)	$\delta_\pi - \delta_\odot$ (deg)
38457.00	0.67	0.09	0.76	-19.11	-19.16	1523	3488.1	238.3	13.3
58.00	0.63	0.07	0.70	.15	.20	1498	3488.3	237.3	14.5
59.00	0.72	0.06	0.78	.11	.16	1520	3488.4	236.2	15.6
60.00	0.71	0.04	0.76	.12	.17	1514	3488.4	235.2	16.8
61.00	0.66	0.03	0.69	.15	.21	1492	3488.4	234.2	18.0
62.00	0.67	0.01	0.68	.16	.21	1489	3489.0	233.1	19.2
63.00	0.75	0.00	0.75	.12	.17	1512	3488.8	232.1	20.4
64.00	0.78	-0.02	0.76	.11	.16	1518	3488.5	231.1	21.6
65.00	0.73	-0.04	0.69	.15	.20	1495	3488.2	230.0	22.9
66.00	0.65	-0.05	0.60	.21	.26	1460	3487.7	229.0	24.1
67.00	0.65	-0.07	0.58	.23	.28	1451	3487.2	228.0	25.4
68.00	0.55	-0.09	0.46	.33	.38	1401	3486.5	227.0	26.6
69.00	0.53	-0.11	0.42	.37	.42	1381	3485.8	225.9	27.8
70.00	0.54	-0.13	0.41	.38	.44	1376	3485.0	224.9	29.1
71.00	0.55	-0.14	0.41	.38	.44	1377	3484.1	223.9	30.3
72.00	0.59	-0.16	0.43	.36	.41	1389	3483.1	222.8	31.6
73.00	0.71	-0.18	0.53	.27	.32	1437	3482.0	221.8	32.8
74.00	0.86						3481.2	220.8	34.0
75.00	1.06						3480.0	219.7	35.2
76.00	1.62						3478.7	218.7	36.4
77.00	1.94						3477.3	217.7	37.6
78.00	1.88						3475.8	216.6	38.7
79.00	1.64						3474.3	215.6	39.9
80.00	1.27						3472.7	214.5	41.0
81.00	1.00						3471.1	213.5	42.1
82.00	0.60						3469.3	212.4	43.2
83.00	0.33						3467.5	211.4	44.2
84.00	0.14						3465.6	210.3	45.3
85.00	-0.07						3463.7	209.2	46.3
86.00	0.16						3461.7	208.2	47.3
87.00	0.26						3459.6	207.1	48.3
88.00	0.48						3457.5	206.0	49.2
89.00	0.91						3455.3	204.9	50.2
90.00	1.78						3453.0	203.8	51.1
91.00	2.65						3450.7	202.7	52.0
92.00	3.32						3448.3	201.6	52.8
93.00	4.22						3445.9	200.5	53.6
94.00	4.79						3442.1	199.4	54.4
95.00	5.76						3439.5	198.2	55.3
96.00	6.74						3436.8	197.1	56.1
97.00	7.69						3434.1	195.9	56.9
98.00	8.60						3431.3	194.7	57.7
99.00	9.44						3428.4	193.5	58.5
38500.00	10.24						3425.5	192.3	59.2
01.00	10.91						3422.6	191.1	60.0
02.00	11.53						3419.6	189.8	60.7
03.00	11.98						3416.6	188.5	61.4
04.00	12.54						3413.6	187.2	62.0
05.00	12.94						3410.5	185.8	62.7
06.00	13.27						3407.5	184.4	63.3
07.00	13.66						3404.4	183.0	64.0
08.00	13.86						3401.3	181.5	64.6
09.00	14.20						3398.2	179.9	65.2
10.00	14.48						3395.1	178.2	65.8
11.00	14.62						3392.0	176.4	66.4
12.00	14.73						3388.8	174.4	67.0
13.00	15.02						3385.6	172.3	67.6
14.00	14.79						3382.4	169.9	68.1
15.00	14.97						3379.2	167.1	68.7
16.00	14.76						3376.0	163.9	69.3

Table 3 (Cont.)

MJD	$-10^7 \dot{P}$	$10^7 \dot{P}_r$	$-10^7 \dot{P}_a$	$\log \rho_\pi$	$\log \rho_s$	T_π (°K)	z (km)	$a_\pi - a_\odot$ (deg)	$\delta_\pi - \delta_\odot$ (deg)
38517.00	14.88					3372.8	159.8	69.8	
18.00	14.55					3369.6	154.6	70.3	
19.00	14.42					3366.4	147.5	70.8	
20.00	14.23					3363.2	136.9	71.2	
21.00	13.83					3359.5	119.9	71.5	
22.00	13.16					3356.4	94.9	71.5	
23.00	12.43					3353.3	66.1	71.2	
24.00	11.58					3350.2	43.7	70.6	
25.00	10.71					3347.2	29.2	69.7	
26.00	9.78					3344.1	19.8	68.8	
27.00	8.85					3341.0	13.3	67.8	
28.00	7.93					3338.0	8.4	66.8	
29.00	6.92					3334.9	4.6	65.8	
30.00	6.01					3331.9	1.4	64.8	
31.00	5.19					3328.9	358.7	63.8	
32.00	4.41					3325.9	356.3	62.8	
33.00	3.74					3322.9	354.2	61.8	
34.00	3.39					3320.0	352.2	60.8	
35.00	3.18					3317.1	350.4	59.9	
36.00	3.11					3314.2	348.7	58.9	
37.00	2.97					3311.3	346.9	58.0	
38.00	3.06					3308.6	345.3	57.0	
39.00	3.27					3305.9	343.8	56.1	
40.00	3.56					3303.3	342.4	55.2	
41.00	3.94					3300.7	341.0	54.3	
42.00	4.37					3298.1	339.6	53.4	
43.00	4.82					3295.6	338.2	52.5	
44.00	5.27					3293.0	336.9	51.6	
45.00	5.69					3290.6	335.6	50.8	
46.00	6.07					3288.1	334.3	49.9	
47.00	6.46					3285.7	333.0	49.1	
48.00	6.73					3283.3	331.7	48.2	
49.00	6.78					3281.0	330.5	47.4	
50.00	6.72					3278.8	329.2	46.6	
51.00	6.66					3276.6	328.0	45.8	
52.00	6.51					3274.5	326.7	45.0	
53.00	6.11					3272.5	325.5	44.2	
54.00	5.14					3270.5	324.3	43.4	
55.00	4.01					3268.7	323.1	42.7	
56.00	0.46					3266.9	321.9	41.9	
57.00	-0.11					3265.2	320.7	41.2	
58.00	0.39	-0.20	0.19	-19.76	-19.86	1253	3263.6	319.5	40.5
59.00	0.40	-0.19	0.21	.72	.81	1279	3262.0	318.3	39.7
60.00	0.26	-0.17	0.10	-20.04	-20.13	1070	3260.5	317.1	39.0
61.00	0.39	-0.15	0.24	-19.66	-19.75	1312	3259.1	315.9	38.3
62.00	0.66	-0.13	0.54	.30	.40	1498	3257.8	314.8	37.6
63.00	0.50	-0.11	0.39	.44	.54	1421	3256.5	313.6	36.9
64.00	0.56	-0.09	0.47	.36	.46	1465	3255.3	312.4	36.2
65.00	0.80	-0.06	0.74	.16	.26	1581	3254.1	311.2	35.5
66.00	0.82	-0.04	0.78	.14	.24	1594	3253.0	310.1	34.8
67.00	0.84	-0.01	0.83	.11	.21	1611	3252.0	308.9	34.1
68.00	0.79	0.01	0.80	.12	.22	1602	3251.0	307.7	33.4
69.00	0.67	0.03	0.71	.17	.27	1570	3250.1	306.6	32.8
70.00	0.49	0.06	0.55	.28	.38	1504	3249.3	305.4	32.1
71.00	0.43	0.07	0.50	.32	.42	1479	3248.4	304.3	31.4
72.00	0.52	0.11	0.63	.22	.32	1537	3247.6	303.1	30.7
73.00	0.47	0.14	0.61	.23	.33	1530	3246.9	301.9	30.0
74.00	0.41	0.15	0.56	.27	.37	1508	3246.2	300.8	29.3
75.00	0.32	0.19	0.51	.31	.41	1483	3245.6	299.6	28.7
76.00	0.29	0.22	0.51	.30	.40	1484	3245.0	298.5	28.0

Table 3 (Cont.)

MJD	$-10^7 \dot{P}$	$10^7 \dot{P}_r$	$-10^7 \dot{P}_a$	$\log p_\pi$	$\log p_s$	T_π (°K)	z (km)	$a_\pi - a_\odot$ (deg)	$\delta_\pi - \delta_\odot$ (deg)
38577.00	0.31	0.25	0.55	-19.27	-19.37	1504	3244.5	297.3	27.3
78.00	0.30	0.27	0.57	.25	.35	1513	3244.1	296.2	26.7
79.00	0.30	0.29	0.59	.23	.34	1519	3243.8	295.1	26.0
80.00	0.36	0.31	0.67	.18	.28	1550	3243.5	293.9	25.4
81.00	0.38	0.34	0.72	.15	.25	1570	3243.3	292.8	24.7
82.00	0.39	0.34	0.73	.14	.24	1575	3243.1	291.7	24.1
83.00	0.51	0.38	0.89	.05	.15	1629	3243.1	290.5	23.4
84.00	0.63	0.40	1.03	-18.99	.09	1669	3243.1	289.4	22.8
85.00	0.68	0.42	1.10	.96	.06	1688	3243.2	288.3	22.2
86.00	0.79	0.44	1.23	.91	.01	1723	3243.3	287.1	21.5
87.00	0.46	0.45	0.91	-19.03	.14	1631	3243.6	286.0	20.9
88.00	0.36	0.47	0.83	.07	.17	1606	3243.9	284.9	20.3
89.00	0.13	0.49	0.62	.20	.30	1526	3244.3	283.8	19.6
90.00	0.19	0.50	0.70	.14	.24	1558	3244.8	282.7	19.0
91.00	0.20	0.52	0.72	.13	.23	1565	3245.3	281.6	18.3
92.00	0.17	0.53	0.70	.14	.24	1557	3246.2	280.5	17.7
93.00	0.19	0.54	0.73	.12	.22	1564	3246.9	279.4	17.0
94.00	0.15	0.55	0.70	.14	.24	1550	3247.7	279.2	16.4
95.00	0.15	0.56	0.71	.13	.23	1552	3248.5	277.1	15.7
96.00	0.04	0.57	0.61	.19	.30	1513	3249.4	276.0	15.1
97.00	0.08	0.58	0.66	.16	.26	1534	3250.3	275.0	14.4
98.00	0.06	0.59	0.65	.16	.26	1529	3251.3	273.9	13.7
99.00	0.03	0.60	0.63	.17	.28	1519	3252.3	272.8	13.0
38600.00	0.13	0.61	0.73	.11	.21	1557	3253.3	271.7	12.3
01.00	0.17	0.61	0.78	.07	.18	1574	3254.4	270.6	11.6
02.00	0.23	0.62	0.85	.04	.14	1596	3255.5	269.5	10.9
03.00	0.22	0.62	0.85	.03	.14	1595	3256.7	268.4	10.2
04.00	0.20	0.63	0.83	.04	.14	1587	3257.8	267.4	9.5
05.00	0.20	0.64	0.83	.04	.14	1584	3259.0	266.3	8.8
06.00	0.18	0.64	0.82	.05	.15	1577	3260.4	265.2	8.1
07.00	0.11	0.64	0.76	.08	.18	1554	3261.6	264.1	7.3
08.00	0.15	0.64	0.79	.06	.16	1564	3262.7	263.1	6.6
09.00	0.19	0.64	0.83	.04	.14	1577	3263.9	262.0	5.8
10.00	0.12	0.63	0.75	.08	.18	1548	3265.1	260.9	5.1
11.00	0.21	0.63	0.83	.04	.14	1570	3266.3	259.9	4.3
12.00	0.18	0.62	0.80	.05	.15	1557	3267.4	258.8	3.5
13.00	0.18	0.61	0.79	.06	.16	1553	3268.6	257.8	2.8
14.00	0.07	0.60	0.68	.12	.22	1513	3269.8	256.7	2.0
15.00	-0.04	0.59	0.55	.21	.31	1461	3271.0	255.7	1.2
16.00	-0.01	0.58	0.57	.19	.29	1468	3272.2	254.6	0.4
17.00	0.00	0.57	0.56	.20	.30	1462	3273.5	253.6	-0.4
18.00	-0.05	0.55	0.50	.25	.35	1433	3274.7	252.5	-1.2
19.00	-0.03	0.54	0.51	.24	.34	1434	3275.9	251.5	-2.0
20.00	-0.01	0.53	0.52	.23	.33	1437	3277.2	250.5	-2.8
21.00	-0.01	0.51	0.50	.25	.34	1428	3278.8	249.4	-3.6
22.00	-0.01	0.49	0.49	.26	.35	1423	3280.1	248.4	-4.4
23.00	-0.06	0.47	0.41	.33	.43	1382	3281.4	247.4	-5.3
24.00	-0.02	0.46	0.43	.31	.41	1390	3282.7	246.3	-6.1
25.00	0.02	0.43	0.45	.29	.39	1398	3283.9	245.3	-7.0
26.00	0.03	0.41	0.44	.30	.39	1392	3285.2	244.3	-7.8
27.00	0.09	0.39	0.48	.26	.35	1410	3286.4	243.3	-8.7
28.00	0.15	0.36	0.51	.23	.33	1422	3287.6	242.2	-9.6
29.00	0.21	0.34	0.55	.20	.29	1436	3288.8	241.2	-10.5
30.00	0.16	0.31	0.47	.27	.36	1400	3289.9	240.2	-11.5
31.00	0.21	0.29	0.49	.25	.34	1409	3291.0	239.2	-12.4
32.00	0.22	0.26	0.48	.26	.35	1402	3292.0	238.2	-13.3
33.00	0.21	0.23	0.44	.30	.39	1381	3293.0	237.2	-14.3
34.00	0.19	0.20	0.39	.35	.44	1354	3293.9	236.1	-15.3
35.00	0.14	0.18	0.32	.43	.53	1314	3294.7	235.1	-16.2
36.00	0.14	0.14	0.28	.49	.58	1289	3295.4	234.1	-17.2

Table 3 (Cont.)

MJD	$-10^7 p$	$10^7 p_r$	$-10^7 p_a$	$\log \rho_\pi$	$\log \rho_g$	T_π (°K)	z (km)	$a_\pi - a_\odot$ (deg)	$\delta_\pi - \delta_\odot$ (deg)
38637.00	0.14	0.11	0.26	-19.52	-19.61	1274	3296.1	233.1	-18.2
38.00	0.14	0.08	0.22	.60	.69	1241	3296.7	232.1	-19.2
39.00	0.18	0.04	0.22	.60	.69	1237	3297.2	231.1	-20.2
40.00	0.09	0.00	0.09	.99	-20.08	1051	3297.6	230.1	-21.2
41.00	0.09	-0.03	0.05	-20.24	.33	961	3297.9	229.1	-22.2
42.00	0.03						3298.6	228.1	-23.3
43.00	0.00						3298.7	227.1	-24.3
44.00	0.03						3298.7	226.0	-25.3
45.00	0.15						3298.6	225.0	-26.3
46.00	0.27						3298.4	224.0	-27.3
47.00	0.35						3298.2	223.0	-28.4
48.00	0.54						3297.9	222.0	-29.4
49.00	0.92						3297.5	221.0	-30.4
50.00	1.90						3297.0	220.0	-31.4
51.00	2.53						3296.5	219.0	-32.4
52.00	2.56						3295.9	218.0	-33.4
53.00	2.47						3295.2	217.0	-34.4
54.00	2.30						3294.5	216.0	-35.4
55.00	1.74						3293.7	214.9	-36.3
56.00	1.67						3292.8	213.9	-37.3
57.00	1.28						3291.9	212.9	-38.3
58.00	1.04						3290.9	211.9	-39.2
59.00	0.83						3289.8	210.9	-40.2
60.00	0.76						3288.6	209.8	-41.1
61.00	0.70						3287.4	208.8	-42.1
62.00	0.85						3286.1	207.8	-43.0
63.00	0.97						3284.7	206.7	-43.9
64.00	1.30						3283.2	205.7	-44.8
65.00	1.66						3281.6	204.6	-45.8
66.00	2.09						3279.9	203.6	-46.7
67.00	2.52						3278.2	202.5	-47.6
68.00	3.05						3276.3	201.5	-48.5
69.00	3.57						3274.4	200.4	-49.3
70.00	4.27						3272.3	199.3	-50.2
71.00	4.90						3270.2	198.3	-51.1
72.00	5.66						3268.0	197.2	-51.9
73.00	6.56						3265.7	196.1	-52.7
74.00	7.38						3263.3	195.0	-53.6
75.00	8.42						3260.8	193.9	-54.4
76.00	9.39						3258.1	192.7	-55.2
77.00	10.54						3255.4	191.6	-56.0
78.00	11.69						3252.7	190.5	-56.8
79.00	12.82						3249.9	189.3	-57.5
80.00	13.97						3247.0	188.1	-58.3
81.00	15.05						3244.1	186.9	-59.1
82.00	16.07						3241.1	185.7	-59.8
83.00	17.15						3238.1	184.5	-60.5
84.00	17.90						3235.1	183.2	-61.2
85.00	18.62						3232.0	181.9	-62.0
86.00	19.05						3228.9	180.6	-62.7
87.00	19.12						3225.8	179.2	-63.4
88.00	18.90						3222.6	177.8	-64.0
89.00	18.67						3219.4	176.4	-64.7
90.00	18.09						3216.2	174.8	-65.4
91.00	17.42						3213.0	173.2	-66.0
92.00	16.44						3209.3	171.5	-66.7
93.00	15.36						3206.0	169.6	-67.4
94.00	14.28						3202.7	167.6	-68.0
95.00	13.22						3199.4	165.4	-68.7
96.00	12.10						3196.1	162.9	-69.3

Table 3 (Cont.)

MJD	$-10^7 \dot{P}$	$10^7 \dot{P}_r$	$-10^7 \dot{P}_a$	$\log \rho_\pi$	$\log \rho_s$	T_π (°K)	z (km)	$a_\pi - a_\odot$ (deg)	$\delta_\pi - \delta_\odot$ (deg)
38697.00	11.14					3192.8	159.9	-69.9	
98.00	10.22					3189.5	156.4	-70.5	
99.00	9.48					3186.2	151.9	-71.1	
38700.00	8.90					3182.9	145.8	-71.7	
01.00	8.32					3179.6	137.0	-72.2	
02.00	7.99					3176.3	123.1	-72.6	
03.00	7.77					3173.1	100.5	-72.8	
04.00	7.50					3169.8	69.5	-72.6	
05.00	7.22					3166.6	42.3	-72.0	
06.00	7.17					3163.4	24.9	-71.1	
07.00	7.24					3160.2	14.1	-70.0	
08.00	7.38					3157.0	7.0	-68.9	
09.00	7.47					3153.6	1.8	-67.8	
10.00	7.65					3150.5	357.9	-66.6	
11.00	7.94					3147.4	354.6	-65.5	
12.00	8.34					3144.3	351.9	-64.4	
13.00	8.61					3141.3	349.5	-63.2	
14.00	8.99					3138.3	347.3	-62.1	
15.00	9.50					3135.3	345.3	-61.0	
16.00	10.08					3132.4	343.5	-59.9	
17.00	10.82					3129.5	341.7	-58.8	
18.00	11.33					3126.7	340.1	-57.8	
19.00	11.81					3123.9	338.5	-56.7	
20.00	12.18					3121.1	336.9	-55.6	
21.00	12.40					3118.4	335.4	-54.6	
22.00	12.56					3115.7	334.0	-53.6	
23.00	12.23					3113.1	332.6	-52.5	
24.00	11.77					3110.6	331.2	-51.5	
25.00	10.94					3108.1	329.8	-50.5	
38726.00	9.87					3105.4	328.4	-49.5	
26.50	9.44					3104.2	327.8	-49.1	
27.00	8.68					3103.0	327.1	-48.6	
27.50	7.81					3101.8	326.4	-48.1	
28.00	7.04					3100.6	325.8	-47.6	
28.50	6.26					3099.4	325.1	-47.1	
29.00	5.42					3098.2	324.5	-46.7	
29.50	4.19					3097.0	323.8	-46.2	
30.00	3.05					3095.8	323.2	-45.7	
30.50	1.95					3094.7	322.5	-45.2	
31.00	1.05					3093.5	321.9	-44.8	
31.50	0.57					3092.4	321.2	-44.3	
32.00	0.29	-0.71	-0.41			3091.3	320.6	-43.9	
32.50	-0.01	-0.69	-0.69			3090.2	319.9	-43.4	
33.50	0.68	-0.67	0.01	-21.00	-21.11	1015	3088.0	318.6	-42.5
34.00	0.63	-0.64	0.00				3086.9	318.0	-42.0
34.50	0.56	-0.62	-0.05				3085.9	317.4	-41.6
35.00	0.62	-0.60	0.02	-20.70	-20.81	1004	3084.8	316.7	-41.1
35.50	0.66	-0.58	0.08	.10	.21	1005	3083.8	316.1	-40.7
36.00	0.55	-0.55	0.00				3082.8	315.5	-40.2
36.50	0.53	-0.52	0.00				3081.9	314.8	-39.8
37.00	0.57	-0.50	0.06	-20.09	-20.21	1041	3080.9	314.2	-39.3
37.50	0.42	-0.47	-0.04				3080.0	313.6	-38.9
38.00	0.35	-0.45	-0.09				3079.1	312.9	-38.4
38.50	0.28	-0.42	-0.13				3078.2	312.3	-38.0
39.00	0.24	-0.39	-0.15				3077.4	311.7	-37.6
39.50	0.15	-0.37	-0.21				3076.5	311.1	-37.1
40.00	0.02	-0.34	-0.31				3075.7	310.4	-36.7

Table 3 (Cont.)

MJD	$-10^7 \dot{P}$	$10^7 \dot{P}_r$	$-10^7 \dot{P}_a$	$\log \rho_\pi$	$\log \rho_s$	T_π (°K)	z (km)	$a_\pi - a_\odot$ (deg)	$\delta_\pi - \delta_\odot$ (deg)
38741.00	0.01	-0.31	-.29			3074.2	309.2	-35.8	
42.00	-0.12	-0.25	-.37			3072.7	307.9	-34.9	
43.00	-0.20	-0.20	-.39			3071.4	306.7	-34.1	
44.00	-0.17	-0.15	-.30			3070.1	305.4	-33.2	
45.00	-0.10	-0.10	-.19			3069.0	304.2	-32.4	
46.00	-0.05	-0.05	-.09			3066.0	302.9	-31.5	
47.00	0.04	0.00	0.04	-20.38	-20.50	1023	3067.1	301.7	-30.7
48.00	0.13	0.05	0.18	-19.73	-19.85	1231	3066.3	300.5	-29.9
49.00	0.21	0.10	0.30	.50	.62	1341	3065.6	299.2	-29.0
50.00	0.22	0.14	0.37	.41	.53	1387	3065.0	298.0	-28.2
51.00	0.14	0.19	0.33	.46	.58	1363	3064.5	296.8	-27.4
52.00	0.02	0.24	0.26	.56	.68	1312	3064.1	295.5	-26.6
53.00	-0.16	0.26	0.12	.89	-20.01	1147	3063.8	294.3	-25.8
54.00	-0.29	0.38	0.08	-20.07	.19	998	3063.9	293.1	-25.0
55.00	-0.30	0.42	0.12	-19.89	.01	1146	3063.8	291.8	-24.2
56.00	-0.30	0.46	0.16	.76	-19.88	1211	3063.7	290.6	-23.4
57.00	-0.28	0.51	0.23	.60	.72	1287	3063.7	289.4	-22.6
58.00	-0.25	0.55	0.30	.49	.61	1341	3063.8	288.2	-21.8
59.00	-0.12	0.59	0.47	.29	.41	1441	3063.9	287.0	-21.1
60.00	-0.07	0.63	0.56	.21	.33	1484	3064.0	285.7	-20.3
61.00	-0.05	0.67	0.62	.17	.29	1509	3064.2	284.5	-19.5
62.00	-0.06	0.71	0.64	.15	.27	1514	3064.4	283.3	-18.8
63.00	-0.13	0.74	0.61	.18	.30	1499	3064.7	282.1	-18.0
64.00	-0.19	0.77	0.58	.20	.32	1487	3065.0	280.9	-17.2
65.00	-0.26	0.81	0.55	.22	.33	1474	3065.4	279.7	-16.5
66.00	-0.34	0.84	0.50	.25	.37	1451	3065.8	278.5	-15.7
67.00	-0.39	0.86	0.47	.28	.40	1435	3066.3	277.3	-14.9
68.00	-0.39	0.89	0.50	.25	.37	1447	3066.8	276.1	-14.1
69.00	-0.40	0.91	0.51	.24	.36	1450	3067.4	274.9	-13.4
70.00	-0.40	0.93	0.53	.22	.34	1459	3068.0	273.7	-12.6
71.00	-0.37	0.95	0.58	.18	.30	1480	3068.7	272.5	-11.8
72.00	-0.26	0.97	0.71	.09	.21	1530	3069.5	271.3	-11.0
73.00	-0.11	0.99	0.88	.00	.12	1584	3070.3	270.1	-10.3
74.00	-0.01	1.00	0.99	-18.94	.07	1616	3071.2	269.0	-9.5
75.00	-0.03	1.01	0.98	.94	.07	1613	3072.1	267.8	-8.7
76.00	0.01	1.02	1.03	.92	.04	1626	3073.1	266.6	-7.9
77.00	0.05	1.03	1.08	.90	.02	1638	3074.5	265.4	-7.1
78.00	-0.02	1.03	1.01	.93	.05	1616	3075.7	264.3	-6.3
79.00	-0.15	1.04	0.89	.98	.10	1579	3076.9	263.1	-5.5
80.00	-0.14	1.04	0.90	.97	.09	1580	3078.2	261.9	-4.7
81.00	-0.16	1.05	0.89	.98	.10	1574	3079.6	260.8	-3.9
82.00	-0.10	1.05	0.95	.95	.07	1587	3080.9	259.6	-3.1
83.00	-0.10	1.05	0.95	.95	.07	1585	3082.3	258.5	-2.3
84.00	-0.10	1.05	0.95	.95	.06	1585	3083.7	257.3	-1.5
85.00	-0.09	1.04	0.95	.94	.06	1585	3085.1	256.2	-0.7
86.00	-0.12	1.03	0.91	.96	.08	1570	3086.5	255.0	0.1
87.00	-0.15	1.02	0.87	.98	.10	1555	3087.9	253.9	0.9
88.00	-0.17	1.01	0.84	-19.00	.11	1543	3089.3	252.8	1.7
89.00	-0.17	1.00	0.83	.00	.12	1537	3090.7	251.6	2.5
90.00	-0.16	0.98	0.82	.01	.12	1532	3092.0	250.5	3.3
91.00	-0.19	0.96	0.77	.03	.15	1514	3093.3	249.4	4.2
92.00	-0.23	0.94	0.71	.07	.18	1491	3094.6	248.2	5.0
93.00	-0.20	0.92	0.72	.06	.17	1493	3095.8	247.1	5.8
94.00	-0.07	0.90	0.83	.00	.11	1527	3097.0	246.0	6.6
95.00	0.02	0.88	0.91	-18.96	.07	1546	3098.2	244.9	7.5
96.00	-0.03	0.86	0.83	-19.00	.11	1519	3099.3	243.8	8.3
97.00	-0.01	0.84	0.83	-18.99	.11	1517	3100.3	242.7	9.2
98.00	0.09	0.81	0.90	.96	.08	1533	3101.3	241.6	10.0
99.00	0.06	0.79	0.85	.99	.10	1517	3102.2	240.5	10.9
38800.00	0.07	0.76	0.83	.99	.11	1509	3103.5	239.4	11.8

Table 3 (Cont.)

MJD	$-10^7 \dot{P}$	$10^7 \dot{P}_r$	$-10^7 \dot{P}_a$	$\log \rho_\pi$	$\log \rho_s$	T_π (°K)	z (km)	$a_\pi - a_\odot$ (deg)	$\delta_\pi - \delta_\odot$ (deg)
38801.00	0.16	0.73	0.89	-18.96	-19.08	1524	3104.4	238.3	12.7
02.00	0.17	0.71	0.88	.97	.08	1520	3105.2	237.2	13.6
03.00	0.12	0.68	0.80	-19.01	.12	1495	3106.0	236.1	14.5
04.00	0.11	0.65	0.76	.03	.14	1481	3106.8	235.0	15.4
05.00	0.08	0.62	0.70	.06	.18	1459	3107.6	234.0	16.3
06.00	0.08	0.59	0.67	.08	.20	1445	3108.3	232.9	17.2
07.00	0.09	0.56	0.65	.09	.21	1437	3108.9	231.8	18.1
08.00	0.27	0.53	0.80	.00	.12	1486	3109.6	230.7	19.0
09.00	0.34	0.50	0.63	-18.98	.10	1494	3110.2	229.7	19.9
10.00	0.38	0.46	0.84	.98	.09	1495	3110.7	228.6	20.9
11.00	0.44	0.42	0.86	.97	.08	1499	3111.2	227.5	21.8
12.00	0.54	0.38	0.92	.94	.06	1513	3111.6	226.5	22.7
13.00	0.51	0.33	0.85	.98	.09	1491	3112.0	225.4	23.6
14.00	0.37	0.28	0.65	-19.09	.21	1427	3112.3	224.3	24.5

Table 4. Accelerations, atmospheric densities, atmospheric temperatures, and geometric parameters from 1963 30D in the interval MJD 40237.00–41045.80.

MJD	$-10^7 \dot{P}$	$10^7 \dot{P}_r$	$-10^7 \dot{P}_a$	$\log \rho_\pi$	$\log \rho_s$	T_π (°K)	z (km)	$a_\pi - a_\odot$ (deg)	$\delta_\pi - \delta_\odot$ (deg)
40237.00	3.89	-3.65	0.24	-19.02	-19.27	769	1811.4	322.9	94.1
38.00	3.41	-3.62	-0.20				1808.5	321.0	92.9
39.00	4.30	-3.60	0.70	-18.56	-18.81	919	1805.6	319.2	91.6
40.00	4.16	-3.56	0.60	.63	.89	890	1802.8	317.4	90.3
41.00	3.93	-3.52	0.41	.80	-19.06	782	1800.1	315.7	89.0
42.00	3.86	-3.48	0.38	.83	.11	773	1797.3	314.0	87.7
43.00	3.42	-3.44	-0.01				1794.7	312.4	86.4
44.00	3.27	-3.39	-0.11				1792.0	310.8	85.1
40246.00	3.22	-3.29	-0.06				1786.9	307.7	82.5
48.00	3.89	-3.18	0.71	-18.57	-18.86	919	1782.0	304.8	79.9
50.00	3.74	-3.06	0.68	.60	.90	907	1777.4	301.9	77.2
52.00	3.54	-2.92	0.62	.66	.96	885	1773.0	299.1	74.5
54.00	3.47	-2.78	0.69	.61	.92	911	1768.8	296.4	71.8
56.00	3.38	-2.62	0.76	.57	.88	934	1764.9	293.8	69.0
58.00	3.27	-2.46	0.81	.55	.86	945	1761.3	291.1	66.3
60.00	3.20	-2.29	0.91	.50	.83	966	1758.0	288.6	63.5
62.00	3.01	-2.11	0.90	.51	.84	966	1755.0	286.0	60.7
64.00	2.83	-1.93	0.90	.52	.85	968	1752.2	283.5	57.9
66.00	2.78	-1.75	1.03	.47	.80	993	1749.8	281.0	55.1
68.00	2.65	-1.56	1.09	.45	.79	1005	1747.6	278.6	52.2
70.00	2.49	-1.36	1.13	.44	.78	1013	1745.7	276.2	49.4
72.00	2.23	-1.19	1.04	.48	.82	1001	1744.1	273.8	46.5
74.00	2.21	-1.01	1.20	.41	.76	1034	1742.7	271.4	43.6
76.00	2.21	-0.84	1.37	.35	.70	1065	1741.5	269.0	40.7
78.00	2.50	-0.68	1.82	.23	.57	1132	1740.6	266.7	37.8
80.00	2.39	-0.52	1.87	.22	.56	1142	1739.9	264.3	34.8
82.00	1.94	-0.38	1.56	.30	.65	1101	1739.4	262.0	31.9
84.00	1.44	-0.24	1.20	.42	.77	1046	1739.1	259.7	28.9
40286.00	1.69	-0.11	1.58	-18.30	-18.65	1107	1738.6	257.4	25.9
87.00	1.46	-0.05	1.41	.35	.70	1084	1738.6	256.3	24.4
88.00	1.87	0.01	1.88	.22	.57	1149	1738.6	255.2	22.9
89.00	1.59	0.06	1.65	.28	.63	1120	1738.7	254.0	21.4
90.00	1.40	0.10	1.50	.32	.67	1100	1738.9	252.9	19.8
91.00	1.30	0.15	1.45	.34	.69	1093	1739.1	251.7	18.3
92.00	1.15	0.19	1.34	.36	.72	1080	1739.3	250.6	16.8
93.00	1.07	0.22	1.29	.38	.73	1073	1739.6	249.5	15.3
94.00	1.19	0.26	1.45	.34	.69	1096	1739.9	248.4	13.8
95.00	1.36	0.29	1.65	.28	.63	1126	1740.2	247.2	12.3
96.00	1.31	0.31	1.62	.28	.63	1124	1740.6	246.1	10.7
97.00	1.16	0.33	1.49	.31	.67	1108	1741.0	245.0	9.2
98.00	1.32	0.34	1.66	.26	.62	1133	1741.4	243.8	7.7
99.00	1.36	0.35	1.71	.25	.60	1139	1741.8	242.7	6.1
40300.00	1.41	0.35	1.76	.24	.59	1148	1742.3	241.6	4.6
01.00	1.47	0.35	1.82	.22	.57	1157	1742.7	240.5	3.1
02.00	1.66	0.34	2.00	.18	.53	1178	1743.2	239.4	1.5
03.00	1.83	0.34	2.17	.15	.50	1197	1743.7	238.2	0.0
04.00	1.86	0.32	2.18	.15	.49	1202	1744.1	237.1	-1.5
05.00	1.85	0.31	2.16	.15	.49	1200	1744.6	236.0	-3.1
40306.00	1.68	0.30	1.98				1745.1	234.9	-4.6
07.00	1.72	0.28	2.00				1745.5	233.7	-6.1
08.00	1.32	0.26	1.58				1746.0	232.6	-7.7
09.00	0.98	0.50	1.48				1746.4	231.5	-9.2
10.00	0.71	0.59	1.30				1746.8	230.4	-10.8
11.00	0.23	1.66	1.89				1747.2	229.2	-12.3
12.00	-0.74	2.64	1.90				1747.6	228.1	-13.8
13.00	-1.54	2.89	1.35				1748.0	227.0	-15.4
14.00	-2.17	2.08	-0.08				1748.3	225.8	-16.9

Table 4 (Cont.)

MJD	$-10^7 \dot{P}$	$10^7 \dot{P}_r$	$-10^7 \dot{P}_a$	$\log p_\pi$	$\log p_s$	T_π (°K)	z (km)	$a_\pi - a_\odot$ (deg)	$\delta_\pi - \delta_\odot$ (deg)
40315.00	-1.72	0.24	-1.47			1748.6	224.7	-18.5	
16.00	0.87	-2.04	-1.16			1748.9	223.6	-20.0	
17.00	5.87	-4.44	1.43			1749.2	222.4	-21.6	
40318.00	5.84	-6.40	-5.55			1749.4	221.3	-23.1	
18.50	7.17	-6.30	0.87			1749.5	220.7	-23.9	
19.00	9.06	-5.90	3.16			1749.6	220.2	-24.6	
19.50	7.25	-5.40	1.85			1749.6	219.6	-25.4	
20.00	7.06	-4.80	2.26			1749.7	219.0	-26.2	
20.50	6.37	-3.80	2.57			1749.7	218.5	-26.9	
21.00	4.63	-2.90	1.73			1749.8	217.9	-27.7	
21.50	1.32	-2.10	-0.77			1749.8	217.3	-28.5	
22.00	1.76	-1.60	0.16			1749.8	216.7	-29.2	
22.50	1.14	-1.10	0.04			1749.8	216.2	-30.0	
23.00	1.08	-1.40	-0.31			1749.8	215.6	-30.8	
23.50	2.10	-1.60	0.50			1749.8	215.0	-31.5	
24.00	2.61	-2.00	0.61			1749.8	214.4	-32.3	
24.50	3.12	-3.40	-0.27			1749.7	213.9	-33.1	
25.00	4.19	-4.80	-0.60			1749.6	213.3	-33.8	
25.50	4.73	-5.30	-0.56			1749.6	212.7	-34.6	
26.00	6.88	-7.60	-0.71			1749.5	212.1	-35.4	
26.50	10.63	-9.70	0.93			1749.4	211.5	-36.1	
27.00	11.73	-11.50	0.23			1749.2	211.0	-36.9	
27.50	13.37	-12.80	0.57			1749.1	210.4	-37.6	
28.00	15.01	-14.20	0.81			1748.9	209.8	-38.4	
28.50	14.53	-14.70	-0.16			1748.8	209.2	-39.2	
29.00	14.58	-15.30	-0.71			1748.6	208.6	-39.9	
29.50	14.10	-15.20	-1.09			1748.4	208.0	-40.7	
30.00	12.55	-14.90	-2.34			1748.2	207.5	-41.4	
30.50	12.61	-14.30	-1.68			1747.9	206.9	-42.2	
31.00	13.19	-13.50	-0.30			1747.7	206.3	-43.0	
31.50	12.70	-12.50	0.20			1747.4	205.7	-43.7	
32.00	11.14	-11.40	-0.25			1747.1	205.1	-44.5	
32.50	10.11	-10.60	-0.48			1746.8	204.5	-45.2	
33.00	10.13	-9.90	0.23			1746.5	203.9	-46.0	
33.50	10.15	-9.10	1.05			1746.1	203.3	-46.7	
34.00	10.15	-9.40	0.75			1745.8	202.7	-47.5	
34.50	9.62	-9.60	0.02			1745.4	202.1	-48.3	
35.00	10.13	-10.50	-0.36			1745.0	201.5	-49.0	
35.50	11.69	-11.30	0.39			1744.6	200.9	-49.8	
36.00	13.24	-12.90	0.34			1744.2	200.3	-50.5	
36.50	13.70	-15.60	-1.89			1743.7	199.7	-51.3	
37.00	15.22	-16.30	-1.07			1743.3	199.1	-52.0	
37.50	16.18	-18.10	-1.91			1742.8	198.5	-52.7	
38.00	17.12	-20.00	-2.87			1742.3	197.9	-53.5	
38.50	18.03	-21.60	-3.56			1741.8	197.3	-54.2	
39.00	22.65	-23.10	-0.44			1741.2	196.7	-55.0	
39.50	26.18	-24.10	2.08			1740.7	196.0	-55.7	
40.00	26.49	-24.90	1.59			1740.1	195.4	-56.5	
40.50	25.71	-25.20	0.51			1739.5	194.8	-57.2	
41.00	24.37	-25.00	-0.62			1738.9	194.2	-58.0	
41.50	25.13	-24.70	0.43			1738.2	193.6	-58.7	
42.00	23.73	-23.80	-0.06			1737.6	192.9	-59.4	
42.50	20.17	-23.00	-2.82			1736.9	192.3	-60.2	
43.00	20.30	-21.80	-1.49			1736.2	191.7	-60.9	
43.50	20.40	-21.00	-0.59			1735.5	191.1	-61.6	
44.00	19.39	-20.00	-0.60			1734.8	190.4	-62.4	
44.50	18.88	-19.50	-0.61			1734.0	189.8	-63.1	
45.00	17.80	-19.00	-1.19			1733.2	189.2	-63.8	
45.50	18.28	-18.80	-0.51			1732.5	188.5	-64.6	

Table 4 (Cont.)

MJD	$-10^7 \dot{P}$	$10^7 \dot{P}_r$	$-10^7 \dot{P}_a$	$\log \rho_\pi$	$\log \rho_s$	T_π (°K)	z (km)	$\alpha_\pi - \alpha_\odot$ (deg)	$\delta_\pi - \delta_\odot$ (deg)
40346.00	19.24	-19.20	0.04			1731.7	187.9	-65.3	
46.50	19.64	-19.70	-.05			1730.8	187.2	-66.0	
47.00	20.52	-20.90	-.37			1730.0	186.6	-66.7	
47.50	20.82	-22.10	-1.27			1729.1	185.9	-67.5	
48.00	24.84	-22.10	2.74			1728.2	185.3	-68.2	
48.50	27.78	-23.80	3.98			1727.5	184.6	-68.9	
49.00	29.62	-25.50	4.12			1726.9	184.0	-69.6	
49.50	30.36	-27.50	2.86			1726.2	183.3	-70.3	
50.00	32.14	-29.20	2.94			1725.5	182.6	-71.0	
50.50	33.34	-30.90	2.44			1724.8	182.0	-71.8	
51.00	33.98	-32.40	1.58			1724.1	181.3	-72.5	
51.50	32.46	-33.50	-1.03			1723.4	180.6	-73.2	
52.00	29.31	-34.40	-5.08			1722.7	179.9	-73.9	
52.50	29.85	-34.80	-4.94			1722.0	179.3	-74.6	
53.00	31.42	-34.80	-3.37			1721.2	178.6	-75.3	
53.50	32.96	-34.60	-1.63			1720.5	177.9	-76.0	
54.00	32.87	-33.80	-.92			1719.7	177.2	-76.7	
54.50	32.74	-33.00	-.25			1718.9	176.5	-77.4	
55.00	32.59	-31.90	0.69			1718.1	175.8	-78.1	
55.50	29.21	-30.60	-1.38			1717.3	175.1	-78.8	
56.00	27.40	-29.80	-2.39			1716.5	174.3	-79.5	
56.50	27.68	-28.70	-1.01			1715.7	173.6	-80.2	
57.00	27.94	-28.10	-.15			1714.9	172.9	-80.9	
57.50	29.22	-27.60	1.62			1714.0	172.2	-81.6	
58.00	28.88	-27.70	1.18			1713.2	171.4	-82.2	
58.50	28.52	-28.10	0.42			1712.3	170.7	-82.9	
59.00	29.18	-28.80	0.38			1711.4	169.9	-83.6	
59.50	31.41	-30.00	1.41			1710.6	169.1	-84.3	
60.00	32.55	-31.10	1.45			1709.6	168.3	-85.0	
60.50	34.19	-32.80	1.39			1708.7	167.6	-85.6	
61.00	35.27	-34.40	0.87			1707.8	166.8	-86.3	
61.50	38.45	-36.20	2.25			1706.9	165.9	-87.0	
62.00	40.01	-37.80	2.21			1705.9	165.1	-87.7	
62.50	40.48	-39.50	0.98			1705.0	164.3	-88.3	
63.00	40.38	-40.60	-.21			1704.0	163.4	-89.0	
63.50	41.86	-41.80	0.06			1703.0	162.6	-89.7	
64.00	42.78	-42.20	0.58			1702.0	161.7	-90.3	
64.50	43.67	-42.70	0.97			1701.0	160.8	-91.0	
65.00	42.41	-42.40	0.01			1700.0	159.9	-91.7	
65.50	41.12	-42.10	-.97			1698.9	159.0	-92.3	
66.00	37.15	-41.30	-4.14			1697.9	158.0	-93.0	
66.50	35.81	-40.40	-4.58			1696.8	157.0	-93.6	
67.00	34.98	-39.20	-4.21			1695.7	156.0	-94.3	
67.50	34.13	-37.70	-3.56			1694.7	155.0	-94.9	
68.00	34.31	-36.90	-2.58			1693.6	153.9	-95.6	
68.50	33.94	-35.70	-1.75			1692.4	152.8	-96.2	
69.00	33.55	-35.00	-1.44			1691.3	151.6	-96.8	
69.50	33.66	-34.50	-.83			1690.2	150.5	-97.5	
70.00	34.81	-34.20	0.61			1689.1	149.2	-98.1	
70.50	34.88	-33.70	1.18			1687.9	147.9	-98.7	
71.00	35.45	-34.70	0.75			1686.7	146.6	-99.4	
71.50	34.94	-35.50	-.55			1685.6	145.1	-100.0	
72.00	36.00	-36.40	-.39			1684.4	143.6	-100.6	
72.50	38.64	-37.50	1.14			1683.2	142.0	-101.2	
73.00	39.66	-38.80	0.86			1682.0	140.3	-101.8	
73.50	40.66	-40.40	0.26			1680.7	138.5	-102.4	
74.00	42.16	-41.60	0.56			1679.5	136.5	-103.0	
74.50	42.59	-43.00	-.40			1678.3	134.4	-103.6	
75.00	43.53	-44.00	-.46			1677.0	132.1	-104.2	
75.50	45.50	-44.80	0.70			1675.7	129.5	-104.7	

Table 4 (Cont.)

MJD	$-10^7 \dot{P}$	$10^7 \dot{P}_r$	$-10^7 \dot{P}_a$	$\log \rho_\pi$	$\log \rho_s$	T_π (°K)	z (km)	$a_\pi - a_\odot$ (deg)	$\delta_\pi - \delta_\odot$ (deg)
40376.00	46.93	-45.40	1.53			1674.5	126.7	-105.3	
76.50	47.28	-45.70	1.58			1673.2	123.5	-105.8	
77.00	45.48	-45.60	-0.11			1671.9	120.0	-106.3	
77.50	44.19	-45.00	-0.80			1670.6	115.9	-106.8	
78.00	44.48	-44.50	-0.01			1669.3	111.4	-107.3	
78.50	43.16	-43.30	-0.13			1667.9	106.1	-107.7	
79.00	41.29	-42.40	-1.10			1666.6	100.1	-108.2	
79.50	38.34	-40.70	-2.35			1665.3	93.3	-108.5	
80.00	36.44	-39.90	-3.45			1663.9	85.6	-108.8	
80.50	36.11	-38.40	-2.28			1662.5	77.1	-109.0	
81.00	36.82	-37.50	-0.67			1661.2	68.1	-109.2	
81.50	36.46	-36.50	-0.03			1659.8	58.7	-109.2	
82.00	36.08	-35.80	0.28			1658.4	49.5	-109.2	
82.50	35.69	-35.30	0.39			1657.0	40.8	-109.1	
83.00	36.34	-35.10	1.24			1655.6	32.8	-108.9	
83.50	35.92	-35.20	0.72			1654.2	25.6	-108.7	
84.00	35.47	-35.30	0.17			1652.8	19.4	-108.4	
84.50	37.14	-36.00	1.14			1651.4	13.9	-108.0	
85.00	37.73	-36.40	1.33			1649.9	9.1	-107.6	
85.50	38.84	-37.30	1.54			1648.5	4.8	-107.2	
86.00	38.88	-37.70	1.18			1647.1	1.1	-106.8	
86.50	39.96	-38.50	1.46			1645.6	357.8	-106.4	
87.00	40.49	-39.00	1.49			1644.2	354.9	-105.9	
87.50	41.55	-39.40	2.15			1642.7	352.2	-105.4	
88.00	44.71	-39.50	5.21			1641.2	349.8	-104.9	
88.50	45.74	-39.50	6.24			1639.8	347.6	-104.5	
89.00	42.51	-39.10	3.41			1638.3	345.6	-104.0	
89.50	38.74	-38.50	0.24			1636.8	343.7	-103.4	
90.00	36.02	-37.60	-1.57			1635.3	341.9	-102.9	
90.50	34.35	-36.70	-2.34			1633.9	340.3	-102.4	
91.00	32.67	-35.10	-2.42			1632.4	338.7	-101.9	
91.50	31.51	-33.40	-1.88			1630.9	337.3	-101.4	
92.00	30.34	-31.90	-1.55			1629.4	335.9	-100.8	
92.50	28.09	-30.30	-2.20			1627.9	334.5	-100.3	
93.00	26.90	-28.50	-1.59			1626.4	333.3	-99.8	
93.50	26.23	-27.00	-0.76			1624.9	332.0	-99.2	
94.00	24.49	-25.00	-0.50			1623.4	330.9	-98.7	
94.50	23.27	-23.50	-0.22			1621.9	329.7	-98.1	
95.00	21.51	-22.60	-1.08			1620.4	328.6	-97.6	
95.50	19.75	-20.00	-0.24			1618.9	327.6	-97.0	
96.00	17.44	-18.10	-0.65			1617.4	326.5	-96.5	
96.50	15.13	-15.30	-0.16			1615.9	325.5	-95.9	
97.00	12.81	-13.30	-0.48			1614.4	324.5	-95.4	
97.50	11.01	-10.00	1.01			1612.9	323.6	-94.8	
98.00	9.21	-4.30	4.91			1611.4	322.6	-94.2	
98.50	7.92	-4.30	3.62			1609.9	321.7	-93.7	
99.00	6.64	-4.30	2.34			1608.5	320.8	-93.1	
99.50	4.81	-4.30	0.51			1607.0	319.9	-92.5	
40400.00	2.45	-4.30	-1.84			1605.5	319.1	-92.0	
00.50	1.15	-4.30	-3.14			1604.0	318.2	-91.4	
01.00	-0.16	-4.30	-4.45			1602.5	317.4	-90.8	
01.50	1.71	-4.30	-2.58			1601.1	316.5	-90.2	
02.00	4.10	-4.20	-0.09			1599.6	315.7	-89.7	
02.50	4.90	-4.20	0.70			1598.2	314.9	-89.1	
03.00	4.63	-4.20	0.43			1596.7	314.1	-88.5	
03.50	6.48	-4.20	2.28			1595.3	313.3	-87.9	
04.00	7.27	-4.10	3.17			1593.8	312.5	-87.3	
04.50	6.99	-4.10	2.89			1592.4	311.7	-86.7	

Table 4 (Cont.)

MJD	$-10^7 \dot{P}$	$10^7 \dot{P}_r$	$-10^7 \dot{P}_a$	$\log \rho_\pi$	$\log \rho_s$	T_π (°K)	z (km)	$a_\pi - a_\odot$ (deg)	$\delta_\pi - \delta_\odot$ (deg)
40405.00	6.71	-4.10	2.61	-17.98	-18.25	1058	1591.0	311.0	-86.2
05.50	4.84	-4.08	0.76	-18.52	.79	824	1589.6	310.2	-85.6
06.00	4.02	-4.06	-.03				1588.2	309.4	-85.0
06.50	4.26	-4.03	0.23	-19.04	-19.31	743	1586.8	308.7	-84.4
07.00	3.97	-4.01	-.03				1585.4	307.9	-83.8
07.50	3.15	-3.98	-.82				1584.0	307.2	-83.2
08.00	3.92	-3.96	-.03				1582.7	306.5	-82.6
08.50	4.69	-3.94	0.75	-18.53	-18.81	822	1581.3	305.7	-82.0
09.00	3.86	-3.92	-.05				1580.0	305.0	-81.4
09.50	3.04	-3.89	-.84				1578.7	304.3	-80.8
10.00	2.21	-3.87	-1.65				1577.4	303.6	-80.2
40411.00	4.09	-3.82	0.27	-18.98	-19.26	746	1574.8	302.2	-78.9
12.00	4.55	-3.77	0.78	.52	-18.81	832	1572.3	300.8	-77.7
13.00	4.84	-3.72	1.12	.37	.66	902	1569.8	299.4	-76.5
14.00	4.71	-3.66	1.05	.40	.69	890	1567.4	298.0	-75.2
15.00	3.75	-3.61	0.14	-19.28	-19.57	750	1565.0	296.6	-74.0
16.00	3.57	-3.56	0.01	-20.43	-20.72	751	1562.8	295.3	-72.7
17.00	3.76	-3.50	0.26	-19.02	-19.32	752	1560.5	294.0	-71.5
18.00	3.79	-3.44	0.35	-18.90	.20	754	1558.4	292.6	-70.2
19.00	3.54	-3.38	0.16	-19.24	.55	756	1556.3	291.3	-69.0
20.00	3.66	-3.33	0.33	-18.94	.25	758	1554.2	290.0	-67.7
21.00	3.37	-3.27	0.10	-19.46	.78	760	1552.3	288.7	-66.4
22.00	3.32	-3.20	0.12	.39	.70	763	1550.4	287.4	-65.1
23.00	2.59	-3.14	-.54				1548.5	286.1	-63.8
24.00	2.77	-3.06	-.28				1546.7	284.8	-62.5
25.00	3.07	-3.00	0.07	-19.63	-19.94	764	1545.0	283.6	-61.2
26.00	2.55	-2.92	-.36				1543.3	282.3	-59.9
27.00	2.29	-2.85	-.55				1541.6	281.0	-58.6
28.00	4.01	-2.78	1.23	-18.39	-18.71	925	1540.1	279.8	-57.2
29.00	6.24	-2.70	3.54	-17.92	.24	1159	1538.5	278.5	-55.9
30.00	3.29	-2.62	0.67	-18.64	.97	767	1537.1	277.3	-54.6
31.00	2.19	-2.54	-.34				1535.7	276.0	-53.2
32.00	1.61	-2.46	-.84				1534.3	274.8	-51.9
33.00	1.82	-2.38	-.55				1533.0	273.6	-50.5
34.00	2.42	-2.30	0.12	-19.40	-19.73	772	1531.7	272.3	-49.2
35.00	2.48	-2.22	0.26	.06	.40	760	1530.5	271.1	-47.8
36.00	3.07	-2.14	0.93	-18.51	-18.84	889	1529.3	269.9	-46.4
37.00	3.65	-2.08	1.57	.28	.61	1000	1528.1	268.7	-45.0
38.00	3.70	-2.00	1.70	.25	.57	1018	1527.0	267.5	-43.6
39.00	3.36	-1.94	1.42	.33	.66	981	1526.0	266.3	-42.3
40.00	3.41	-1.86	1.55	.29	.63	999	1524.9	265.1	-40.8
41.00	3.06	-1.80	1.26	.38	.72	959	1524.0	263.9	-39.4
42.00	3.11	-1.74	1.37	.34	.68	978	1523.0	262.7	-38.0
43.00	2.90	-1.68	1.22	.39	.74	956	1522.1	261.5	-36.6
44.00	2.70	-1.62	1.08	.45	.80	931	1521.2	260.3	-35.2
45.00	2.50	-1.56	0.94	.51	.86	904	1520.4	259.1	-33.8
46.00	2.43	-1.50	0.93	.51	.86	904	1519.6	257.9	-32.3
47.00	2.25	-1.46	0.79	.59	.93	866	1518.8	256.8	-30.9
48.00	2.20	-1.41	0.79	.60	.93	869	1518.0	255.6	-29.4
49.00	2.29	-1.36	0.93	.54	.86	911	1517.3	254.4	-28.0
50.00	2.26	-1.33	0.93	.54	.86	911	1516.6	253.2	-26.5
51.00	2.38	-1.30	1.08	.47	.80	944	1515.9	252.1	-25.1
52.00	2.50	-1.26	1.24	.41	.74	973	1515.2	250.9	-23.6
53.00	2.51	-1.24	1.27	.40	.73	979	1514.6	249.8	-22.1
54.00	2.40	-1.20	1.20	.42	.75	970	1513.9	248.6	-20.7
55.00	2.17	-1.19	0.98	.52	.84	930	1513.3	247.4	-19.2
56.00	1.82	-1.18	0.64	.69	-19.03	793	1512.7	246.3	-17.7
57.00	1.23	-1.16	0.07	-19.64	.99	793	1512.1	245.1	-16.2
58.00	2.24	-1.16	1.08	-18.45	-18.80	948	1511.5	244.0	-14.7

Table 4 (Cont.)

MJD	$-10^7 \dot{P}$	$10^7 \dot{P}_r$	$-10^7 \dot{P}_a$	$\log \rho_\pi$	$\log \rho_s$	T_π (°K)	z (km)	$a_\pi - a_\odot$ (deg)	$\delta_\pi - \delta_\odot$ (deg)
40459.00	3.14	-1.16	1.98	-18.19	-18.54	1078	1510.9	242.8	-13.2
60.00	3.67	-1.16	2.51	.07	.44	1138	1510.3	241.7	-11.7
61.00	3.02	-1.17	1.85	.21	.57	1066	1509.7	240.5	-10.2
62.00	1.60	-1.18	0.42	.85	-19.22	793	1509.1	239.4	-8.7
63.00	1.80	-1.20	0.60	.70	.06	793	1508.5	238.2	-7.2
64.00	2.01	-1.22	0.79	.58	-18.94	877	1508.0	237.1	-5.7
65.00	2.26	-1.24	1.02	.47	.83	935	1507.3	235.9	-4.1
40466.00	2.93	-1.26	1.67				1506.7	234.8	-2.6
67.00	3.75	-1.28	2.47				1506.1	233.7	-1.1
68.00	4.35	-1.32	3.03				1505.4	232.5	0.4
40468.50	3.94	-1.80	2.14				1504.7	231.9	1.2
69.00	4.78	-2.10	2.68				1504.4	231.4	2.0
69.50	5.10	-3.20	1.90				1504.2	230.8	2.7
70.00	6.48	-4.30	2.18				1503.9	230.2	3.5
70.50	6.81	-5.20	1.61				1503.6	229.7	4.3
71.00	7.14	-5.90	1.24				1503.4	229.1	5.0
71.50	7.48	-7.00	0.48				1503.1	228.5	5.8
72.00	8.35	-8.90	-.54				1502.8	227.9	6.6
72.50	9.76	-9.30	0.46				1502.4	227.4	7.3
73.00	10.11	-9.90	0.21				1502.1	226.8	8.1
73.50	11.53	-11.00	0.53				1501.8	226.2	8.9
74.00	12.42	-11.80	0.62				1501.4	225.7	9.6
74.50	13.85	-12.70	1.15				1501.1	225.1	10.4
75.00	13.69	-13.30	0.39				1500.7	224.5	11.2
75.50	14.59	-13.70	0.89				1500.4	223.9	12.0
76.00	14.44	-14.20	0.24				1500.0	223.4	12.7
76.50	14.82	-14.20	0.62				1499.6	222.8	13.5
77.00	15.74	-14.40	1.34				1499.2	222.2	14.3
77.50	15.07	-14.10	0.97				1498.8	221.7	15.0
78.00	15.47	-14.00	1.47				1498.4	221.1	15.8
78.50	14.27	-13.50	0.77				1497.9	220.5	16.6
79.00	14.15	-13.20	0.95				1497.5	219.9	17.4
79.50	14.02	-12.60	1.42				1497.0	219.4	18.1
80.00	14.43	-12.30	2.13				1496.6	218.8	18.9
80.50	13.25	-12.00	1.25				1496.1	218.2	19.7
81.00	12.61	-11.80	0.81				1495.6	217.6	20.5
81.50	12.49	-11.80	0.69				1495.2	217.1	21.2
82.00	12.39	-11.70	0.69				1494.7	216.5	22.0
82.50	12.28	-12.10	0.18				1494.2	215.9	22.8
83.00	12.18	-12.40	-.21				1493.6	215.3	23.6
83.50	12.61	-13.20	-.58				1493.1	214.8	24.3
84.00	14.63	-13.90	0.73				1492.6	214.2	25.1
84.50	15.59	-15.00	0.59				1492.0	213.6	25.9
85.00	17.09	-16.20	0.89				1491.5	213.0	26.7
85.50	18.06	-17.30	0.76				1490.9	212.4	27.5
86.00	20.09	-18.90	1.19				1490.3	211.9	28.2
86.50	21.59	-20.50	1.09				1489.8	211.3	29.0
87.00	22.57	-21.80	0.77				1489.2	210.7	29.8
87.50	24.61	-23.30	1.31				1488.6	210.1	30.6
88.00	25.06	-24.50	0.56				1488.0	209.5	31.3
88.50	26.04	-25.50	0.54				1487.3	208.9	32.1
89.00	27.02	-26.60	0.42				1486.7	208.3	32.9
89.50	27.47	-27.40	0.07				1486.1	207.8	33.7
90.00	28.46	-27.90	0.56				1485.4	207.2	34.5
90.50	28.92	-28.50	0.42				1484.7	206.6	35.2
91.00	28.32	-28.30	0.02				1484.1	206.0	36.0
91.50	28.25	-28.20	0.05				1483.4	205.4	36.8
92.00	28.18	-27.90	0.28				1482.7	204.8	37.6

Table 4 (Cont.)

MJD	$-10^7 \dot{P}$	$10^7 \dot{P}_r$	$-10^7 \dot{P}_a$	$\log \rho_\pi$	$\log \rho_s$	T_π (°K)	z (km)	$a_\pi - a_\odot$ (deg)	$\delta_\pi - \delta_\odot$ (deg)
40492.50	29.17	-27.40	1.77			1482.0	204.2	38.3	
93.00	29.63	-27.00	2.63			1481.3	203.6	39.1	
93.50	30.09	-26.20	3.89			1480.5	203.0	39.9	
94.00	30.03	-25.70	4.33			1479.8	202.4	40.7	
94.50	27.31	-24.80	2.51			1479.0	201.8	41.4	
95.00	25.66	-24.60	1.06			1478.3	201.2	42.2	
95.50	21.89	-24.20	-2.30			1477.5	200.6	43.0	
96.00	22.35	-24.00	-1.64			1476.7	200.0	43.8	
96.50	23.88	-24.20	-.31			1475.9	199.4	44.6	
97.00	24.87	-24.30	0.57			1475.1	198.8	45.3	
97.50	25.87	-25.00	0.87			1474.3	198.2	46.1	
98.00	26.34	-25.50	0.84			1473.5	197.6	46.9	
98.50	26.80	-26.80	0.00			1472.7	197.0	47.7	
99.00	28.33	-27.60	0.73			1471.8	196.4	48.4	
99.50	29.32	-29.10	0.22			1471.0	195.7	49.2	
40500.00	30.32	-31.40	-1.07			1470.1	195.1	50.0	
00.50	32.37	-32.10	0.27			1469.2	194.5	50.8	
01.00	33.36	-33.60	-.23			1468.3	193.9	51.5	
01.50	35.41	-35.40	0.01			1467.4	193.3	52.3	
02.00	36.40	-36.80	-.39			1466.5	192.6	53.1	
02.50	38.45	-38.10	0.35			1465.6	192.0	53.9	
03.00	39.97	-39.50	0.47			1464.7	191.4	54.6	
03.50	40.43	-40.40	0.03			1463.7	190.7	55.4	
04.00	41.95	-41.40	0.55			1462.8	190.1	56.2	
04.50	43.46	-41.90	1.56			1461.8	189.5	56.9	
05.00	43.91	-42.40	1.51			1460.8	188.8	57.7	
05.50	44.37	-42.50	1.87			1459.9	188.2	58.5	
06.00	43.23	-42.30	0.93			1458.9	187.5	59.2	
06.50	42.62	-42.00	0.62			1457.8	186.9	60.0	
07.00	42.54	-41.40	1.14			1456.8	186.2	60.8	
07.50	42.46	-40.70	1.76			1455.8	185.5	61.5	
08.00	40.78	-40.00	0.78			1454.7	184.9	62.3	
08.50	39.64	-38.80	0.64			1453.7	184.2	63.1	
09.00	39.55	-38.50	1.05			1452.6	183.5	63.8	
09.50	38.92	-37.60	1.32			1451.5	182.9	64.6	
10.00	37.77	-37.30	0.47			1450.4	182.2	65.4	
10.50	37.14	-36.90	0.24			1449.3	181.5	66.1	
11.00	37.57	-36.80	0.77			1448.2	180.8	66.9	
11.50	37.47	-36.60	0.87			1447.1	180.1	67.7	
12.00	37.37	-37.20	0.17			1446.0	179.4	68.4	
12.50	38.32	-37.60	0.72			1444.8	178.7	69.2	
13.00	39.27	-38.50	0.77			1443.7	178.0	69.9	
13.50	40.21	-39.40	0.81			1442.5	177.3	70.7	
14.00	40.62	-40.80	-.17			1441.3	176.5	71.4	
14.50	42.62	-41.80	0.82			1440.1	175.8	72.2	
15.00	43.55	-43.70	-.14			1438.9	175.1	73.0	
15.50	45.54	-45.00	0.54			1437.7	174.3	73.7	
16.00	47.00	-46.90	0.10			1436.5	173.6	74.5	
16.50	49.51	-48.30	1.21			1435.2	172.8	75.2	
17.00	51.49	-49.80	1.69			1434.0	172.0	76.0	
17.50	51.87	-51.00	0.87			1432.7	171.2	76.7	
18.00	52.26	-52.20	0.06			1431.4	170.4	77.5	
18.50	53.17	-52.90	0.27			1430.2	169.6	78.2	
19.00	54.07	-53.60	0.47			1428.9	168.8	78.9	
19.50	55.50	-54.00	1.50			1427.6	168.0	79.7	
20.00	57.98	-53.90	4.08			1426.2	167.1	80.4	
20.50	57.81	-53.60	4.21			1424.9	166.2	81.2	
21.00	56.58	-53.30	3.28			1423.6	165.4	81.9	
21.50	56.41	-52.40	4.01			1422.2	164.5	82.6	
22.00	55.17	-51.90	3.27			1420.8	163.5	83.4	

Table 4 (Cont.)

MJD	$-10^7 \dot{P}_r$	$10^7 \dot{P}_a$	$-10^7 \dot{P}_a$	$\log \rho_\pi$	$\log \rho_s$	T_π (°K)	z (km)	$a_\pi - a_\odot$ (deg)	$\delta_\pi - \delta_\odot$ (deg)
40522.50	53.93	-50.80	3.13			1419.5	162.6	34.1	
23.00	53.21	-50.10	3.11			1418.1	161.6	84.8	
23.50	52.48	-48.80	3.68			1416.7	160.7	85.6	
24.00	51.76	-48.30	3.46			1415.3	159.6	86.3	
24.50	51.02	-47.60	3.42			1413.9	158.6	87.0	
25.00	50.81	-46.90	3.91			1412.4	157.5	87.7	
25.50	49.01	-46.60	2.41			1411.0	156.4	88.5	
26.00	48.26	-46.30	1.96			1409.5	155.3	89.2	
26.50	48.03	-46.40	1.63			1408.1	154.1	89.9	
27.00	48.33	-46.60	1.73			1406.6	152.8	90.6	
27.50	48.00	-47.30	0.70			1405.1	151.5	91.3	
28.00	48.21	-47.80	0.41			1403.6	150.2	92.0	
28.50	48.43	-49.00	-0.56			1402.2	148.8	92.7	
29.00	49.17	-49.90	-0.72			1400.7	147.3	93.4	
29.50	52.56	-51.20	1.36			1399.3	145.7	94.1	
30.00	53.31	-52.40	0.91			1397.8	144.0	94.8	
30.50	55.11	-53.80	1.31			1396.3	142.2	95.5	
31.00	55.85	-55.00	0.85			1394.8	140.2	96.2	
31.50	57.65	-56.30	1.35			1393.3	138.2	96.8	
32.00	58.91	-57.20	1.71			1391.8	135.9	97.5	
32.50	60.70	-58.10	2.60			1390.3	133.4	98.1	
33.00	61.42	-58.80	2.62			1388.8	130.7	98.8	
33.50	61.60	-59.30	2.30			1387.2	127.7	99.4	
34.00	62.30	-59.40	2.90			1385.7	124.3	100.0	
34.50	62.98	-59.40	3.58			1384.1	120.6	100.6	
35.00	62.60	-58.90	3.70			1382.6	116.4	101.2	
35.50	62.73	-58.30	4.43			1381.0	111.6	101.7	
36.00	62.31	-57.50	4.81			1379.5	106.2	102.2	
36.50	57.12	-56.50	0.62			1377.9	100.1	102.7	
37.00	56.14	-55.40	0.74			1376.3	93.3	103.1	
37.50	55.14	-53.80	1.34			1374.8	85.8	103.4	
38.00	54.64	-53.00	1.64			1373.2	77.6	103.7	
38.50	54.11	-51.70	2.41			1371.6	69.1	103.9	
39.00	54.09	-50.80	3.29			1370.0	60.4	104.1	
39.50	51.93	-49.80	2.13			1368.4	51.9	104.1	
40.00	51.86	-48.90	2.96			1366.8	43.9	104.1	
40.50	50.69	-48.20	2.49			1365.2	36.6	104.0	
41.00	50.03	-47.80	2.23			1363.6	29.9	103.8	
41.50	50.38	-47.50	2.88			1362.0	24.0	103.6	
42.00	49.65	-47.50	2.15			1360.4	18.7	103.3	
42.50	49.93	-47.70	2.23			1358.8	14.1	103.1	
43.00	50.71	-48.00	2.71			1357.2	10.0	102.8	
43.50	50.92	-48.50	2.42			1355.6	6.3	102.4	
44.00	51.61	-48.90	2.71			1354.0	3.1	102.1	
44.50	52.80	-49.50	3.30			1352.4	0.1	101.7	
45.00	53.93	-50.00	3.93			1350.8	357.4	101.3	
45.50	53.97	-50.60	3.37			1349.2	355.0	101.0	
46.00	54.49	-51.00	3.49			1347.6	352.7	100.6	
46.50	54.96	-51.30	3.66			1346.0	350.7	100.2	
47.00	54.86	-51.40	3.46			1344.4	348.7	99.7	
47.50	55.76	-51.40	4.36			1342.8	346.9	99.3	
48.00	55.55	-50.90	4.65			1341.2	345.2	98.9	
48.50	55.82	-50.20	5.62			1339.6	343.6	98.5	
49.00	53.92	-49.50	4.42			1338.0	342.1	98.0	
49.50	53.02	-48.30	4.72			1336.4	340.7	97.6	
50.00	51.53	-47.20	4.33			1334.8	339.3	97.2	
50.50	49.99	-45.50	4.49			1333.2	338.0	96.7	
51.00	48.38	-44.00	4.38			1331.7	336.7	96.3	
51.50	46.71	-42.10	4.61			1330.1	335.5	95.8	
52.00	45.51	-40.30	5.21			1328.5	334.3	95.4	

Table 4 (Cont.)

MJD	$-10^7 \dot{P}$	$10^7 \dot{P}_r$	$-10^7 \dot{P}_a$	$\log \rho_\pi$	$\log \rho_s$	T_π (°K)	z (km)	$a_\pi - a_\odot$ (deg)	$\delta_\pi - \delta_\odot$ (deg)
40552.50	44.24	-38.50	5.74				1327.0	333.1	94.9
53.00	41.85	-36.30	5.55				1325.4	332.0	94.4
53.50	38.86	-34.50	4.36				1323.9	330.9	94.0
54.00	35.81	-32.10	3.71				1322.3	329.9	93.5
54.50	33.74	-30.00	3.74				1320.8	328.8	93.0
55.00	32.12	-27.90	4.22				1319.3	327.8	92.6
55.50	29.37	-25.30	4.07				1317.8	326.8	92.1
56.00	27.08	-23.20	3.88				1316.3	325.9	91.6
56.50	23.66	-20.00	3.66				1314.8	324.9	91.1
57.00	21.21	-16.80	4.41				1313.3	324.0	90.7
40558.00	9.97	-5.22	4.75				1310.3	322.2	89.7
40560.00	9.37	-5.14	4.23	-17.71	-17.87	953	1304.6	318.6	87.7
62.00	8.93	-5.04	3.89	.75	.92	934	1299.0	315.3	85.8
64.00	8.61	-4.94	3.67	.78	.96	920	1293.6	312.0	83.7
66.00	8.14	-4.84	3.30	.83	-18.02	899	1288.2	308.8	81.7
68.00	7.85	-4.72	3.14	.86	.05	889	1283.0	305.7	79.6
70.00	7.67	-4.61	3.06	.87	.07	885	1278.0	302.7	77.4
72.00	8.13	-4.48	3.65	.80	.01	922	1273.1	299.7	75.3
74.00	8.37	-4.36	4.01	.77	-17.98	943	1268.5	296.8	73.1
76.00	8.69	-4.24	4.45	.73	.94	969	1264.0	293.8	70.9
78.00	8.54	-4.11	4.43	.74	.96	973	1259.7	290.9	68.6
80.00	8.05	-3.99	4.06	.78	-18.00	957	1255.6	288.1	66.3
82.00	7.20	-3.87	3.33	.87	.10	917	1251.7	285.2	64.0
84.00	7.00	-3.75	3.25	.88	.12	915	1248.1	282.4	61.6
86.00	6.87	-3.64	3.23	.89	.13	917	1244.7	279.6	59.2
88.00	6.98	-3.52	3.46	.87	.11	938	1241.6	276.8	56.8
90.00	7.02	-3.42	3.60	.85	.10	951	1238.7	274.0	54.3
92.00	6.00	-3.31	2.69	.98	.24	891	1236.1	271.3	51.8
40593.00	4.96	-3.26	1.70	-18.18	-18.44	792	1235.1	269.9	50.5
94.00	5.20	-3.21	1.99	.11	.38	831	1233.8	268.5	49.2
95.00	5.01	-3.16	1.85	.14	.41	818	1232.6	267.1	48.0
96.00	4.91	-3.12	1.79	.16	.43	813	1231.5	265.8	46.7
97.00	4.51	-3.08	1.43	.26	.53	725	1230.3	264.4	45.4
98.00	4.46	-3.04	1.42	.26	.53	737	1229.2	263.1	44.1
99.00	4.23	-2.99	1.24	.33	.59	729	1228.2	261.7	42.7
40600.00	6.58	-2.95	3.63	-17.86	.12	982	1227.2	260.4	41.4
01.00	7.70	-2.92	4.78	.74	.01	1054	1226.2	259.0	40.1
02.00	7.85	-2.88	4.97	.73	-17.99	1069	1225.2	257.7	38.7
03.00	6.88	-2.86	4.02	.82	-18.08	1019	1224.3	256.3	37.4
04.00	6.25	-2.83	3.42	.89	.16	982	1223.4	255.0	36.0
05.00	5.43	-2.81	2.62	-18.01	.27	924	1222.5	253.7	34.6
06.00	5.20	-2.79	2.41	.04	.31	908	1221.6	252.4	33.3
07.00	5.18	-2.77	2.41	.04	.31	911	1220.8	251.0	31.9
08.00	4.29	-2.76	1.53	.24	.51	807	1219.9	249.7	30.5
09.00	4.92	-2.75	2.17	.09	.36	892	1219.1	248.4	29.1
40618.00	8.74	-8.50	0.24				1212.0	236.7	16.2
19.00	12.62	-11.40	1.22				1211.2	235.4	14.7
20.00	17.33	-13.60	3.73				1210.4	234.1	13.2
21.00	18.25	-15.30	2.95				1209.6	232.8	11.8
22.00	17.49	-16.30	1.19				1208.8	231.6	10.3
23.00	16.51	-16.70	.18				1208.0	230.3	8.8
24.00	16.07	-16.60	.52				1207.1	229.0	7.3
25.00	16.71	-16.30	0.41				1206.3	227.8	5.8
26.00	17.11	-15.90	1.21				1205.4	226.5	4.3
27.00	17.80	-15.90	1.90				1204.5	225.2	2.8

Table 4 (Cont.)

MJD	$-10^7 \dot{P}$	$10^7 P_r$	$-10^7 P_a$	$\log \rho_\pi$	$\log \rho_s$	T_π (°K)	z (km)	$a_\pi - a_\odot$ (deg)	$\delta_\pi - \delta_\odot$ (deg)
40628.00	18.37	-16.50	1.87			1203.6	224.0	1.3	
29.00	19.22	-17.70	1.52			1202.6	222.7	-0.3	
30.00	20.61	-19.50	1.11			1201.7	221.4	-1.8	
31.00	22.53	-22.10	0.43			1200.7	220.2	-3.3	
32.00	25.79	-24.90	0.89			1199.7	218.9	-4.8	
33.00	31.15	-27.00	4.15			1198.6	217.7	-6.4	
34.00	33.88	-30.20	3.68			1197.5	216.4	-7.9	
35.00	34.64	-32.10	2.54			1196.4	215.2	-9.5	
36.00	33.96	-33.20	0.76			1195.3	213.9	-11.0	
37.00	33.14	-33.60	-0.45			1194.1	212.7	-12.6	
38.00	33.63	-33.30	0.33			1192.9	211.4	-14.1	
39.00	33.19	-32.40	0.79			1191.6	210.2	-15.7	
40.00	33.26	-31.40	1.86			1190.4	208.9	-17.2	
41.00	30.30	-30.50	-0.19			1189.0	207.7	-18.8	
42.00	31.27	-30.20	1.07			1187.7	206.4	-20.4	
43.00	32.10	-30.60	1.50			1186.3	205.2	-21.9	
44.00	33.03	-31.80	1.23			1184.8	203.9	-23.5	
45.00	34.73	-33.90	0.83			1183.3	202.7	-25.1	
46.00	37.73	-35.60	1.13			1181.9	201.4	-26.6	
47.00	40.82	-39.70	1.12			1180.2	200.2	-28.2	
48.00	44.16	-42.90	1.26			1178.5	198.9	-29.8	
49.00	46.80	-45.80	1.00			1176.8	197.6	-31.4	
50.00	51.51	-48.00	3.51			1175.1	196.4	-32.9	
51.00	53.03	-49.30	3.73			1173.3	195.1	-34.5	
52.00	52.28	-49.70	2.58			1171.5	193.8	-36.1	
40653.00	52.33	-48.80	3.53			1169.6	192.5	-37.7	
53.50	53.47	-48.00	5.47			1168.6	191.9	-38.5	
54.00	55.16	-47.80	7.36			1167.7	191.3	-39.3	
54.50	50.56	-46.90	3.66			1166.7	190.6	-40.1	
55.00	49.14	-46.50	2.64			1165.7	190.0	-40.8	
55.50	47.74	-45.80	1.94			1164.7	189.3	-41.6	
56.00	45.84	-45.40	0.44			1163.7	188.7	-42.4	
56.50	46.58	-45.10	1.48			1162.6	188.0	-43.2	
57.00	47.35	-44.70	2.65			1161.6	187.4	-44.0	
57.50	46.55	-44.70	1.85			1160.6	186.7	-44.8	
58.00	46.83	-44.70	2.13			1159.5	186.1	-45.6	
58.50	46.60	-45.00	1.60			1158.4	185.4	-46.4	
59.00	47.43	-45.60	1.83			1157.4	184.8	-47.2	
59.50	48.29	-46.50	1.79			1156.3	184.1	-48.0	
60.00	48.10	-47.30	0.80			1155.2	183.4	-48.8	
60.50	48.98	-48.50	0.48			1154.1	182.8	-49.6	
61.00	49.35	-49.70	-0.34			1152.9	182.1	-50.3	
61.50	49.73	-51.10	-1.36			1151.8	181.4	-51.1	
62.00	51.18	-52.60	-1.41			1150.7	180.7	-51.9	
62.50	53.16	-54.20	-1.03			1149.5	180.0	-52.7	
63.00	55.67	-55.60	0.07			1148.3	179.4	-53.5	
63.50	56.62	-57.30	-0.67			1147.2	178.7	-54.3	
64.00	59.16	-58.50	0.66			1146.0	178.0	-55.1	
64.50	60.65	-59.80	0.85			1144.8	177.3	-55.9	
65.00	61.62	-60.80	0.82			1143.6	176.6	-56.7	
65.50	63.13	-61.70	1.43			1142.4	175.9	-57.5	
66.00	65.16	-62.40	2.76			1141.1	175.2	-58.2	
66.50	65.10	-63.00	2.10			1139.9	174.4	-59.0	
67.00	66.10	-63.10	3.00			1138.7	173.7	-59.8	
67.50	66.04	-63.10	2.94			1137.4	173.0	-60.6	
68.00	66.52	-62.90	3.62			1136.1	172.3	-61.4	
68.50	66.47	-62.40	4.07			1134.9	171.5	-62.2	
69.00	65.90	-61.90	4.00			1133.6	170.8	-63.0	
69.50	64.80	-61.20	3.60			1132.3	170.0	-63.7	

Table 4 (Cont.)

MJD	$-10^7 \dot{P}$	$10^7 \dot{P}_r$	$-10^7 \dot{P}_a$	$\log \rho_\pi$	$\log \rho_s$	T_π (°K)	z (km)	$a_\pi - a_\odot$ (deg)	$\delta_\pi - \delta_\odot$ (deg)
40670.00	64.75	-60.50	4.25			1131.0	169.2	-64.5	
70.50	63.66	-59.70	3.96			1129.7	168.5	-65.3	
71.00	63.61	-58.90	4.71			1128.4	167.7	-66.1	
71.50	63.03	-57.90	5.13			1127.0	166.9	-66.9	
72.00	62.97	-57.40	5.57			1125.7	166.1	-67.7	
72.50	62.39	-56.80	5.59			1124.4	165.3	-68.4	
73.00	61.27	-56.70	4.57			1123.0	164.4	-69.2	
73.50	60.68	-56.10	4.58			1121.6	163.6	-70.0	
74.00	60.07	-56.20	3.87			1120.3	162.7	-70.8	
74.50	59.99	-56.50	3.49			1118.9	161.9	-71.5	
75.00	59.89	-56.70	3.19			1117.5	161.0	-72.3	
75.50	59.79	-57.60	2.19			1116.1	160.1	-73.1	
76.00	60.20	-58.00	2.20			1114.7	159.1	-73.9	
76.50	62.18	-59.40	2.78			1113.3	158.2	-74.6	
77.00	63.09	-60.00	3.09			1111.9	157.2	-75.4	
77.50	64.00	-61.50	2.50			1110.5	156.2	-76.2	
78.00	64.89	-62.40	2.49			1109.0	155.2	-77.0	
78.50	65.76	-63.80	1.96			1107.6	154.1	-77.7	
79.00	67.15	-64.90	2.25			1106.1	153.0	-78.5	
79.50	68.52	-66.10	2.42			1104.7	151.9	-79.2	
80.00	69.35	-67.10	2.25			1103.2	150.7	-80.0	
80.50	71.21	-68.20	3.01			1101.8	149.5	-80.8	
81.00	72.53	-68.70	3.83			1100.3	148.2	-81.5	
81.50	74.36	-69.50	4.86			1098.8	146.9	-82.3	
82.00	76.16	-69.60	6.56			1097.3	145.5	-83.0	
82.50	79.00	-69.90	9.10			1095.8	144.0	-83.8	
83.00	78.14	-69.60	8.54			1094.3	142.5	-84.5	
83.50	76.75	-69.10	7.65			1092.8	140.9	-85.2	
84.00	76.37	-68.70	7.67			1091.3	139.1	-86.0	
84.50	75.45	-67.80	7.65			1089.8	137.2	-86.7	
85.00	75.56	-67.00	8.56			1088.3	135.2	-87.4	
85.50	75.11	-66.00	9.11			1086.8	133.0	-88.1	
86.00	74.64	-65.00	9.64			1085.3	130.7	-88.8	
86.50	74.15	-63.90	10.25			1083.7	128.1	-89.5	
87.00	74.15	-62.80	11.35			1082.2	125.2	-90.2	
87.50	72.55	-61.30	11.25			1080.7	122.1	-90.9	
88.00	71.45	-60.80	10.65			1079.1	118.6	-91.5	
88.50	69.28	-59.50	9.78			1077.6	114.7	-92.1	
89.00	68.64	-59.10	9.54			1076.0	110.3	-92.7	
89.50	66.93	-58.30	8.63			1074.5	105.4	-93.3	
90.00	65.18	-58.10	7.08			1072.9	99.9	-93.8	
90.50	64.46	-57.80	6.66			1071.3	93.7	-94.3	
91.00	64.22	-57.80	6.42			1069.8	86.9	-94.8	
91.50	62.90	-57.90	5.00			1068.2	79.5	-95.1	
92.00	62.59	-58.10	4.49			1066.7	71.6	-95.4	
92.50	63.30	-58.50	4.80			1065.1	63.5	-95.6	
93.00	63.97	-58.90	5.07			1063.5	55.3	-95.8	
93.50	65.13	-59.50	5.63			1061.9	47.4	-95.8	
94.00	66.25	-59.90	6.35			1060.4	40.0	-95.8	
94.50	68.38	-60.50	7.88			1058.8	33.1	-95.8	
95.00	68.37	-60.80	7.57			1057.2	26.9	-95.6	
95.50	67.80	-61.30	6.50			1055.6	21.3	-95.5	
96.00	69.29	-61.30	7.99			1054.1	16.4	-95.3	
96.50	69.16	-61.50	7.66			1052.5	12.0	-95.0	
97.00	69.52	-61.30	8.22			1050.9	8.0	-94.7	
97.50	69.83	-61.00	8.83			1049.3	4.5	-94.5	
98.00	74.81	-60.40	14.41			1047.8	1.3	-94.1	
98.50	70.32	-59.40	10.92			1046.2	358.5	-93.8	
99.00	68.41	-58.70	9.71			1044.6	355.9	-93.5	
99.50	66.45	-57.10	9.35			1043.0	353.5	-93.1	

Table 4 (Cont.)

MJD	$-10^7 \dot{P}$	$10^7 \dot{P}_r$	$-10^7 \dot{P}_a$	$\log \rho_\pi$	$\log \rho_s$	T_π (°K)	z (km)	$a_\pi - a_\odot$ (deg)	$\delta_\pi - \delta_\odot$ (deg)
40700.00	64.97	-56.10	8.87				1041.5	351.3	-92.8
00.50	63.97	-54.40	9.57				1039.9	349.2	-92.4
01.00	61.87	-53.00	8.87				1038.3	347.3	-92.0
01.50	59.72	-51.00	8.72				1036.8	345.6	-91.7
02.00	58.04	-49.40	8.64				1035.2	343.9	-91.3
02.50	56.84	-47.50	9.34				1033.6	342.3	-90.9
03.00	56.11	-45.40	10.71				1032.1	340.9	-90.5
03.50	54.28	-43.50	10.78				1030.5	339.4	-90.1
04.00	52.40	-41.40	11.00				1029.0	338.1	-89.7
04.50	49.95	-39.30	10.65				1027.4	336.8	-89.3
05.00	49.00	-37.30	11.70				1025.9	335.6	-88.9
05.50	46.96	-35.00	11.96				1024.4	334.4	-88.5
06.00	43.82	-33.00	10.82				1022.8	333.2	-88.1
06.50	40.62	-30.00	10.62				1021.3	332.1	-87.7
07.00	37.88	-28.10	9.78				1019.8	331.0	-87.3
07.50	35.61	-24.50	11.11				1018.3	330.0	-86.9
08.00	32.24	-20.00	12.24				1016.8	328.9	-86.4
40709.00	17.31	-5.96	11.35				1013.9	326.9	-85.6
40710.00	17.76	-5.91	11.85	-17.23	-17.42	1004	1010.9	325.1	-84.7
11.00	18.01	-5.85	12.16	.22	.42	1009	1007.9	323.2	-83.9
12.00	17.81	-5.79	12.02	.23	.43	1003	1005.0	321.5	-83.0
13.00	17.80	-5.73	12.07	.23	.43	1002	1002.1	319.8	-82.1
14.00	18.24	-5.67	12.57	.21	.42	1012	999.3	318.1	-81.3
15.00	18.50	-5.61	12.89	.20	.41	1017	996.5	316.5	-80.4
16.00	18.84	-5.54	13.30	.19	.40	1025	993.7	314.9	-79.5
17.00	19.12	-5.48	13.64	.18	.40	1031	991.0	313.3	-78.6
18.00	19.21	-5.42	13.79	.17	.40	1032	988.3	311.8	-77.7
19.00	19.39	-5.36	14.03	.17	.40	1034	985.6	310.3	-76.8
20.00	19.26	-5.29	13.97	.17	.41	1031	983.0	308.8	-75.9
21.00	19.47	-5.23	14.24	.16	.41	1035	980.4	307.3	-74.9
22.00	19.91	-5.17	14.74	.15	.40	1045	977.8	305.9	-74.0
23.00	20.30	-5.12	15.18	.13	.39	1053	975.3	304.4	-73.1
24.00	20.26	-5.06	15.20	.14	.39	1053	972.9	303.0	-72.1
25.00	20.32	-5.00	15.32	.14	.39	1057	970.4	301.5	-71.2
26.00	20.48	-4.94	15.54	.13	.39	1061	968.0	300.1	-70.2
27.00	20.34	-4.88	15.46	.13	.40	1059	965.7	298.7	-69.3
28.00	20.18	-4.82	15.36	.14	.41	1059	963.4	297.3	-68.3
29.00	20.12	-4.76	15.36	.14	.41	1060	961.1	295.9	-67.3
30.00	19.77	-4.70	15.07	.15	.43	1055	958.9	294.5	-66.4
31.00	19.41	-4.64	14.77	.16	.44	1050	956.7	293.1	-65.4
32.00	18.89	-4.58	14.31	.18	.46	1042	954.5	291.8	-64.4
33.00	19.01	-4.52	14.49	.17	.46	1048	952.4	290.4	-63.4
34.00	19.25	-4.46	14.79	.16	.46	1055	950.3	289.0	-62.4
35.00	19.99	-4.41	15.58	.14	.44	1072	948.2	287.7	-61.4
36.00	18.90	-4.31	14.59	.17	.47	1055	946.2	286.3	-60.4
37.00	18.46	-4.31	14.15	.19	.49	1048	944.3	284.9	-59.3
38.00	17.62	-4.26	13.36	.21	.52	1033	942.3	283.6	-58.3
39.00	17.17	-4.21	12.96	.23	.54	1027	940.4	282.2	-57.2
40.00	16.98	-4.17	12.81	.23	.55	1027	938.6	280.9	-56.2
40758.00	11.01	-3.85	7.16	-17.49	-17.88	931	910.6	256.7	-36.0
59.00	11.00	-3.87	7.13	.50	.88	937	909.3	255.3	-34.8
60.00	10.66	-3.90	6.76	.52	.90	928	908.0	254.0	-33.6
61.00	10.62	-3.92	6.70	.53	.91	930	906.8	252.7	-32.4
62.00	10.63	-3.90	6.73	.53	.91	936	905.5	251.3	-31.1
63.00	10.83	-4.00	6.83	.52	.91	944	904.3	250.0	-29.9
64.00	11.09	-4.04	7.05	.50	.90	955	903.1	248.6	-28.7

Table 4 (Cont.)

MJD	$-10^7 \dot{P}$	$10^7 \dot{P}_r$	$-10^7 \dot{P}_a$	$\log \rho_\pi$	$\log \rho_s$	T_π (°K)	z (km)	$a_\pi - a_\odot$ (deg)	$\delta_\pi - \delta_\odot$ (deg)
40765.00	12.06	-4.08	7.98	-17.44	-17.85	993	901.9	247.3	-27.4
66.00	12.69	-4.12	8.57	.42	.82	1019	900.7	246.0	-26.2
67.00	13.66	-4.16	9.50	.37	.77	1052	899.5	244.6	-24.9
68.00	15.34	-6.30	9.04	.39	.80	1041	898.3	243.3	-23.6
69.00	17.09	-10.63	6.46	.53	.95	951	897.1	242.0	-22.3
70.00	20.34	-12.75	7.59	.46	.89	997	895.9	240.6	-21.1
40771.00	23.14	-15.53	7.61				894.8	239.3	-19.8
72.00	23.68	-16.47	7.21				893.6	238.0	-18.5
40772.50	20.76	-17.50	3.26				893.1	237.3	-17.8
73.00	21.00	-18.70	2.30				892.4	236.6	-17.1
73.50	21.76	-20.00	1.76				891.7	236.0	-16.5
74.00	23.03	-21.30	1.73				891.0	235.3	-15.8
74.50	24.81	-22.70	2.11				890.3	234.6	-15.2
75.00	26.07	-24.10	1.97				889.6	234.0	-14.5
75.50	26.28	-25.30	0.98				888.8	233.3	-13.8
76.00	34.83	-26.80	8.03				888.1	232.7	-13.2
76.50	39.72	-28.10	11.62				887.4	232.0	-12.5
77.00	40.43	-29.20	11.23				886.6	231.3	-11.9
77.50	39.06	-30.30	8.76				885.9	230.7	-11.2
78.00	36.63	-31.00	5.63				885.1	230.0	-10.5
78.50	35.24	-31.50	3.74				884.3	229.3	-9.8
79.00	35.94	-32.10	3.84				883.5	228.7	-9.2
79.50	36.62	-32.40	4.22				882.7	228.0	-8.5
80.00	36.26	-32.60	3.66				881.9	227.3	-7.8
80.50	36.94	-32.50	4.44				881.1	226.7	-7.1
81.00	37.62	-32.50	5.12				880.3	226.0	-6.5
81.50	38.29	-32.30	5.99				879.5	225.4	-5.8
82.00	38.44	-32.10	6.34				878.7	224.7	-5.1
82.50	38.58	-31.70	6.88				877.8	224.0	-4.4
83.00	38.72	-31.70	7.02				877.0	223.4	-3.7
83.50	38.33	-31.70	6.63				876.2	222.7	-3.0
84.00	36.38	-31.80	4.58				875.3	222.0	-2.3
84.50	35.46	-32.20	3.26				874.4	221.4	-1.6
85.00	34.54	-32.30	2.24				873.5	220.7	-1.0
85.50	34.67	-33.40	1.27				872.7	220.1	-0.3
86.00	33.74	-34.00	-.25				871.8	219.4	0.4
86.50	35.42	-35.80	-.37				870.9	218.7	1.1
87.00	36.58	-36.40	0.18				870.0	218.1	1.8
87.50	37.74	-38.00	-.25				869.0	217.4	2.5
88.00	38.89	-39.40	-.50				868.1	216.7	3.2
88.50	45.77	-41.00	4.77				867.2	216.1	3.9
89.00	46.92	-42.70	4.22				866.2	215.4	4.6
89.50	47.02	-44.50	2.52				865.3	214.7	5.4
90.00	47.13	-45.80	1.33				864.3	214.1	6.1
40790.50	48.79						863.4	213.4	6.8
91.00	49.93						862.4	212.8	7.5
91.50	55.76						861.4	212.1	8.2
92.00	64.72						860.4	211.4	8.9
92.50	63.77						859.4	210.8	9.6
93.00	58.66						858.4	210.1	10.3
93.50	56.67						857.4	209.4	11.1
94.00	54.68						856.4	208.8	11.8
94.50	53.74						855.3	208.1	12.5
95.00	55.39						854.3	207.4	13.2
95.50	57.05						853.2	206.8	13.9
96.00	58.71						852.2	206.1	14.7
96.50	61.41						851.1	205.4	15.4

Table 4 (Cont.)

MJD	$-10^7 \dot{P}$	$10^7 \dot{P}_r$	$-10^7 \dot{P}_a$	$\log \rho_\pi$	$\log \rho_s$	T_π (°K)	z (km)	$a_\pi - a_\odot$ (deg)	$\delta_\pi - \delta_\odot$ (deg)
40797.00	61.51					850.0	204.8	16.1	
97.50	53.79					848.9	204.1	16.8	
98.00	54.41					847.8	203.4	17.6	
98.50	53.99					846.7	202.8	18.3	
99.00	54.61					845.6	202.1	19.0	
99.50	54.19					844.5	201.4	19.8	
40800.00	53.78					843.4	200.7	20.5	
00.50	53.88					842.2	200.1	21.2	
01.00	55.03					841.1	199.4	22.0	
01.50	57.22					839.9	198.7	22.7	
02.00	58.37					838.8	198.0	23.4	
02.50	59.53					837.6	197.4	24.2	
03.00	61.20					836.4	196.7	24.9	
03.50	62.36					835.2	196.0	25.7	
04.00	65.08					834.0	195.3	26.4	
04.50	67.81					832.8	194.7	27.1	
05.00	70.01					831.6	194.0	27.9	
05.50	70.66					830.4	193.3	28.6	
06.00	72.36					829.2	192.6	29.4	
06.50	74.05					827.9	191.9	30.1	
07.00	75.75					826.7	191.2	30.9	
07.50	75.89					825.4	190.5	31.6	
08.00	72.92					824.2	189.8	32.4	
08.50	72.03					822.9	189.1	33.1	
09.00	71.67					821.6	188.4	33.9	
09.50	70.78					820.3	187.7	34.6	
10.00	70.95					819.0	187.0	35.4	
10.50	70.08					817.7	186.3	36.1	
11.00	69.21					816.4	185.6	36.9	
11.50	70.43					815.1	184.9	37.6	
12.00	70.09					813.7	184.2	38.4	
12.50	70.28					812.4	183.5	39.2	
13.00	69.95					811.0	182.7	39.9	
13.50	70.67					809.7	182.0	40.7	
14.00	71.92					808.3	181.3	41.4	
14.50	75.77					806.9	180.6	42.2	
15.00	86.38					805.6	179.8	42.9	
15.50	89.20					804.2	179.1	43.7	
16.00	82.67					802.8	178.3	44.5	
16.50	82.90					801.4	177.6	45.2	
17.00	83.15					800.0	176.8	46.0	
17.50	84.43					798.5	176.0	46.8	
18.00	85.73					797.1	175.3	47.5	
18.50	87.03					795.7	174.5	48.3	
19.00	88.34					794.2	173.7	49.0	
19.50	90.17					792.8	172.9	49.8	
20.00	91.49					791.3	172.1	50.6	
20.50	92.82					789.9	171.3	51.3	
21.00	93.12					788.4	170.5	52.1	
21.50	92.91					786.9	169.6	52.9	
22.00	93.22					785.4	168.8	53.6	
22.50	94.06					783.9	167.9	54.4	
23.00	94.91					782.4	167.0	55.2	
23.50	95.25					780.9	166.2	55.9	
24.00	97.16					779.4	165.3	56.7	
24.50	98.03					777.9	164.3	57.4	
25.00	96.32					776.4	163.4	58.2	
25.50	94.11					774.9	162.5	59.0	
26.00	92.93					773.3	161.5	59.7	
26.50	93.33					771.8	160.5	60.5	

Table 4 (Cont.)

MJD	$-10^6 \dot{P}$	$10^6 \dot{P}_r$	$-10^6 \dot{P}_a$	$\log \rho_\pi$	$\log \rho_s$	T_π (°K)	z (km)	$a_\pi - a_\odot$ (deg)	$\delta_\pi - \delta_\odot$ (deg)
40827.00	9.37					770.3	159.4	61.3	
27.50	9.21					768.7	158.4	62.0	
28.00	9.15					767.1	157.3	62.8	
28.50	9.45					765.6	156.2	63.5	
29.00	9.54					764.0	155.0	64.3	
29.50	10.57					762.4	153.9	65.1	
30.00	10.98					760.9	152.6	65.8	
30.50	11.60					759.3	151.3	66.6	
31.00	11.83					757.7	150.0	67.3	
31.50	11.85					756.1	148.6	68.1	
32.00	11.96					754.5	147.1	68.8	
32.50	11.70					752.9	145.6	69.6	
33.00	11.75					751.3	143.9	70.3	
33.50	11.80					749.7	142.2	71.0	
34.00	12.07					748.8	140.3	71.8	
34.50	12.12					747.3	138.3	72.5	
35.00	12.09					745.7	136.2	73.2	
35.50	12.05					744.2	133.9	73.9	
36.00	11.93					742.6	131.4	74.6	
36.50	11.96					741.0	128.6	75.3	
37.00	11.90					739.5	125.6	76.0	
37.50	11.74					737.9	122.3	76.7	
38.00	11.69					736.2	118.7	77.3	
38.50	11.48					734.6	114.6	77.9	
39.00	11.54					733.0	110.1	78.5	
39.50	11.56					731.4	105.0	79.1	
40.00	11.62					729.7	99.4	79.6	
40.50	11.64					728.1	93.3	80.1	
41.00	11.92					726.4	86.5	80.5	
41.50	12.20					724.8	79.3	80.8	
42.00	12.89					723.1	71.8	81.1	
42.50	13.43					721.5	64.1	81.3	
43.00	13.76					719.8	56.5	81.4	
43.50	13.78					718.1	49.1	81.5	
44.00	12.97					716.5	42.2	81.5	
44.50	12.79					714.8	35.8	81.4	
45.00	11.98					713.1	30.0	81.3	
45.50	11.84					711.4	24.8	81.1	
46.00	11.85					709.8	20.0	81.0	
46.50	12.17					708.1	15.8	80.7	
47.00	12.33					706.4	12.0	80.5	
47.50	12.43					704.7	8.5	80.2	
48.00	12.74					703.1	5.4	79.9	
48.50	12.88					701.4	2.6	79.6	
49.00	13.38					699.7	360.0	79.3	
49.50	13.62					698.1	357.6	79.0	
40850.00	13.74	-6.54	7.20	-16.17	-16.30	1073	696.4	355.4	78.6
50.50	13.96	-6.41	7.55	.14	.28	1078	694.8	353.4	78.3
51.00	13.61	-6.27	7.34	.15	.30	1071	693.1	351.5	77.9
51.50	13.50	-6.12	7.38	.15	.31	1066	691.5	349.7	77.6
52.00	13.49	-5.96	7.53	.15	.31	1064	689.9	348.0	77.2
52.50	13.58	-5.78	7.80	.13	.30	1065	688.2	346.4	76.9
53.00	13.55	-5.58	7.97	.12	.30	1064	686.6	344.9	76.5
53.50	13.51	-5.37	8.14	.11	.30	1063	685.0	343.5	76.1
54.00	13.51	-5.14	8.37	.10	.30	1064	683.4	342.2	75.8
54.50	13.55	-4.88	8.67	.08	.29	1066	681.8	340.9	75.4
55.00	13.74	-4.60	9.14	.06	.28	1069	680.3	339.6	75.0
55.50	13.86	-4.29	9.57	.04	.26	1071	678.7	338.4	74.6
56.00	14.07	-3.95	10.12	.01	.24	1077	677.1	337.2	74.2

Table 4 (Cont.)

MJD	$-10^6 \dot{P}$	$10^6 \dot{P}_r$	$-10^6 \dot{P}_a$	$\log p_\pi$	$\log p_s$	T_π (°K)	z (km)	$a_\pi - a_\odot$ (deg)	$\delta_\pi - \delta_\odot$ (deg)
40856.50	15.19	-3.52	11.67	-15.94	-16.18	1098	675.6	336.1	73.9
57.00	14.81	-3.00	11.81	.93	.18	1096	674.1	335.0	73.5
57.50	12.97	-2.00	10.97	.97	.23	1077	672.6	334.0	73.1
58.00	9.93	-0.58	9.35	-16.05	.32	1046	671.1	332.9	72.7
58.50	8.43	-0.57	7.86	.13	.40	1016	669.6	331.9	72.3
59.00	8.60	-0.56	8.04	.11	.40	1016	668.1	330.9	71.9
59.50	8.81	-0.55	8.26	.10	.39	1018	666.7	330.0	71.5
60.00	9.57	-0.55	9.02	.06	.36	1027	665.2	329.0	71.1
60.50	10.01	-0.55	9.46	.04	.35	1030	663.8	328.1	70.7
61.00	10.17	-0.54	9.63	.03	.35	1029	662.4	327.2	70.4
61.50	10.26	-0.54	9.72	.03	.35	1027	661.0	326.3	70.0
62.00	10.18	-0.54	9.64	.03	.36	1022	659.6	325.5	69.6
40862.20	10.37	-0.54	9.83	-16.02	-16.36	1024	659.1	325.1	69.4
62.40	10.24	-0.54	9.70	.03	.37	1021	658.6	324.8	69.2
62.60	10.12	-0.53	9.59	.04	.38	1016	658.0	324.4	69.1
62.80	10.31	-0.53	9.78	.03	.37	1017	657.5	324.1	68.9
63.00	14.03	-0.52	13.51	-15.88	.23	1067	657.0	323.8	68.8
63.20	16.47	-0.52	15.95	.80	.15	1094	656.5	323.4	68.6
63.40	15.04	-0.52	14.52	.84	.19	1080	655.9	323.1	68.4
63.60	12.97	-0.51	12.46	.91	.26	1054	655.4	322.7	68.3
63.80	10.57	-0.51	10.06	-16.00	.36	1019	654.9	322.4	68.1
64.00	10.42	-0.51	9.91	.01	.37	1014	654.4	322.1	68.0
40864.50	9.58	-0.50	9.08	-16.05	-16.42	997	653.5	321.3	67.6
65.00	9.27	-0.50	8.77	.07	.45	988	652.2	320.5	67.2
65.50	8.27	-0.47	7.80	.13	.50	967	651.0	319.7	66.8
66.00	7.67	-0.48	7.19	.16	.55	952	649.7	318.9	66.4
66.50	7.68	-0.48	7.20	.17	.56	948	648.5	318.1	66.0
67.00	7.41	-0.47	6.94	.18	.58	939	647.3	317.3	65.6
67.50	7.54	-0.46	7.08	.18	.58	938	646.0	316.6	65.2
68.00	7.66	-0.45	7.21	.17	.58	938	644.8	315.8	64.7
68.50	7.92	-0.45	7.47	.15	.57	941	643.6	315.1	64.3
69.00	8.88	-0.45	8.43	.10	.52	956	642.4	314.3	63.9
69.50	10.45	-0.44	10.01	.01	.45	979	641.3	313.6	63.5
70.00	12.99	-0.44	12.55	-15.91	.35	1013	640.1	312.8	63.1
70.50	15.10	-0.43	14.67	.83	.28	1035	639.0	312.1	62.7
71.00	16.68	-0.42	16.26	.79	.24	1049	637.8	311.4	62.3
71.50	15.17	-0.42	14.75	.83	.29	1030	636.7	310.6	61.9
72.00	13.34	-0.41	12.93	.90	.36	1004	635.6	309.9	61.5
72.50	12.38	-0.40	11.98	.93	.40	989	634.5	309.2	61.1
73.00	11.66	-0.40	11.26	.95	.43	979	633.4	308.5	60.7
73.50	11.08	-0.39	10.69	.98	.47	967	632.3	307.8	60.2
74.00	10.86	-0.39	10.47	-16.00	.48	961	631.2	307.1	59.8
74.50	10.93	-0.38	10.55	.00	.49	958	630.2	306.4	59.4
75.00	10.69	-0.36	10.33	.01	.50	952	629.2	305.7	59.0
40875.20	14.01	-0.36	13.65	-15.89	-16.38	991	628.8	305.4	58.8
75.40	15.33	-0.35	14.98	.85	.35	1004	628.3	305.1	58.7
75.60	30.78	-0.35	30.43	.52	.03	1119	627.9	304.8	58.5
75.80	31.46	-0.35	31.11	.50	.01	1130	627.5	304.5	58.3
76.00	25.08	-0.35	24.73	.60	.10	1092	627.1	304.3	58.2
76.20	22.23	-0.35	21.88	.65	.17	1069	626.7	304.0	58.0
76.40	24.19	-0.34	23.85	.62	.14	1078	626.3	303.7	57.8
76.60	27.43	-0.34	27.09	.57	.09	1097	626.0	303.4	57.7
76.80	28.42	-0.34	28.08	.55	.07	1103	625.6	303.1	57.5
77.00	33.59	-0.34	33.25	.47	-15.99	1133	625.2	302.9	57.3
77.20	21.75	-0.34	21.41	.66	-16.18	1063	624.8	302.6	57.2
77.40	14.73	-0.34	14.39	.83	.35	1002	624.4	302.3	57.0
77.60	12.51	-0.34	12.17	.91	.44	974	624.0	302.0	56.8

Table 4 (Cont.)

MJD	$-10^6 \dot{P}$	$10^6 \dot{P}_r$	$-10^6 \dot{P}_a$	$\log p_\pi$	$\log p_s$	T_π (°K)	z (km)	$a_\pi - a_\odot$ (deg)	$\delta_\pi - \delta_\odot$ (deg)
40877.80	11.90	-0.34	11.56	-15.94	-16.47	962	623.6	301.8	56.6
40878.00	12.60	-0.33	12.27	-15.91	-16.45	969	623.3	301.5	56.5
78.50	11.18	-0.33	10.85	.97	.51	948	622.3	300.8	56.1
79.00	10.87	-0.32	10.55	.98	.53	941	621.4	300.1	55.6
79.50	10.41	-0.31	10.10	-16.00	.55	933	620.5	299.4	55.2
80.00	11.33	-0.31	11.02	-15.97	.18	941	619.6	298.7	54.8
80.50	12.08	-0.30	11.78	.95	.17	946	618.8	298.1	54.4
81.00	13.29	-0.30	12.99	.91	.13	959	617.9	297.4	53.9
81.50	14.76	-0.29	14.47	.85	.07	976	617.1	296.7	53.5
82.00	16.52	-0.28	16.24	.79	.01	995	616.2	296.0	53.1
82.50	19.67	-0.27	19.40	.71	-15.94	1021	615.4	295.3	52.6
83.00	18.20	-0.26	17.94	.74	.98	1007	614.6	294.7	52.2
83.50	14.52	-0.26	14.26	.84	-16.08	972	613.8	294.0	51.8
84.00	11.81	-0.26	11.55	.94	.18	939	613.1	293.3	51.3
84.50	11.35	-0.26	11.09	.95	.21	931	612.3	292.6	50.9
85.00	11.25	-0.25	11.00	.96	.22	929	611.6	292.0	50.5
85.50	11.10	-0.25	10.85	.96	.23	925	610.9	291.3	50.0
86.00	11.05	-0.25	10.80	.97	.23	923	610.2	290.6	49.6
86.50	12.27	-0.25	12.02	.92	.19	937	609.5	289.9	49.2
87.00	14.88	-0.25	14.63	.82	.10	967	608.8	289.3	48.7
87.50	17.23	-0.24	16.99	.76	.03	989	608.1	288.6	48.3
88.00	18.45	-0.24	18.21	.72	.00	998	607.4	287.9	47.8
88.50	19.15	-0.24	18.91	.71	-15.99	1003	606.8	287.2	47.4
89.00	18.99	-0.23	18.76	.71	.99	1002	606.2	286.6	46.9
89.50	17.30	-0.23	17.07	.75	-16.04	986	605.6	285.9	46.5
90.00	16.06	-0.22	15.84	.79	.09	970	605.0	285.2	46.1
90.50	15.70	-0.21	15.49	.80	.11	965	604.4	284.6	45.6
91.00	14.31	-0.20	14.11	.85	.16	949	603.8	283.9	45.2
91.50	14.10	-0.20	13.90	.86	.17	945	603.2	283.2	44.7
92.00	14.00	-0.20	13.80	.86	.18	942	602.7	282.5	44.2
92.50	14.45	-0.20	14.25	.84	.17	947	602.1	281.9	43.8
93.00	14.81	-0.20	14.61	.83	.15	951	601.6	281.2	43.3
93.50	15.69	-0.19	15.50	.80	.13	958	601.0	280.5	42.9
94.00	15.74	-0.19	15.55	.80	.13	959	600.5	279.8	42.4
94.50	15.81	-0.19	15.62	.80	.13	959	600.0	279.2	42.0
95.00	15.93	-0.19	15.74	.80	.14	958	599.6	278.5	41.5
95.50	15.84	-0.18	15.66	.80	.14	957	599.1	277.8	41.0
96.00	16.53	-0.18	16.35	.78	.12	964	598.7	277.1	40.6
96.50	17.19	-0.17	17.02	.76	.10	970	598.2	276.5	40.1
40897.00	19.13	-0.17	18.96	-15.71	-16.07	983	597.7	275.8	39.6
97.20	20.69	-0.16	20.53	.67	.02	997	597.5	275.5	39.4
97.40	24.48	-0.15	24.33	.59	-15.93	1029	597.4	275.2	39.2
97.60	28.92	-0.15	28.77	.51	.85	1057	597.2	275.0	39.1
97.80	27.61	-0.15	27.46	.54	.88	1047	597.0	274.7	38.9
98.00	20.56	-0.15	20.41	.67	-16.02	999	596.8	274.4	38.7
40898.50	13.03	-0.15	12.88	-15.88	-16.24	930	596.4	273.8	38.2
99.00	12.16	-0.15	12.01	.91	.28	917	595.9	273.1	37.7
99.50	12.83	-0.15	12.68	.89	.26	924	595.5	272.4	37.3
40900.00	13.30	-0.15	13.15	.87	.24	930	595.1	271.7	36.8
00.50	14.64	-0.15	14.49	.82	.19	945	594.6	271.0	36.3
01.00	15.12	-0.15	14.97	.81	.18	950	594.2	270.4	35.8
01.50	15.30	-0.15	15.15	.80	.17	952	593.8	269.7	35.3
02.00	14.52	-0.15	14.37	.82	.20	944	593.4	269.0	34.8
02.50	13.74	-0.15	13.59	.85	.23	937	593.0	268.3	34.4
03.00	13.68	-0.16	13.52	.85	.24	934	592.5	267.6	33.9
03.50	13.62	-0.16	13.46	.85	.24	934	592.1	267.0	33.4
04.00	13.51	-0.16	13.35	.85	.24	934	591.7	266.3	32.9

Table 4 (Cont.)

MJD	$-10^6 \dot{P}$	$10^6 \dot{P}_r$	$-10^6 \dot{P}_a$	$\log \rho_\pi$	$\log \rho_s$	T_π (°K)	z (km)	$a_\pi - a_\odot$ (deg)	$\delta_\pi - \delta_\odot$ (deg)
40904.50	13.35	-0.17	13.18	-15.86	-16.25	932	591.3	265.6	32.4
05.00	13.29	-0.17	13.12	.86	.26	931	590.9	264.9	31.9
05.50	13.17	-0.17	13.00	.86	.26	929	590.5	264.2	31.4
06.00	13.16	-0.17	12.99	.86	.26	930	590.1	263.5	30.9
06.50	13.15	-0.17	12.98	.86	.26	931	589.6	262.8	30.4
07.00	13.13	-0.17	12.96	.86	.26	933	589.2	262.1	29.9
07.50	13.11	-0.17	12.94	.86	.26	932	588.8	261.5	29.4
08.00	13.13	-0.17	12.96	.86	.27	930	588.4	260.8	28.9
40908.40	12.72	-0.17	12.55	-15.87	-16.29	926	588.1	260.2	28.5
08.60	13.35	-0.17	13.18	.85	.27	933	587.9	259.9	28.3
08.80	18.42	-0.17	18.25	.70	.12	980	587.8	259.7	28.1
09.00	19.99	-0.17	19.82	.67	.08	994	587.6	259.4	27.9
09.20	20.93	-0.17	20.76	.65	.05	1002	587.4	259.1	27.7
09.40	20.27	-0.17	20.10	.66	.06	999	587.3	258.8	27.5
09.60	17.39	-0.17	17.22	.73	.14	974	587.1	258.6	27.3
09.80	14.51	-0.18	14.33	.81	.23	945	586.9	258.3	27.1
10.00	13.53	-0.18	13.35	.85	.28	932	586.8	258.0	26.9
10.20	12.23	-0.18	12.05	.89	.32	918	586.6	257.7	26.6
10.40	11.25	-0.18	11.07	.93	.36	907	586.4	257.4	26.4
10.60	10.91	-0.18	10.73	.94	.38	903	586.3	257.2	26.2
10.80	11.83	-0.19	11.64	.91	.34	914	586.1	256.9	26.0
11.00	14.03	-0.19	13.84	.83	.27	937	585.9	256.6	25.8
11.20	15.58	-0.19	15.39	.78	.21	953	585.8	256.3	25.6
11.40	16.50	-0.19	16.31	.75	.18	964	585.6	256.1	25.4
11.60	22.19	-0.19	22.00	.62	.04	1010	585.4	255.8	25.2
11.80	25.01	-0.19	24.82	.57	-15.98	1029	585.3	255.5	25.0
12.00	24.65	-0.19	24.46	.57	-16.00	1023	585.1	255.2	24.8
12.20	22.07	-0.19	21.88	.62	.06	1004	584.9	254.9	24.6
12.40	19.80	-0.19	19.61	.67	.10	990	584.8	254.7	24.4
12.60	17.53	-0.19	17.34	.72	.16	972	584.6	254.4	24.2
40913.00	13.83	-0.19	13.64	-15.83	-16.27	939	584.3	253.8	23.7
13.50	14.56	-0.20	14.36	.80	.25	946	583.8	253.1	23.2
14.00	14.67	-0.20	14.47	.80	.25	946	583.4	252.4	22.7
14.50	12.27	-0.20	12.07	.88	.34	920	583.0	251.7	22.1
15.00	11.07	-0.20	10.87	.93	.39	906	582.6	251.0	21.6
15.50	10.67	-0.20	10.47	.94	.41	901	582.2	250.3	21.1
16.00	10.10	-0.20	9.90	.97	.44	893	581.7	249.6	20.5
16.50	9.36	-0.20	9.16	-16.01	.49	882	581.3	248.9	20.0
17.00	8.81	-0.20	8.61	.03	.52	874	580.9	248.2	19.5
17.50	9.60	-0.40	9.20	.00	.49	883	580.5	247.5	18.9
18.00	10.48	-0.66	9.82	-15.97	.46	892	580.1	246.8	18.4
18.50	10.97	-0.93	10.04	.96	.45	895	579.7	246.1	17.8
19.00	10.84	-1.16	9.68	.98	.47	889	579.3	245.4	17.3
19.50	11.04	-1.34	9.70	.98	.48	888	578.9	244.7	16.7
20.00	10.68	-1.50	9.18	-16.00	.15	882	578.9	243.9	16.2
20.50	10.97	-1.65	9.32	.00	.15	883	578.5	243.2	15.6
21.00	10.89	-1.79	9.10	.01	.16	881	578.0	242.5	15.1
21.50	10.95	-1.92	9.03	.01	.17	880	577.6	241.8	14.5
22.00	11.06	-2.05	9.01	.01	.17	880	577.1	241.1	14.0
22.50	11.65	-2.17	9.48	-15.98	.15	887	576.6	240.4	13.4
23.00	12.18	-2.28	9.90	.96	.13	894	576.1	239.6	12.8
23.50	12.75	-2.39	10.36	.94	.11	900	575.6	238.9	12.3
24.00	13.56	-2.51	11.05	.91	.09	906	575.0	238.2	11.7
24.50	14.81	-2.62	12.19	.87	.05	918	574.5	237.5	11.1
25.00	15.90	-2.72	13.18	.83	.01	931	573.9	236.8	10.5
25.50	16.76	-2.83	13.93	.80	-15.98	940	573.3	236.0	10.0
26.00	17.82	-2.93	14.89	.77	.96	947	572.7	235.3	9.4
26.50	18.55	-3.04	15.51	.76	.95	953	572.0	234.6	8.8

Table 4 (Cont.)

MJD	$-10^6 \dot{P}$	$10^6 \dot{P}_r$	$-10^6 \dot{P}_a$	$\log \rho_\pi$	$\log \rho_s$	T_π (°K)	z (km)	$a_\pi - a_\odot$ (deg)	$\delta_\pi - \delta_\odot$ (deg)
40927.00	19.31	-3.13	16.18	-15.74	-15.93	959	571.4	233.9	8.2
40927.20	19.62	-3.17	16.45	-15.73	-15.93	959	571.1	233.6	8.0
27.40	20.45	-3.21	17.24	.71	.91	966	570.9	233.3	7.8
27.60	21.91	-3.25	18.66	.67	.87	978	570.6	233.0	7.5
27.80	23.37	-3.29	20.08	.64	.84	988	570.3	232.7	7.3
28.00	26.41	-3.33	23.08	.58	.78	1009	570.1	232.4	7.1
28.20	28.17	-3.37	24.80	.55	.75	1022	569.8	232.1	6.8
28.40	29.62	-3.41	26.21	.52	.72	1032	569.5	231.8	6.6
28.60	27.27	-3.46	23.81	.57	.76	1017	569.2	231.5	6.4
28.80	24.29	-3.50	20.79	.62	.83	995	568.9	231.2	6.1
29.00	23.20	-3.53	19.67	.65	.86	986	568.7	230.9	5.9
40929.50	20.91	-3.63	17.28	-15.70	-15.92	966	567.9	230.2	5.3
30.00	19.91	-3.72	16.19	.73	.95	955	567.2	229.5	4.7
30.50	20.24	-3.82	16.42	.72	.96	956	566.4	228.7	4.1
31.00	20.46	-3.92	16.54	.72	.96	956	565.7	228.0	3.5
31.50	19.90	-4.02	15.88	.74	.98	950	564.9	227.3	2.9
32.00	19.93	-4.12	15.81	.74	.99	948	564.1	226.5	2.3
32.50	21.25	-4.22	17.03	.70	.96	958	563.3	225.8	1.7
33.00	21.79	-4.32	17.47	.69	.95	962	562.5	225.1	1.1
33.50	22.21	-4.42	17.79	.68	.95	963	561.7	224.3	0.5
40934.00	23.73	-4.52	19.21	-15.65	-15.92	974	560.8	223.6	-0.1
34.20	25.40	-4.56	20.84	.62	.88	987	560.5	223.3	-0.4
34.40	41.90	-4.60	37.30	.37	.62	1081	560.1	223.0	-0.6
34.60	63.13	-4.64	58.49	.18	.42	1164	559.8	222.7	-0.9
34.80	47.12	-4.68	42.44	.31	.57	1102	559.5	222.4	-1.1
35.00	44.35	-4.72	39.63	.34	.60	1088	559.1	222.1	-1.3
35.20	33.06	-4.76	28.30	.48	.75	1033	558.8	221.8	-1.6
35.40	25.24	-4.79	20.45	.62	.89	983	558.4	221.5	-1.8
35.60	23.10	-4.84	18.26	.67	.95	965	558.1	221.2	-2.1
35.80	22.85	-4.88	17.97	.68	.96	962	557.7	220.9	-2.3
40936.00	23.82	-4.91	18.91	-15.65	-15.94	967	557.4	220.6	-2.6
36.50	23.34	-5.01	18.33	.67	.97	960	556.5	219.8	-3.2
37.00	23.25	-5.09	18.16	.67	.98	957	555.6	219.1	-3.8
37.50	21.92	-5.19	16.73	.70	-16.02	944	554.7	218.3	-4.4
38.00	19.41	-5.29	14.12	.78	.11	920	553.8	217.6	-5.1
38.50	20.00	-5.38	14.62	.76	.10	923	552.9	216.8	-5.7
39.00	21.52	-5.47	16.05	.72	.06	935	552.0	216.1	-6.3
39.50	22.97	-5.56	17.41	.68	.02	947	551.0	215.3	-7.0
40.00	27.61	-5.64	21.97	.58	-15.92	979	550.1	214.6	-7.6
40.50	28.30	-5.74	22.56	.57	.92	981	549.2	213.8	-8.2
41.00	25.99	-5.84	20.15	.62	.98	963	548.2	213.0	-8.9
41.50	24.91	-5.94	18.97	.64	-16.01	952	547.3	212.3	-9.5
42.00	23.80	-6.03	17.77	.67	.05	942	546.4	211.5	-10.2
42.50	22.42	-6.12	16.30	.71	.09	929	545.4	210.8	-10.8
43.00	22.01	-6.20	15.81	.72	.11	924	544.5	210.0	-11.4
43.50	22.83	-6.31	16.52	.70	.10	929	543.5	209.2	-12.1
44.00	23.32	-6.40	16.92	.69	.09	931	542.6	208.5	-12.7
44.50	25.59	-6.50	19.09	.64	.05	945	541.7	207.7	-13.4
40945.00	23.31	-6.59	16.72	-15.69	-16.11	925	540.8	206.9	-14.0
45.25	22.71	-6.63	16.08	.71	.14	918	540.4	206.5	-14.4
45.50	22.73	-6.67	16.06	.71	.15	916	539.9	206.1	-14.7
45.75	23.36	-6.72	16.64	.69	.14	920	539.4	205.8	-15.0
46.00	23.40	-6.76	16.64	.69	.13	921	538.9	205.4	-15.3
46.25	23.85	-6.80	17.05	.68	.12	924	538.4	205.0	-15.7
46.50	24.92	-6.85	18.07	.66	.10	930	537.9	204.6	-16.0

Table 4 (Cont.)

MJD	$-10^5 \dot{P}$	$10^5 \dot{P}_r$	$-10^5 \dot{P}_a$	$\log p$	$\log \rho_s$	T_π (°K)	z (km)	$a_\pi - a_\odot$ (deg)	$\delta_\pi - \delta_\odot$ (deg)
40946.75	2.50	-0.69	1.81	-15.66	-16.11	928	537.4	204.2	-16.3
47.00	2.51	-0.69	1.82	.65	.11	928	536.9	203.8	-16.6
47.25	2.70	-0.80	1.90	.64	.10	934	536.4	203.4	-17.0
47.50	2.83	-0.70	2.13	.59	.05	948	535.9	203.0	-17.3
47.75	2.86	-0.71	2.16	.58	.04	950	535.4	202.6	-17.6
48.00	2.91	-0.71	2.21	.57	.03	954	534.9	202.2	-18.0
48.25	3.01	-0.71	2.30	.55	.01	959	534.4	201.9	-18.3
48.50	3.18	-0.72	2.47	.52	-15.99	968	533.8	201.5	-18.6
48.75	3.48	-0.72	2.76	.47	.94	983	533.3	201.1	-19.0
49.00	3.70	-0.73	2.97	.44	.91	995	532.8	200.7	-19.3
49.25	3.43	-0.73	2.70	.49	.95	979	532.2	200.3	-19.6
49.50	3.15	-0.73	2.41	.53	-16.02	960	531.7	199.9	-20.0
49.75	2.83	-0.74	2.09	.59	.09	938	531.2	199.5	-20.3
50.00	2.81	-0.74	2.06	.60	.74	936	530.6	199.1	-20.6
50.25	2.75	-0.75	2.00	.62	.75	933	530.1	198.7	-21.0
50.50	2.77	-0.75	2.02	.61	.75	933	529.5	198.3	-21.3
50.75	2.79	-0.76	2.03	.60	.76	931	528.9	197.9	-21.7
51.00	2.85	-0.76	2.09	.59	.75	934	528.4	197.5	-22.0
51.25	2.73	-0.76	1.97	.62	.78	923	527.8	197.1	-22.3
51.50	2.74	-0.77	1.97	.61	.78	922	527.2	196.7	-22.7
51.75	2.84	-0.77	2.07	.59	.77	928	526.6	196.3	-23.0
52.00	2.93	-0.78	2.15	.58	.75	932	526.0	195.9	-23.4
52.25	2.99	-0.78	2.21	.57	.74	936	525.4	195.5	-23.7
52.50	3.04	-0.79	2.25	.56	.74	938	524.8	195.1	-24.0
52.75	3.10	-0.79	2.31	.55	.73	940	524.2	194.7	-24.4
53.00	3.17	-0.79	2.38	.53	.72	943	523.6	194.3	-24.7
53.25	3.46	-0.80	2.66	.49	.68	958	523.0	193.9	-25.1
53.50	3.70	-0.80	2.90	.45	.64	971	522.4	193.5	-25.4
53.75	3.75	-0.81	2.94	.45	.64	972	521.8	193.1	-25.8
54.00	3.90	-0.81	3.09	.43	.63	978	521.1	192.7	-26.1
54.25	4.27	-0.81	3.45	.38	.58	993	520.5	192.3	-26.4
54.50	4.57	-0.82	3.76	.34	.55	1006	519.9	191.8	-26.8
54.75	4.72	-0.82	3.90	.33	.54	1011	519.2	191.4	-27.1
55.00	5.07	-0.82	4.25	.29	.50	1024	518.6	191.0	-27.5
55.25	4.80	-0.83	3.97	.32	.54	1011	517.9	190.6	-27.8
55.50	4.49	-0.83	3.66	.35	.58	996	517.2	190.2	-28.2
55.75	4.42	-0.83	3.58	.36	.59	990	516.6	189.8	-28.5
56.00	4.35	-0.84	3.51	.37	.61	986	515.9	189.4	-28.9
56.25	4.30	-0.84	3.45	.37	.62	981	515.2	189.0	-29.2
56.50	4.32	-0.84	3.48	.37	.62	981	514.5	188.5	-29.6
56.75	4.31	-0.85	3.46	.37	.63	979	513.9	188.1	-29.9
57.00	4.36	-0.85	3.51	.37	.62	979	513.2	187.7	-30.3
57.25	4.35	-0.85	3.50	.37	.63	977	512.5	187.3	-30.6
57.50	4.38	-0.86	3.52	.36	.63	976	511.8	186.9	-31.0
57.75	4.35	-0.86	3.49	.37	.64	973	511.1	186.4	-31.3
58.00	4.24	-0.86	3.37	.38	.66	966	510.4	186.0	-31.7
58.25	4.19	-0.87	3.32	.39	.67	962	509.7	185.6	-32.0
58.50	4.20	-0.87	3.32	.38	.68	960	509.0	185.2	-32.4
58.75	4.20	-0.87	3.33	.38	.68	959	508.2	184.7	-32.7
59.00	4.21	-0.88	3.33	.38	.69	957	507.5	184.3	-33.1
59.25	4.20	-0.88	3.32	.38	.70	955	506.8	183.9	-33.4
59.50	4.19	-0.88	3.30	.39	.70	952	506.1	183.4	-33.8
59.75	4.07	-0.89	3.19	.40	.72	945	505.4	183.0	-34.1
60.00	3.94	-0.89	3.05	.42	.75	937	504.6	182.6	-34.5
60.25	3.81	-0.89	2.92	.44	.77	929	503.9	182.1	-34.8
60.50	4.11	-0.89	3.22	.40	.73	942	503.2	181.7	-35.2
60.75	4.46	-0.90	3.56	.35	.70	955	502.4	181.3	-35.5
61.00	4.62	-0.90	3.72	.33	.68	960	501.7	180.8	-35.9
61.25	4.94	-0.90	4.04	.30	.65	971	501.0	180.4	-36.3
61.50	5.01	-0.91	4.10	.29	.65	972	500.2	179.9	-36.6

Table 4 (Cont.)

MJD	$-10^5 \dot{P}$	$10^5 \dot{P}_r$	$-10^5 \dot{P}_a$	$\log \rho$	$\log \rho_s$	T_π (°K)	z (km)	$a_\pi - a_\odot$ (deg)	$\delta_\pi - \delta_\odot$ (deg)
40961.75	5.53	-0.91	4.62	-15.24	-16.60	990	499.5	179.5	-37.0
62.00	5.73	-0.91	4.82	.23	.58	997	499.3	179.0	-37.3
62.25	5.98	-0.91	5.07	.21	.56	1003	498.5	178.6	-37.7
62.50	6.03	-0.92	5.11	.20	.56	1002	497.7	178.1	-38.0
62.75	5.97	-0.92	5.05	.21	.57	999	496.9	177.7	-38.4
63.00	6.11	-0.92	5.18	.20	.57	1001	496.1	177.2	-38.8
63.25	5.84	-0.92	4.91	.22	.60	989	495.2	176.7	-39.1
63.50	5.96	-0.93	5.04	.20	.59	991	494.4	176.3	-39.5
63.75	5.98	-0.93	5.06	.20	.60	989	493.6	175.8	-39.8
64.00	6.00	-0.93	5.07	.20	.60	987	492.7	175.3	-40.2
64.25	6.02	-0.93	5.08	.20	.61	986	491.9	174.9	-40.6
64.50	6.32	-0.93	5.39	.18	.58	994	491.0	174.4	-40.9
64.75	6.73	-0.94	5.79	.15	.56	1004	490.1	173.9	-41.3
65.00	7.32	-0.94	6.38	.10	.18	1018	489.3	173.4	-41.6
65.25	7.62	-0.94	6.68	.08	.17	1024	488.4	173.0	-42.0
65.50	7.82	-0.94	6.87	.07	.16	1027	487.5	172.5	-42.4
65.75	8.50	-0.95	7.56	.03	.12	1042	486.7	172.0	-42.7
40970.25	8.26	-0.97	7.29	-15.05	-15.24	991	471.2	162.4	-49.3
70.50	8.27	-0.97	7.29	.05	.25	989	470.4	161.8	-49.6
70.75	9.06	-0.97	8.09	.00	.21	1005	469.6	161.2	-50.0
71.00	9.66	-0.97	8.69	-14.98	.18	1016	468.7	160.6	-50.4
71.25	11.54	-0.97	10.57	.90	.10	1052	467.9	160.0	-50.7
71.50	12.05	-0.97	11.08	.88	.09	1059	467.1	159.4	-51.1
71.75	10.21	-0.97	9.24	.96	.17	1021	466.3	158.8	-51.5
72.00	9.65	-0.97	8.68	.98	.20	1006	465.5	158.1	-51.8
72.25	9.30	-0.97	8.32	-15.00	.23	996	464.7	157.5	-52.2
72.50	9.34	-0.97	8.36	-14.99	.23	994	463.9	156.8	-52.6
72.75	9.48	-0.97	8.50	.99	.23	995	463.1	156.1	-52.9
73.00	9.72	-0.97	8.75	.97	.22	998	462.4	155.4	-53.3
73.25	10.07	-0.97	9.10	.96	.21	1003	461.6	154.7	-53.7
73.50	10.14	-0.97	9.16	.95	.21	1002	460.8	154.0	-54.0
73.75	10.40	-0.97	9.43	.94	.20	1004	460.0	153.3	-54.4
74.00	10.38	-0.97	9.40	.94	.21	1001	459.3	152.6	-54.8
74.25	10.46	-0.97	9.49	.94	.21	1001	458.5	151.8	-55.1
74.50	10.84	-0.97	9.87	.92	.20	1006	457.7	151.0	-55.5
74.75	11.04	-0.97	10.07	.91	.20	1007	457.0	150.2	-55.8
75.00	11.33	-0.97	10.37	.90	.19	1010	456.2	149.4	-56.2
75.25	11.54	-0.97	10.58	.89	.18	1012	455.5	148.6	-56.6
75.50	11.86	-0.97	10.89	.88	.18	1015	454.7	147.7	-56.9
75.75	12.28	-0.96	11.31	.86	.16	1020	454.0	146.8	-57.3
76.00	13.00	-0.96	12.04	.84	.14	1030	453.2	145.9	-57.7
76.25	13.15	-0.96	12.18	.83	.14	1030	452.5	145.0	-58.0
76.50	13.40	-0.96	12.44	.82	.14	1031	451.7	144.0	-58.4
76.75	12.30	-0.96	11.34	.86	.18	1010	451.0	143.1	-58.7
77.00	12.48	-0.96	11.52	.85	.18	1011	450.2	142.0	-59.1
77.25	12.08	-0.96	11.12	.86	.20	1001	449.5	141.0	-59.4
77.50	11.60	-0.96	10.64	.88	.23	990	448.7	139.9	-59.8
77.75	11.12	-0.95	10.17	.89	.26	979	447.9	138.7	-60.2
78.00	11.83	-0.95	10.87	.87	.23	989	447.2	137.6	-60.5
78.25	15.24	-0.95	14.29	.75	.12	1041	446.4	136.3	-60.9
78.50	25.72	-0.95	24.77	.52	-14.87	1167	445.6	135.1	-61.2
78.75	20.75	-0.95	19.80	.63	.97	1108	444.9	133.7	-61.5
79.00	20.72	-0.94	19.77	.62	.98	1105	444.1	132.4	-61.9
79.25	20.89	-0.94	19.94	.62	.98	1104	443.3	130.9	-62.2
79.50	20.78	-0.94	19.84	.62	.99	1100	442.5	129.4	-62.6
79.75	21.17	-0.94	20.23	.61	.99	1101	441.7	127.8	-62.9
80.00	22.05	-0.94	21.11	.60	.66	1109	440.9	126.2	-63.2
80.25	20.32	-0.93	19.38	.64	.69	1088	440.7	124.4	-63.5

Table 4 (Cont.)

MJD	$-10^4 \dot{P}$	$10^4 \dot{P}_r$	$-10^4 \dot{P}_a$	$\log \rho_\pi$	$\log \rho_s$	T_π (°K)	z (km)	$a_\pi - a_\odot$ (deg)	$\delta_\pi - \delta_\odot$ (deg)
40980.50	1.77	-0.09	1.68	-14.69	-14.75	1055	440.6	122.6	-63.9
80.75	1.80	-0.09	1.70	.68	.75	1056	440.3	120.6	-64.2
81.00	1.88	-0.09	1.79	.66	.72	1066	440.0	118.6	-64.5
81.25	2.00	-0.09	1.91	.63	.70	1079	439.6	116.4	-64.8
81.50	2.08	-0.09	1.99	.62	.69	1087	439.1	114.2	-65.1
81.75	2.13	-0.09	2.04	.60	.68	1091	438.6	111.8	-65.4
82.00	2.15	-0.09	2.06	.60	.68	1091	438.0	109.3	-65.6
82.25	2.19	-0.09	2.10	.59	.68	1093	437.4	106.6	-65.9
82.50	2.21	-0.09	2.12	.59	.68	1092	436.7	103.8	-66.2
82.75	2.20	-0.09	2.11	.59	.68	1088	436.0	100.9	-66.4
83.00	2.22	-0.09	2.13	.58	.68	1087	435.2	97.8	-66.6
83.25	2.24	-0.09	2.15	.58	.68	1086	434.4	94.6	-66.8
83.50	2.24	-0.09	2.15	.58	.69	1083	433.5	91.2	-67.0
83.75	2.23	-0.09	2.14	.59	.70	1079	432.6	87.7	-67.2
84.00	2.26	-0.09	2.17	.57	.70	1078	431.7	84.1	-67.4
84.25	2.27	-0.09	2.18	.57	.70	1076	430.7	80.4	-67.5
84.50	2.26	-0.09	2.17	.57	.71	1071	429.8	76.6	-67.7
84.75	2.26	-0.09	2.17	.57	.71	1067	428.8	72.7	-67.8
85.00	2.25	-0.09	2.16	.57	.72	1062	427.7	68.8	-67.9
85.25	2.26	-0.09	2.17	.57	.73	1059	426.7	64.9	-67.9
85.50	2.27	-0.09	2.18	.56	.73	1056	425.6	61.0	-68.0
85.75	2.26	-0.08	2.17	.56	.74	1051	424.5	57.1	-68.0
86.00	2.25	-0.08	2.17	.56	.75	1046	423.4	53.3	-68.0
86.25	2.25	-0.08	2.17	.56	.76	1042	422.3	49.6	-68.0
86.50	2.29	-0.08	2.21	.55	.76	1042	421.2	46.1	-68.0
86.75	2.33	-0.08	2.24	.55	.76	1041	420.1	42.6	-67.9
87.00	2.36	-0.08	2.27	.54	.76	1040	419.0	39.3	-67.9
87.25	2.49	-0.08	2.41	.51	.74	1049	417.9	36.1	-67.8
87.50	2.51	-0.08	2.43	.51	.74	1047	416.7	33.1	-67.7
87.75	2.52	-0.08	2.44	.50	.75	1043	415.6	30.2	-67.6
88.00	2.53	-0.08	2.45	.50	.76	1040	414.5	27.5	-67.5
88.25	2.57	-0.08	2.49	.50	.76	1039	413.4	24.9	-67.3
88.50	2.59	-0.08	2.51	.49	.76	1037	412.3	22.4	-67.2
88.75	2.58	-0.08	2.50	.49	.77	1031	411.2	20.1	-67.0
89.00	2.59	-0.08	2.51	.49	.78	1028	410.1	17.8	-66.9
89.25	2.59	-0.08	2.52	.49	.78	1025	409.0	15.7	-66.7
89.50	2.60	-0.08	2.52	.49	.79	1021	408.0	13.8	-66.6
89.75	2.62	-0.08	2.55	.48	.79	1019	406.9	11.9	-66.4
90.00	2.64	-0.08	2.56	.48	.80	1016	405.9	10.1	-66.2
90.25	2.65	-0.07	2.58	.48	.80	1014	404.9	8.3	-66.0
90.50	2.66	-0.07	2.59	.48	.81	1010	403.9	6.7	-65.8
90.75	2.69	-0.07	2.62	.47	.81	1009	402.9	5.2	-65.6
91.00	2.70	-0.07	2.63	.47	.81	1006	401.9	3.7	-65.4
91.25	2.69	-0.07	2.62	.47	.82	1001	401.0	2.3	-65.2
91.50	2.68	-0.07	2.61	.47	.83	997	400.0	0.9	-65.0
91.75	2.65	-0.07	2.58	.48	.84	991	399.1	359.6	-64.8
92.00	2.60	-0.10	2.50	.48	.86	980	398.2	358.4	-64.6
92.25	2.45	-0.07	2.38	.50	.90	966	397.4	357.1	-64.3
92.50	2.42	-0.07	2.35	.50	.91	960	396.5	356.0	-64.1
92.75	2.43	-0.07	2.37	.50	.91	959	395.7	354.9	-63.9
93.00	2.47	-0.06	2.40	.50	.91	958	394.9	353.8	-63.7
93.25	2.52	-0.06	2.45	.49	.91	959	394.1	352.8	-63.4
93.50	2.52	-0.06	2.45	.48	.92	956	393.3	351.8	-63.2
93.75	2.54	-0.06	2.48	.48	.92	956	392.5	350.8	-63.0
94.00	2.56	-0.06	2.50	.48	.92	954	391.8	349.9	-62.7
94.25	2.62	-0.06	2.56	.47	.91	956	391.1	348.9	-62.5
94.50	2.67	-0.06	2.61	.45	.91	958	390.4	348.1	-62.3
94.75	2.78	-0.06	2.73	.44	.89	965	389.7	347.2	-62.0
95.00	2.86	-0.06	2.80	.43	.51	967	389.1	346.4	-61.8
95.25	2.90	-0.06	2.85	.42	.51	968	388.4	345.5	-61.5

Table 4 (Cont.)

MJD	$-10^4 \dot{P}$	$10^4 \dot{P}_r$	$-10^4 \dot{P}_a$	$\log \rho_\pi$	$\log \rho_s$	T _π (°K)	z (km)	$a_{\pi} - a_\odot$ (deg)	$\delta_{\pi} - \delta_\odot$ (deg)
40995.50	2.93	-0.05	2.88	-14.41	-14.50	968	387.8	344.7	-61.3
95.75	2.95	-0.05	2.90	.40	.50	967	387.2	344.0	-61.1
96.00	3.08	-0.05	3.03	.38	.49	974	386.6	343.2	-60.8
96.25	3.14	-0.05	3.09	.37	.49	976	386.1	342.5	-60.6
96.50	3.36	-0.05	3.31	.35	.46	989	385.5	341.7	-60.3
96.75	3.87	-0.05	3.82	.30	.41	1021	385.0	341.0	-60.1
97.00	3.85	-0.05	3.81	.30	.42	1018	384.4	340.3	-59.8
97.25	3.89	-0.04	3.85	.29	.41	1018	383.9	339.6	-59.6
97.50	3.87	-0.04	3.83	.30	.42	1014	383.4	339.0	-59.3
97.75	3.94	-0.04	3.90	.29	.42	1016	382.9	338.3	-59.1
98.00	4.01	-0.04	3.97	.29	.41	1019	382.4	337.7	-58.8
98.25	4.30	-0.04	4.26	.26	.39	1034	381.9	337.0	-58.6
98.50	4.49	-0.03	4.46	.24	.37	1043	381.4	336.4	-58.3
98.75	4.17	-0.03	4.14	.26	.40	1022	380.9	335.8	-58.1
99.00	3.93	-0.03	3.90	.29	.43	1005	380.5	335.2	-57.8
99.25	3.86	-0.03	3.84	.30	.44	999	380.0	334.6	-57.6
99.50	3.81	-0.02	3.79	.30	.45	994	379.5	334.0	-57.3
99.75	3.81	-0.02	3.79	.30	.45	992	379.1	333.4	-57.0
41000.00	3.85	-0.01	3.84	.29	.45	993	378.6	332.9	-56.8
00.25	3.92	-0.01	3.91	.29	.45	995	378.2	332.3	-56.5
00.50	4.00	-0.01	3.99	.28	.44	998	377.7	331.7	-56.3
00.75	4.07	-0.01	4.07	.27	.44	1000	377.3	331.2	-56.0
01.00	4.13	-0.01	4.13	.26	.43	1002	376.8	330.7	-55.7
01.25	4.09	-0.01	4.08	.27	.44	997	376.4	330.1	-55.5
01.50	4.03	-0.01	4.03	.27	.45	992	375.9	329.6	-55.2
01.75	4.04	-0.01	4.04	.27	.45	990	375.5	329.1	-54.9
02.00	4.03	-0.01	4.03	.26	.45	987	375.0	328.5	-54.7
02.25	4.16	-0.01	4.16	.25	.44	993	374.5	328.0	-54.4
02.50	4.30	-0.01	4.29	.24	.43	998	374.0	327.5	-54.1
02.75	4.38	-0.01	4.37	.23	.43	1000	373.6	327.0	-53.9
03.00	4.44	-0.01	4.43	.23	.43	1001	373.1	326.5	-53.6
03.25	4.52	0.00	4.51	.22	.42	1003	372.6	326.0	-53.3
03.50	4.60	0.00	4.59	.21	.42	1005	372.0	325.5	-53.1
03.75	4.62	0.00	4.62	.21	.42	1004	371.5	325.0	-52.8
04.00	4.67	0.00	4.66	.20	.42	1004	371.0	324.6	-52.5
04.25	4.70	0.00	4.69	.19	.42	1002	370.4	324.1	-52.3
04.50	4.74	0.00	4.74	.19	.42	1003	369.9	323.6	-52.0
04.75	4.70	0.00	4.70	.19	.43	998	369.3	323.1	-51.7
05.00	4.66	0.00	4.66	.19	.44	993	368.7	322.7	-51.4
05.25	4.69	0.00	4.68	.19	.44	991	368.1	322.2	-51.2
05.50	4.73	0.00	4.72	.19	.44	990	367.5	321.7	-50.9
05.75	5.05	0.00	5.04	.17	.42	1004	366.9	321.3	-50.6
06.00	5.86	0.00	5.86	.11	.35	1040	366.3	320.8	-50.3
06.25	5.91	0.00	5.91	.10	.35	1039	365.6	320.4	-50.1
06.50	5.96	0.00	5.96	.09	.36	1038	365.0	319.9	-49.8
06.75	6.04	0.00	6.04	.09	.36	1039	364.3	319.5	-49.5
07.00	6.52	0.00	6.51	.06	.33	1056	363.7	319.0	-49.2
07.25	6.41	0.00	6.41	.07	.34	1048	363.0	318.6	-48.9
07.50	6.18	0.00	6.18	.09	.36	1035	362.3	318.1	-48.7
07.75	6.34	0.00	6.34	.08	.35	1038	361.6	317.7	-48.4
08.00	7.06	0.00	7.05	.04	.31	1064	360.9	317.3	-48.1
08.25	7.90	0.00	7.89	-13.99	.26	1094	360.1	316.8	-47.8
08.50	7.14	0.00	7.14	-14.03	.31	1060	359.4	316.4	-47.5
08.75	6.19	0.00	6.18	.09	.38	1016	358.7	316.0	-47.2
09.00	5.94	0.00	5.93	.10	.41	1002	357.9	315.5	-46.9
09.25	5.65	0.00	5.65	.12	.43	986	357.2	315.1	-46.6
09.50	5.59	0.00	5.58	.12	.45	979	356.4	314.7	-46.4
09.75	5.54	0.00	5.53	.12	.46	973	355.7	314.3	-46.1
10.00	5.77	0.00	5.77	.11	.14	980	354.9	313.8	-45.8
10.25	5.76	0.00	5.76	.11	.15	976	354.1	313.4	-45.5

Table 4 (Cont.)

MJD	$-10^4 \dot{P}$	$10^4 \dot{P}_r$	$-10^4 \dot{P}_a$	$\log \rho_\pi$	$\log \rho_s$	T_π (°K)	z (km)	$a_\pi - a_\odot$ (deg)	$\delta_\pi - \delta_\odot$ (deg)
41010.50	5.57	0.00	5.56	-14.12	-14.17	963	353.4	313.0	-45.2
10.75	5.55	0.00	5.55	.11	.17	959	352.6	312.6	-44.9
11.00	5.60	0.00	5.60	.10	.17	957	351.9	312.2	-44.6
11.25	5.60	0.00	5.60	.11	.18	954	351.1	311.8	-44.3
11.50	5.58	0.00	5.58	.11	.19	949	350.3	311.3	-44.0
11.75	5.55	0.00	5.55	.11	.19	944	349.6	310.9	-43.7
12.00	5.54	0.00	5.54	.10	.20	940	348.9	310.5	-43.4
12.25	5.53	0.00	5.53	.11	.20	936	348.1	310.1	-43.1
12.50	5.68	0.00	5.68	.09	.20	939	347.4	309.7	-42.8
12.75	5.86	0.00	5.86	.08	.19	943	346.7	309.3	-42.5
13.00	6.00	0.00	5.99	.07	.18	945	346.0	308.9	-42.2
13.25	6.11	0.00	6.11	.07	.18	947	345.3	308.5	-41.9
13.50	6.13	0.00	6.12	.07	.19	944	344.7	308.1	-41.6
13.75	6.14	0.00	6.14	.06	.19	941	344.0	307.7	-41.3
14.00	6.41	0.00	6.40	.05	.18	948	343.4	307.3	-41.0
14.25	6.59	0.00	6.59	.04	.17	952	342.8	306.9	-40.7
14.50	6.66	0.00	6.65	.04	.17	952	342.2	306.5	-40.4
14.75	6.63	0.00	6.62	.03	.18	947	341.6	306.1	-40.0
15.00	6.57	0.00	6.57	.03	.22	919	336.3	305.7	-39.6
15.25	6.26	0.00	6.26	.05	.24	907	336.1	305.3	-39.3
15.50	6.03	0.00	6.03	.06	.26	897	335.9	304.9	-39.0
15.75	5.65	0.00	5.64	.09	.29	882	335.8	304.5	-38.7
16.00	5.58	0.00	5.57	.09	.29	879	335.8	304.1	-38.4
16.25	5.55	0.00	5.55	.09	.30	878	335.9	303.7	-38.0
16.50	5.54	0.00	5.54	.09	.29	878	336.0	303.3	-37.7
16.75	5.50	0.00	5.50	.09	.30	877	336.1	302.9	-37.4
17.00	5.49	0.00	5.49	.09	.30	877	336.3	302.5	-37.1
17.25	5.49	0.00	5.49	.09	.29	878	336.5	302.1	-36.8
17.50	5.48	0.00	5.47	.09	.29	878	336.7	301.7	-36.5
17.75	5.51	0.00	5.51	.09	.29	880	337.0	301.3	-36.1
18.00	5.59	0.00	5.59	.08	.28	884	337.2	300.9	-35.8
18.25	5.69	0.00	5.69	.09	.27	889	337.5	300.6	-35.5
18.50	5.78	0.00	5.78	.08	.26	894	337.8	300.2	-35.2
18.75	5.82	0.00	5.82	.08	.25	896	338.0	299.8	-34.8
19.00	5.87	0.00	5.87	.07	.25	899	338.3	299.4	-34.5
19.25	5.90	0.00	5.90	.07	.24	901	338.5	299.0	-34.2
19.50	5.78	0.00	5.78	.07	.25	897	338.8	298.6	-33.8
19.75	5.66	0.00	5.66	.08	.26	893	339.0	298.2	-33.5
20.00	5.33	0.00	5.33	.10	.28	881	339.2	297.9	-33.2
20.25	5.28	0.00	5.28	.11	.28	879	339.3	297.5	-32.8
20.50	5.51	0.00	5.51	.10	.27	889	339.4	297.1	-32.5
20.75	5.55	0.00	5.55	.10	.26	891	339.5	296.7	-32.2
21.00	5.46	0.00	5.46	.10	.27	887	339.6	296.3	-31.8
21.25	5.50	0.00	5.50	.09	.26	889	339.6	295.9	-31.5
21.50	5.51	0.00	5.51	.09	.26	889	339.6	295.6	-31.1
21.75	5.63	0.00	5.63	.08	.25	893	339.5	295.2	-30.8
22.00	5.46	0.00	5.46	.09	.27	885	339.4	294.8	-30.4
22.25	5.52	0.00	5.52	.08	.26	887	339.3	294.4	-30.1
22.50	5.62	0.00	5.62	.08	.26	890	339.1	294.0	-29.8
22.75	5.71	0.00	5.71	.08	.25	892	338.9	293.6	-29.4
23.00	6.77	0.00	6.77	.02	.18	930	338.6	293.3	-29.0
23.25	8.92	0.00	8.92	-13.90	.06	1001	338.3	292.9	-28.7
23.50	8.14	0.00	8.14	.94	.11	973	338.0	292.5	-28.3
23.75	7.65	0.00	7.65	.97	.14	955	337.6	292.1	-28.0
24.00	7.55	0.00	7.55	.98	.15	949	337.1	291.7	-27.6
24.25	7.44	0.00	7.44	.98	.16	942	336.6	291.3	-27.2
24.50	7.43	0.00	7.43	.98	.16	939	336.1	291.0	-26.9
24.75	7.42	0.00	7.42	.98	.17	936	335.5	290.6	-26.5
25.00	7.39	0.00	7.39	.98	.17	931	334.9	290.2	-26.1
25.25	7.38	0.00	7.38	.98	.18	927	334.3	289.8	-25.8

Table 4 (Cont.)

MJD	$-10^4 \dot{P}$	$10^4 \dot{P}_r$	$-10^4 \dot{P}_a$	$\log \rho_\pi$	$\log \rho_s$	T_π (°K)	z (km)	$a_\pi - a_\odot$ (deg)	$\delta_\pi - \delta_\odot$ (deg)
41025.50	7.09	0.00	7.09	-14.00	-14.20	914	333.6	289.4	-25.4
25.75	6.83	0.00	6.83	.00	.22	902	332.9	289.0	-25.0
26.00	6.57	0.00	6.57	.02	.25	889	332.2	288.7	-24.6
26.25	6.30	0.00	6.30	.03	.27	876	331.4	288.3	-24.3
26.50	6.40	0.00	6.40	.03	.27	875	330.6	287.9	-23.9
26.75	6.50	0.00	6.50	.02	.27	874	329.8	287.5	-23.5
27.00	6.55	0.00	6.55	.02	.27	872	329.0	287.1	-23.1
27.25	6.75	0.00	6.75	.00	.27	874	328.2	286.7	-22.7
27.50	6.95	0.00	6.95	-13.99	.26	876	327.3	286.4	-22.3
27.75	7.07	0.00	7.07	.98	.26	876	326.5	286.0	-21.9
28.00	7.01	0.00	7.01	.98	.27	870	325.6	285.6	-21.6
28.25	6.99	0.00	6.99	.98	.28	865	324.8	285.2	-21.2
28.50	6.82	0.00	6.82	.99	.30	856	324.0	284.8	-20.8
28.75	6.61	0.00	6.61	.99	.33	846	323.1	284.4	-20.4
29.00	6.38	0.00	6.38	-14.01	.33	843	324.3	284.1	-19.9
29.25	6.47	0.00	6.47	.01	.33	842	323.6	283.7	-19.5
29.50	6.56	0.00	6.56	.00	.33	841	322.9	283.3	-19.1
29.75	7.52	0.00	7.52	-13.95	.27	866	322.2	282.9	-18.7
30.00	8.03	0.00	8.03	.93	.24	875	321.5	282.5	-18.3
30.25	8.44	0.00	8.44	.91	.23	883	320.9	282.1	-17.9
30.50	7.67	0.00	7.67	.95	.27	857	320.2	281.7	-17.5
30.75	7.03	0.00	7.03	.97	.32	837	319.6	281.4	-17.1
31.00	6.71	0.00	6.71	.98	.36	827	319.0	281.0	-16.6
31.25	6.83	0.00	6.83	.97	.36	829	318.4	280.6	-16.2
31.50	6.26	0.00	6.26	-14.01	.40	809	317.8	280.2	-15.8
31.75	6.09	0.00	6.09	.02	.42	801	317.3	279.8	-15.4
32.00	6.13	0.00	6.14	.01	.42	800	316.8	279.4	-14.9
32.25	6.34	0.00	6.34	.00	.41	804	316.3	279.0	-14.5
32.50	6.40	0.00	6.40	-13.99	.42	805	315.9	278.6	-14.1
32.75	6.37	0.00	6.37	-14.00	.42	802	315.5	278.2	-13.6
33.00	6.35	0.00	6.35	.00	.42	799	315.1	277.8	-13.2
33.25	6.36	0.00	6.36	.00	.43	799	314.8	277.5	-12.8
33.50	6.45	0.00	6.45	-13.99	.43	801	314.5	277.1	-12.3
33.75	6.55	0.00	6.55	.99	.42	801	314.3	276.7	-11.9
34.00	6.58	0.00	6.58	.99	.41	798	314.1	276.3	-11.4
34.25	6.84	0.00	6.84	.97	.40	804	313.9	275.9	-11.0
34.50	7.39	0.00	7.40	.95	.36	816	313.8	275.5	-10.5
34.75	7.23	0.00	7.23	.96	.37	810	313.7	275.1	-10.1
35.00	7.17	0.00	7.17	.96	.37	807	313.6	274.7	-9.6
35.25	7.28	0.00	7.28	.96	.36	809	313.6	274.3	-9.1
35.50	7.36	0.00	7.36	.95	.36	811	313.6	273.9	-8.7
35.75	7.10	0.00	7.10	.97	.37	804	313.6	273.5	-8.2
36.00	6.81	0.00	6.81	.98	.40	798	313.7	273.1	-7.8
36.25	7.08	0.00	7.08	.97	.38	805	313.8	272.7	-7.3
36.50	7.61	0.00	7.61	.94	.34	818	313.9	272.3	-6.8
36.75	7.48	0.00	7.48	.95	.34	815	314.1	271.9	-6.4
37.00	6.94	0.00	6.94	.98	.38	802	314.2	271.5	-5.9
37.25	7.04	0.00	7.04	.97	.38	807	314.4	271.1	-5.4
37.50	6.94	0.00	6.94	.97	.38	805	314.6	270.7	-4.9
37.75	6.48	0.00	6.48	-14.00	.41	791	314.8	270.3	-4.5
38.00	6.44	0.00	6.44	.01	.41	792	315.1	269.9	-4.0
38.25	6.29	0.00	6.29	.01	.43	790	315.3	269.5	-3.5
38.50	5.87	0.00	5.87	.03	.47	781	315.5	269.1	-3.0
38.75	5.78	0.00	5.78	.04	.48	780	315.7	268.7	-2.5
39.00	5.75	0.00	5.75	.04	.47	778	316.0	268.3	-2.1
39.25	5.72	0.00	5.72	.05	.47	778	316.2	267.9	-1.6
39.50	5.67	0.00	5.68	.05	.47	777	316.4	267.5	-1.1
39.75	5.62	0.00	5.62	.05	.48	776	316.6	267.1	-0.6
40.00	5.53	0.00	5.53	.06	.49	773	316.7	266.7	-0.1
40.25	5.91	0.00	5.91	.04	.45	784	316.9	266.2	0.4

Table 4 (Cont.)

MJD	$-10^4 \dot{P}$	$10^4 \dot{P}_r$	$-10^4 \dot{P}_a$	$\log \rho_\pi$	$\log \rho_s$	T_π (°K)	z (km)	$a_\pi - a_\odot$ (deg)	$\delta_\pi - \delta_\odot$ (deg)
41040.50	6.42	0.00	6.42	-14.00	-14.41	800	317.0	265.8	0.9
40.75	6.63	0.00	6.63	-13.99	.40	806	317.0	265.4	1.4
41.00	6.89	0.00	6.89	.99	.37	809	317.1	265.0	1.9
41041.20	7.94	0.00	7.94	-13.94	-14.30	835	317.0	264.7	2.3
41.40	8.66	0.00	8.66	.90	.26	852	317.0	264.3	2.7
41.60	8.39	0.00	8.39	.91	.28	846	316.9	264.0	3.1
41.80	8.50	0.00	8.50	.91	.27	848	316.8	263.7	3.5
42.00	8.61	0.00	8.61	.90	.27	848	316.6	263.4	3.9
42.20	8.18	0.00	8.18	.92	.30	838	316.4	263.0	4.3
42.40	8.01	0.00	8.01	.93	.31	832	316.1	262.7	4.7
42.60	7.87	0.00	7.87	.94	.32	826	315.8	262.4	5.1
42.80	7.33	0.00	7.33	.96	.37	812	315.4	262.0	5.5
43.00	6.46	0.00	6.46	-14.01	.44	787	315.0	261.7	5.9
43.20	6.73	0.00	6.73	-13.99	.43	793	314.5	261.3	6.3
43.40	6.95	0.00	6.95	.97	.42	798	313.9	261.0	6.7
43.60	7.11	0.00	7.11	.97	.41	796	313.3	260.7	7.1
43.80	7.23	0.00	7.23	.97	.40	793	312.5	260.3	7.5
44.00	7.34	0.00	7.34	.96	.41	792	311.8	260.0	8.0
44.20	7.61	0.00	7.61	.95	.40	795	310.9	259.7	8.4
44.40	7.80	0.00	7.80	.94	.39	793	309.9	259.3	8.8
44.60	7.92	0.00	7.92	.94	.39	790	308.9	259.0	9.2
44.80	8.06	0.00	8.06	.92	.40	789	307.8	258.6	9.6
45.00	8.55	0.00	8.55	.90	.39	794	306.6	258.3	10.0
45.20	9.84	0.00	9.84	.85	.32	809	305.2	257.9	10.4
45.40	10.80	0.00	10.80	.81	.29	820	303.8	257.6	10.8
45.60	9.01	0.00	9.01	.88	.40	779	302.3	257.3	11.2
45.80	9.55	0.00	9.55	.86	.39	782	300.6	256.9	11.7

Table 5. Standard heights to which densities in Tables 3 and 4 are referred.

Interval (MJD)	\bar{z} (km)
38397.00–38473.00	3660
38558.00–38641.00	3590
38732.00–38814.00	3470
40237.00–40305.00	2035
40405.00–40465.00	1810
40560.00–40609.00	1415
40710.00–40770.00	1120
40850.00–40879.50	720
40880.00–40919.50	655
40920.00–40949.75	600
40950.00–40964.75	550
40965.00–40979.75	500
40980.00–40994.75	450
40995.00–41009.75	400
41010.00–41045.80	360